

ENCLOSURE 2

MFN 06-042

GE Licensing Topical Report NEDO-32906-A, Revision 1,
“TRACG Application for Anticipated Operational Occurrences
(AOO) Transient Analyses

Non-Proprietary Version

IMPORTANT NOTICE

This is a non-proprietary version of Enclosure 1 to MFN 06-042, which has the proprietary information removed. The proprietary information of the GE Company was indicated by “bars” drawn in the right-hand margin of the text of the report (as shown to the right of this paragraph). Portions of the document that have been removed are indicated by white space with a side bar in the right margin.



GE Nuclear Energy

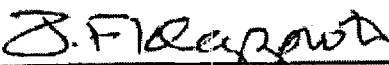
175 Curtner Avenue
San Jose, CA 95125

NEDO-32906-A
Revision 1
Class I
DRF 0000-0017-7858
June 2003
(Issued January 2006)

Licensing Topical Report

**TRACG Application
for
Anticipated Operational Occurrences (AOO)
Transient Analyses**

J. G. M. Andersen (GNF-A)
F. T. Bolger
C. L. Heck (GNF-A)
B. S. Shiralkar

Approved: 

J.F. Klapproth, Manager
Engineering and Technology, GE Nuclear Energy

CHANGES FROM PROPRIETARY VERION

This document is the GE non-proprietary version of NRC accepted GE proprietary Licensing Topical Report (LTR) NEDE-32906P-A. From the GE proprietary version, (1) the copy of the original GE transmittal letter, (2) proprietary information affidavit, (3) the information denoted as GE proprietary (denoted by blanks with dark sidebars in the right margins), and (4) documents no longer referenced were deleted to generate this version. Some minor editorial changes have been made for clarity.

**IMPORTANT NOTICE REGARDING CONTENTS OF THIS REPORT
PLEASE READ CAREFULLY**

Neither the General Electric Company nor any of the contributors to this document makes any warranty or representation (express or implied) with respect to the accuracy, completeness, or usefulness of the information contained in this document; or that the use of such information may not infringe privately owned rights; nor do they assume any responsibility for liability or damage of any kind which may result from the use of any of the information contained in this document.



UNITED STATES
NUCLEAR REGULATORY COMMISSION

WASHINGTON, D.C. 20555-0001

October 22, 2001

MFN 01-062

Mr. James F. Klapproth, Manager
Engineering & Technology
GE Nuclear Energy
175 Curtner Ave
San Jose, CA 95125

SUBJECT: SAFETY EVALUATION REPORT ON GENERAL ELECTRIC NUCLEAR ENERGY TOPICAL REPORT NEDE-32906P, REVISION 0, "TRACG APPLICATION FOR ANTICIPATED OPERATIONAL OCCURRENCES (AOO) TRANSIENT ANALYSES," (TAC NO. MA7779)

Dear Mr. Klapproth:

By letter dated January 25, 2000, General Electric Nuclear Energy (GENE) submitted for review and approval topical report (TR), NEDE-32906P, Revision 0, "TRACG Application for Anticipated Operational Occurrences (AOO) Transient Analyses," for the use of the TRACG code for application to boiling water reactor (BWR) AOO's. The primary document describing the TRACG code is NEDE-32176P, Rev. 2, "TRACG Model Description," December 1999, provided by letter dated December 15, 1999. The TR describes the TRACG analysis code and the assessment of the code's capabilities based on application of the Code Scaling, Applicability, and Uncertainty evaluation methodology (CSAU).

The staff finds that the subject TR is acceptable for referencing in licensing applications to the extent specified and under the limitations delineated in the TR and in the associated NRC safety evaluation (SE). The SE, which is enclosed, defines the basis for acceptance of the TR.

The NRC requests that GENE publish an accepted version of the revised NEDE-32906P within 3 months of receipt of this letter. The accepted version shall incorporate this letter and the enclosed SE between the title page and the abstract, and add an "-A" (designating accepted) following the report identification number (i.e., NEDE-32906P-A).

If the NRC's criteria or regulations change so that its conclusion in this letter, that the TR is acceptable, is invalidated, GENE and/or the applicant referencing the TR will be expected to revise and resubmit its respective documentation, or submit justification for the continued applicability of the TR without revision of the respective documentation.

Pursuant to 10 CFR 2.790, we have determined that the enclosed SE does not contain proprietary information. However, we will delay placing this document in the public document room for a period of ten (10) working days from the date of the letter to provide you with the

Mr. James F. Klapproth

- 2 -

opportunity to comment on the proprietary aspects only. If you believe that any information in the enclosure is proprietary, please identify such information line by line and define the basis pursuant to the criteria of 10 CFR 2.790.

The subject TR and supporting documentation has been reviewed by the Advisory Committee on Reactor Safeguards which has agreed with the staff recommendation for approval by their letter of September 17, 2001.

If you have any further questions regarding this review, please contact Robert M. Pulsifer at (301) 415-3016.

Sincerely,

A handwritten signature in black ink, appearing to read "SARICHARDS", written over a horizontal line.

Stuart A. Richards, Director
Project Directorate IV
Division of Licensing Project Management
Office of Nuclear Reactor Regulation

Project No. 710

Enclosure: Safety Evaluation

cc: See next page

GE Nuclear Energy

Project No. 710

cc:

**Mr. George B. Stramback
Regulatory Services Project Manager
GE Nuclear Energy
175 Curtner Avenue
San Jose, CA 95125**

**Mr. Charles M. Vaughan, Manager
Facility Licensing
Global Nuclear Fuel
P.O. Box 780
Wilmington, NC 28402**

**Mr. Glen A. Watford, Manager
Nuclear Fuel Engineering
Global Nuclear Fuel
P.O. Box 780
Wilmington, NC 28402**



UNITED STATES
NUCLEAR REGULATORY COMMISSION
WASHINGTON, D.C. 20555-0001

SAFETY EVALUATION BY THE OFFICE OF NUCLEAR REACTOR REGULATION

**NEDE-32906P, "TRACG APPLICATION FOR ANTICIPATED OPERATIONAL
OCCURRENCES (AOO) TRANSIENT ANALYSES"**

GE NUCLEAR ENERGY

PROJECT NO. 710

1.0 INTRODUCTION

General Electric Nuclear Energy (GENE) and its subsidiary Global Nuclear Fuel (GNF) submitted TRACG02A (referred to hereafter as TRACG) for NRC review for application to anticipated operational occurrence (AOO) transient events on January 25, 2000 (Reference 1). The submittal includes the code model documents related to the TRACG code (Reference 2). The TRACG code is a thermal/hydraulic analysis code intended to be used in a realistic analysis mode. The approach taken by GENE in the proposed application is to qualify the code under the code scaling, applicability, and uncertainty (CSAU) evaluation methodology (References 3 and 4), rather than the conservative approach of the past.

The TRAC family of codes began as a pressurized water reactor analysis code developed for the NRC at Los Alamos National Laboratory. A boiling water reactor (BWR) version of the code was developed jointly by the NRC and GENE at the Idaho National Engineering Laboratory (INEL) as TRAC-BD1/MOD1 (Reference 5). GENE developed a proprietary version of the code designated as TRACG. The objective of the proprietary code development was to have a code capable of realistic analysis of transient, stability, and anticipated transients without scram (ATWS) events. The code was modified to include a three-dimensional kinetics capability in addition to the multi-dimensional, two-fluid thermal-hydraulics modeling.

The plant types for which the TRACG code is to be applied include the BWR/2s, BWR/3s, BWR/4s, BWR/5s, and BWR/6s. The code has not been submitted for review for application to any other plant design.

2.0 CODE APPLICABILITY

TRACG is a multi-dimensional, two-fluid reactor thermal-hydraulics analysis code with three-dimensional neutron kinetics capability. The code is designed to perform in a realistic manner with conservatism added, where appropriate, via the input specifications.

Table 1 - Applicable Standard Review Plan (SRP) Chapter 15 Events

Event	SRP No.
15.1 - Increase in Heat Removal by the Secondary System	
Decrease in Feedwater Flow	15.1.1
Increase in Feedwater Flow	15.1.2
Increase in Steam Flow	15.1.3
Inadvertent Opening of Steam Generator Relief/Safety Valve	15.1.4
15.2 - Decrease in Heat Removal by Secondary System	
Loss of External Load (LOEL)	15.2.1
Turbine Trip (TT)	15.2.2
Loss of Condenser Vacuum	15.2.3
Closure of Main Steam Isolation Valve (BWR)	15.2.4
Steam Pressure Regulator Failure (closed)	15.2.5
Loss of Non-Emergency AC Power to the Station Auxiliaries	15.2.6
Loss of Normal Feedwater Flow	15.2.7
15.3 - Decrease in Reactor Coolant Flow Rate	
Loss of Forced Reactor Coolant Flow (LOCF)	15.3.1
Flow Controller Malfunction	15.3.2
15.4 - Reactivity and Power Distribution Anomalies	
Startup of an Inactive, or Recirculation, Loop at an Incorrect Temperature	15.4.4
Flow Controller Malfunction Causing an Increase in BWR Core Flow Rate	15.4.5
15.5 - Increase in Reactor Coolant Inventory	
Inadvertent Operation of Emergency Core Cooling System (ECCS) that Increases Reactor Coolant Inventory	15.5.1
Chemical Volume Control System (CVCS) Malfunction that Increases Reactor Coolant Inventory	15.5.2
15.6 - Decrease in Reactor Coolant Inventory	
Inadvertent Opening of a PWR Pressurizer Relief Valve or a BWR Pressure Relief Valve	15.6.1

The current application of the TRACG code does not include transients involving stability analysis.

3.0 STAFF APPROACH TO REVIEW

The staff performed an extensive review of the TRACG code for application to the loss-of-coolant accident (LOCA) during the course of the simplified boiling water reactor (SBWR) review. At that time the code was examined carefully with regards to the thermal-hydraulic construction of the code. For the application to the AOO transients, the staff has built upon the previous review. The most intense review for the AOO transients was performed in the areas of kinetics and statistical analysis. The staff does note that a significant addition has been made to the thermal-hydraulic field equations in the addition of kinetic energy to the equations.

In the early stages of the review, the staff issued two draft documents (References 6 and 7) for public comment. The draft Regulatory Guide and draft Standard Review Plan outline the approach and guidance the staff is using in the review of thermal-hydraulic analysis codes. In addition, the staff has stated its guidance for code uncertainty analysis in References 3 and 4. These four documents provide the basis under which the TRACG review has been conducted. In the course of the review, the staff developed a number of requests for additional information (Reference 8) and received responses from GENE (Reference 9).

As the review progressed, GENE and the staff held several meetings to discuss the application.

May 25, 1999 - preliminary information meeting
July 15, 1999 - preliminary information meeting
March 16, 2000 - detailed presentation of code methodology
September 11, 2000 - staff review concerns
November 13/14, 2000 - ACRS T/H Subcommittee
August 22, 2001 - ACRS T/H Subcommittee
September 6, 2001 - ACRS

4.0 CODE ASSESSMENT

Assessment of computer codes is normally performed by comparison of code results with data from appropriate test facilities. The assessment process involves comparisons with data obtained via phenomenological experiments, separate effects tests, component tests, integral system tests, and plant tests. Assessment of code capability should also include sensitivity studies of time step size and nodalization. Nodalization of test facilities is expected to be done in a manner consistent with the nodalization to be used in a full scale plant analysis.

The TRACG documentation (Reference 2) provides extensive description of the code assessment that has been performed. Each of the phenomena identified in the Phenomena Identification and Ranking Table (PIRT) is correlated against the tests, separate effects tests, component tests, integral system tests, and plant tests and plant data, for which there has been quantitative assessment performed. The assessment descriptions cover the test facility, where applicable, the test results, TRACG sensitivity studies and nodalization studies, where applicable. All medium and high ranked phenomena have been assessed.

The assessment that has been performed to support the intended application of TRACG to AOO transients is appropriate in that it includes assessment of phenomenological models with data from separate effects tests, the entire code with systems tests, and the entire code versus full scale operating plant data. The assessment program has shown the capability of the code to represent the experimental and operating data.

5.0 STAFF EVALUATION OF TRACG

5.1 Thermal-Hydraulics

TRACG uses a two-fluid model, with six conservation equations for both the liquid and gas phases along with phasic constitutive relations for closure. A boron transport equation and a noncondensable gas mass equation are also solved. The spatially discretized equations are solved by donor-cell differencing in staggered meshes in one, two, or three dimensions. A unified flow regime map is also used.

The two-phase level tracking model invokes some approximations for the void fraction above and below the mixture level that may not be accurate if significant voiding occurs below the mixture level. In addition, the model uses an arbitrary cutpoint, α_{cut} , for level detection. This is significant for LOCAs, rather than the current application of TRACG, AOO transients, since they are not expected to result in significant void formation beyond that which is normal for BWR operation. Should significant voiding occur, such as in the case of a LOCA, the two-phase level tracking model will be reevaluated by the staff.

The TRAC-B code from which TRACG was derived had eliminated the kinetic energy term from the energy equations by algebraic manipulations. The kinetic energy term has been retained in TRACG to avoid the energy balance errors that occurred in the TRAC-B codes due to nonconservation of energy.

The two-fluid conservation equations contain a mixing term to account for turbulent mixing and molecular diffusion. This is a good addition which the staff accepts due to the acceptable qualitative results, but notes that the mixing model is qualitative and lacks experimental data necessary for validation. While there is a lack of direct experimental data for assessment, the overall performance of the model versus the more global data which do exist is acceptable.

TRACG solves the heat conduction equation for the fuel rods in cylindrical geometry and for structural materials in slab geometry. The latter case uses either a lumped slab model or a one-dimensional slab model. A strength of the TRACG heat conduction model is the sophisticated gap conductance model and the implicit solution method that couples implicitly the heat transfer between the fuel rod and the coolant by iteration. Although TRACG solves the heat conduction equations in only one-dimension, it does account for axial conduction by means of a correlation developed from two-dimensional (r,z) parametric calculations of the heat conduction in a fuel element. This is only important in modeling quenching or reflood in the core in a LOCA.

The TRACG code has had the GEXL heat transfer correlation installed. The GEXL correlation development is independent of the TRACG development. During the week of March 26, 2001, the NRC staff visited the GENE facility at Wilmington, North Carolina, as part of the review of the power uprate for Duane Arnold to audit material pertinent to the licensee's power uprate.

Material reviewed included the data base used for the development of the GEXL14 correlation for the GE14 fuel, analyses of ATWS event, and LOCA related analyses. In the early stages of the audit, the staff discovered that GENE was using data generated by the computer code COBRAG, instead of experimental data obtained from their CHF test facility in San Jose, California. The use of artificial data instead of raw data called into question the validity of the statistical results obtained from this methodology. The statistical results are important because they are used to establish the validity of the minimum critical power ratio (MCPR) safety limit. GENE has proposed to resolve this issue by agreeing to remove the COBRAG reliance and recalculating the uncertainty associated with the development of GEXL14 correlation. GENE will then submit this re-calculation of the correlation uncertainty for staff review. GENE has not indicated whether it will submit the COBRAG code for staff review, nor has GENE indicated whether it intends to obtain additional data to complete their data base for the GE14 fuel in the future. Based on this ongoing review of the correlation, the staff concludes that it is acceptable to use the GEXL14 correlation in TRACG, provided that when the NRC approves the critical boiling length correlation uncertainty, that same uncertainty is also applied in use of TRACG.

The thermal-hydraulic models are acceptable for the intended application to AOO transients.

5.2 Component Models

TRACG uses basic component models as building blocks to construct physical models for intended applications. This provides a general and flexible tool to simulate a wide variety of systems. The components modeled include the pipe, pump, valve, tee, channel, jet pump, steam separator, steam dryer, vessel, upper plenum, heat exchanger, and break and fill as boundary conditions. The code is limited in that the heat exchanger contains simplifying approximations which may not be appropriate for simulating the isolation condenser or the condenser in the balance of plant. Should the code be applied to transients requiring a condenser, a separate model will be needed or the ability to adequately model the condenser must be demonstrated.

TRACG uses a first-principle mechanistic model for the steam separator. The model has been validated against full-scale performance test data for two-stage and three-stage steam separators. The important parameters that have been assessed are the pressure drop, carryunder and carryover which match the test data by means of correlation constants. The data base covers the applicable range for the intended AOO transients and the model is therefore acceptable.

5.3 Control Systems

TRACG uses control systems constructed by the user from 63 basic control block types. The types of control blocks available are sufficient to represent any control system. This allows both a flexible tool and flexible interface with the hydraulic component models. A wide variety of possible dynamic processes can be simulated with the control system models.

5.4 Numerics

The TRACG numerics represent a significant improvement over its predecessor, TRAC-BD1/MOD1. By default, TRACG uses a fully implicit integration for hydraulic equations and heat conduction equations, accomplished by a predictor-corrector iterative technique. The heat transfer coupling between the heat conduction and coolant hydraulics is also treated implicitly by an iterative technique. This implicit coupling is an improvement over explicit coupling since it is less prone to an error on the phase shift and amplitude in a thermally-induced oscillation. The coolant hydraulic solution has the option of an explicit integration for time-domain stability analyses where implicit integration may suppress real physical oscillations. The staff notes, however, that the current application of the code does not include stability analyses. TRACG was accepted in a limited way by the staff (Reference 10) as part of the detect and suppress solutions licensing basis methodology to define setpoints. Should the applicant want to apply the code to stability analyses beyond that limited approval, the staff will review the methodology for that purpose.

The control system equations are solved sequentially based on the order in which the control blocks are specified in the input. This makes it a potentially explicit integration scheme. If a feedback loop exists in the control system, an implicit solution of the control system equations is impossible. To make sure that the control system will be stable, TRACG uses a sufficiently small time step size (always less than or equal to the hydraulic time step size) to integrate the control system equations.

5.5 Neutron Kinetics

5.5.1 Model Description

The TRACG kinetics review focused on evaluating the derivation of the equations, their implementation in the code and using the code to predict several test problems. The derivation of the equations is discussed in chapter 9 of the Models and Correlations document (Reference 2). Starting with three group theory for the neutron flux, the model is simplified to a one group representation of the neutron flux. Delayed neutrons are modeled with a six group model and a five group model is available for decay heat. The flux model is then further simplified by imposing a quasi-static assumption which allows for the space and time dependence to be decoupled. This decomposition leads to an amplitude equation which is analogous to the point reactor kinetics equations and an equation for the shape function which is equivalent to the three-dimensional flux distribution.

Several auxiliary models are used to account for the affects of direct moderator heating, energy deposition in structural materials, and gamma smearing. Direct moderator heating accounts for prompt energy deposition in the fluid from neutron moderation and prompt gamma heating. This energy is then further subdivided into an in-channel and a bypass component. The in-channel component refers to energy deposited into the voided region inside the fuel channel and the bypass component is the energy deposited into the regions between the fuel channel. This model accounts for void effects for which the uncertainty and bias was quantified using the Monte Carlo Code for Neutron, Photon and Electron Transport (MCNP). Similarly, the uncertainty and bias in the fuel structure and gamma smearing modes were quantified using MCNP calculations.

The kinetics equations are solved using standard finite differencing techniques. Typically they are solved on a rectangular grid six inches square which is equivalent to the mean free path of a fast neutron. The calculation uses two governing time intervals; one in which only the amplitude equation is solved and one in which the shape function is updated. The shape function update is synchronized to the thermal-hydraulic time step and the amplitude function time step is deduced by applying extrapolation techniques and using a user input convergence criterion. The thermal-hydraulic time step is governed by the rate of change of many variables, one of which is the total power. If the system is changing too rapidly within a time step, the entire solution is returned to the previous time step value, the thermal-hydraulic time step is reduced and the procedure is repeated.

Lattice-averaged neutron cross sections in three energy groups are generated using GENE lattice physics methods. This information is fed into TRACG via the GENE three-dimensional steady state design code PANACEA which is used to define the TRACG initial condition. Cross sections are represented by functional fits over the expected range of density, square root of fuel temperature and boron concentration. The functional fits also account for the historical impacts due to water density and exposure. The density used in the fitting procedure is the "effective" nodal value which is a weighted average of the in-channel, water rod and bypass density. This model imposes the assumption that all neutrons behave similarly whether they slow down in the fuel or bypass region. The "effective" density model has no effect on the proposed application under review because for AOO analyses no significant water rod or bypass voiding (or density change) is expected. Therefore, the staff has not reviewed this model. This model would need to be re-considered and reviewed by the staff before TRACG was applied to ATWS analyses beyond previously accepted use for bench marking ODDYN (Reference 11).

5.5.2 Review of GNF Submittal

The staff reviewed the TRACG kinetics model in three ways: first, the staff judged the written material presented in the Models and Correlations document, the Assessment Manual and responses to staff's RAs; second, the staff reviewed the results from the assessments against experimental data; and, third, the staff completed a performance-based assessment of the code by evaluating its predictions to another set of results to a sample problem. The model was well developed from the three group diffusion theory model which was the assumed starting point. Although not currently widely used, the use of the factored one group diffusion theory model is well established and has been successfully applied in the past (Reference 12). The GNF factorization method is an extension of traditional quasi-static methods because the shape function is also a function of time. The cross-section formulation captures all of the relevant physics, and formulations such as those used in TRACG have been demonstrated by the Peach Bottom turbine trip benchmark study discussed in the Assessment Manual to be accurate enough to successfully model the small perturbations expected for AOO analyses. The auxiliary models for direct moderator heating, energy deposition in the structure and gamma smearing capture all of the relevant physics. It is difficult to assess each contribution separately because they will have a small effect on the predictions. However, based on the integral benchmarks presented in the Qualification document, these models are appropriate. One model which is not documented in the Models and Correlations manual, but is discussed in References 1 and 9, attempts to modify the lattice physics prediction of void reactivity based

upon MCNP calculations. Discussion of this model is contained in the next section where the performance-based review is discussed.

The decay heat model is predicated on the assumption that delayed neutron decay is exponential in nature. The fission precursors are grouped into five distinct bins each with a representative decay constant and fission fraction. The model for decay power for each "group" is then integrated using an exponential integrating factor. The model has a set of default or "built in" decay constants and fission fractions based on the May-Witt decay heat curves. This model used in its default mode has the ability to model decay power either as an average of different fuel types similar to the ANS 5.1 model or it can capture the detailed spectral effects on decay heat by overriding the default values and using fuel specific decay constants and fission fractions. The default parameters have been shown to be acceptable for AOO analyses by comparing the results to the latest ANS 5.1 standard.

The solution procedure leverages the factorization concept by solving the amplitude and shape function equations on a different temporal grid. Each governing time step is chosen by the code based on logic which is controlled by user input convergence criteria. This model is best reviewed by evaluating its ability to model experimental data representative of the expected application and sensitivity studies. Time step and sensitivity studies discussed in Reference 1 demonstrate that this model is acceptable because the chosen convergence criteria are shown to be insensitive to further reductions.

All of these models are combined into a code which will be applied by GNF to model AOO transients. AOO analysis is designed to evaluate whether or not specified acceptable fuel design limits (SAFDLs) are exceeded. The figure of merit for these types of analyses is the MCPR. Kinetics codes are needed to predict the direct heating of the coolant via gamma absorption and the energy deposited in the fuel. The energy deposited in the fuel is the dominant parameter. Energy deposition in the fuel is important because for a correlation such as the one used by GNF one must know the boiling length in order to predict the critical power. The boiling length is directly proportional to the fuel heat flux which is dependent on the fuel temperature. The fuel temperature is derived from the energy deposition. For convenience the fission power is often used as the metric for energy deposition. In this study, both energy deposition and power are considered.

5.5.3 Review of Experimental Benchmarks

GNF assessed TRACG against the Peach Bottom turbine trip tests. Three turbine trips were performed at the Peach Bottom Nuclear Power Plant to generate data for code assessment. These tests were initiated at three different power and flow conditions during the coastdown following Cycle 2 operation in 1977. The core consisted of initial load 7x7 fuel and retrofit 8x8 fuel. The 7x7 fuel was the dominant fuel type. These results show that TRACG correctly predicts the Peach Bottom test's fission power data to within an acceptable error.

Another kinetics assessment which is presented in the topical report is a prediction of one of the cold SPERT III E-Core experiments. The SPERT III E-Core is a challenging experiment to model and of limited usefulness when considering applications to AOO transients given the differences between the test parameters and the conditions expected during an AOO. The SPERT tests were initiated by ejecting a control rod and were intended to develop data for code

assessment for reactivity insertion accidents (RIA). This being said, it is evident from a cursory review of the results presented by GNF in the TRACG assessment manual that TRACG overpredicts the flux peak by 40 percent, but predicts the total energy with an error in the integrated energy of 10 percent. As the staff learned when it demonstrated the capability of our methods to predict the SPERT III E-core, the SPERT reactor is difficult to predict. The staff has not attempted to identify the reason for the discrepancy between the TRACG results and the SPERT data. The GNF results are mentioned to reinforce the point that due to the differences between the test conditions and the conditions expected during AOO events, the staff has not considered the TRACG SPERT calculations in our assessment.

5.5.4 Independent Analyses of TRACG

As is its current practice, the staff ran many TRACG cases on NRC computers at headquarters. The VMS operating system was installed on a staff DEC Alpha system and TRACG was installed on the machine. GNF personnel assisted the staff in this initial installation and with subsequent software issues. A test problem provided by GNF was run to check the installation. This case confirmed that the installation was successful and that the code predicted answers equivalent to those calculated at GNF.

The staff and GNF defined a problem intended to reduce the variability of the generated cross sections which would allow the focus to be on the differences in the kinetics modeling. The staff carefully defined this model because it was expected that there would be some variability in lattice physics inputs. In addition, due to the GNF kinetics solver and its use of three-group cross-sections with neutron energy spectrums characteristic of BWR lattices, the staff was unable to provide GNF with physics input to ensure that the lattice physics was not influencing the kinetics results. The initial core consisted of five different modern GNF fuel types at zero exposure. The model contained no components other than the channels and a vessel used to model the core bypass and the upper and lower plenum. Core inlet and exit conditions were modeled with velocity and pressure boundary conditions, respectively. Even with all of the care put into the model definition, unacceptably large differences in predicted lattice void reactivity were evident based on an assessment of the first transient analyses of the test core. Based on differences in input void reactivity, this model was further simplified to two fuel types. This void reactivity effect was caused by differences in the input cross sections because the staff and GNF lattice physics methods predicted different trends in the infinite eigenvalue as a function of void reactivity for certain GNF fuel lattices. Although the cause of this difference has not been identified and the staff is still considering this problem, it was appropriate to define a simpler core based on fuel types that did agree well to allow the TRACG review to proceed because the lattice physics analysis is not part of this review.

The staff and GNF predictions of the two fuel type core are compared in Figures 1 and 2. Figure 1 shows a three-dimensional view of the initial steady state power distribution and Figure 2 shows the infinite eigenvalue as a function of time for the two fuel types used in the core. One difference between the two predictions in Figure 1 is the fact that the staff results are not as smooth as the GNF analyses. This difference is typical when comparing modern nodal methods to finite difference methods, possibly because nodal methods attempt to more accurately account for inter-assembly gradients. Otherwise, Figure 1 demonstrates that the two methods quantitatively agree well with one another. Figure 2 shows that the void reactivity input into the two respective kinetics codes is equivalent.

Both TRACG and staff models were used to evaluate three transient problems: first, a slow pressure increase was modeled; second, an inlet flow decrease was modeled; and, finally, a main steam isolation valve (MSIV) closure transient was simulated. The first two transients were run to evaluate TRACG's ability to predict changes in total reactivity. The figure of merit for a test such as this is total power. In Figures 3 and 4, the two codes compare well with one another with regard to the change in reactivity from the imposed transient. The final transient is intended to assess TRACG's ability to predict prompt critical power changes similar to those expected during limiting AOO transients.

The MSIV closure simulation is modeled by imposing changes to the inlet and outlet boundary conditions. These changes were predicted from another TRAC model which modeled the entire reactor system and the balance of plant. Conditions as a function of time in the upper and lower plenum were extracted from this case, scaled to the test problem, and entered into the velocity and pressure boundary conditions. The staff compared the affects of many of the TRACG models on the results of this problem and many different cases were run. Only one model was found to significantly alter the results from the base case. The staff will refer to this model as the PIRT18 model. This model was previously mentioned in Section 5.5.2 of this safety evaluation. This model uses a set of precalculated MCNP results for various GNF fuel types as a function of void fraction and exposure to adjust the results from the standard GNF lattice physics methods. This adjustment is accomplished by modifying the reference density used in the TRACG fitting algorithm.

The staff independently assessed this model because the TRACG results are sensitive to it. The staff ran many MCNP calculations of a GNF fuel lattice using different modeling assumptions and different cross sections based on ENDF/B-V and ENDF/B-VI data. The results of the assessment identified a weakness in the GNF model. The GNF model uses the MCNP code, which is a Monte Carlo solver, to predict point values. Monte Carlo methods do not yield point answers; rather, they provide statistically significant ranges of answers. As the staff results in Figure 6 show, a wide range of different, but statistically equivalent answers, can be attained by using different cross section formulations and different (but equivalent) modeling assumptions. *The differences presented in Figure 6 would not typically be of concern if it were not for the fact that BWRs are sensitive to void reactivity changes on the order of magnitude of the 95th percentile confidence intervals of the MCNP results.*

Based on the results of the three review efforts, the staff considers that the TRACG kinetics code can adequately model AOO transients. The written material allowed the staff to conclude that there is reasonable assurance that the model captures all of the relevant phenomena and that the equations are appropriately derived. The method of solution has been used in other methods and the description provided in Reference 2 allows the informed reader to conclude that the mathematical formulations are adequate. Although the staff discounted the SPERT experimental validation, the results of the Peach Bottom assessment provide enough experimental evidence for the staff to make a finding that there is reasonable assurance that TRACG can predict AOO transients. The Peach Bottom benchmarking presented by GNF is a valuable result when one considers whether a code can adequately model the phenomena relevant to pressurization AOO transients. These results demonstrate that the TRACG kinetics model is capable of predicting the reactor power during a pressurization transient.

As one can see from the previous section, the staff spent considerable effort attempting to reconcile the differences between the TRACG and the TRAC/NESTLE independent assessment results. In the end this work focused on understanding the PIRT18 model. As one can see from Figure 5, it does significantly affect the peak power. However, after considering that the proposed application of TRACG is to AOO analyses, the staff concluded that this effect on peak power is not significant because when the peak is under-predicted, the global reactivity balance will force the tail to be over-predicted and TRACG has been shown to adequately predict the global reactivity balance. This has the affect of compensating for the effect that the PIRT18 model has on the key parameter of interest from the kinetics solver in AOO analyses, which is energy. Energy, not power, drives changes in critical power ratio. As one can see from Figures 7 and 8 both codes predict similar energy deposition. Figure 7 shows the energy as a function of time and Figure 8 shows the relative difference in energy as function of time between TRACG and TRAC/NESTLE. The staff has, therefore, determined that although the basis for this model has not been well established, its effect on AOO transient results will be minimal as demonstrated in Reference 9. In this evaluation, the affect of the PIRT18 model on the Δ CPR/ICPR results has been shown to be insignificant. This model will have to be reassessed and better justified should GNF desire to use it for RIA analyses.

Returning to the discussion of Figure 5, the staff results and the TRACG results are in reasonable agreement. Although the TRACG results without the PIRT18 model agree better with the staff results, the results with the PIRT18 model are acceptable when one considers the following:

1. TRACG compares well with the Peach Bottom turbine trip tests. Although these tests were not as limiting as the transient considered in the test problem and the Peach Bottom core used older BWR fuel that was easier to analyze, the results do provide evidence that TRACG adequately simulates pressurization transients; and
2. The TRACG results, when compared to the staff's results, do not differ significantly enough to affect predictions of Δ CPR/ICPR values. This is true because as mentioned earlier critical power is a function of energy deposition, not power.

5.5.5 Summary of Findings

In summary, the staff has reviewed the theoretical development of the TRACG code, the validation presented by GNF, and the information generated during our own analytical assessment of TRACG. The staff finds that the information presented on the theoretical development of the kinetics solver and its associated models is adequate to support the conclusion that these models are correctly derived and account for the important phenomena involved in AOO analyses. The benchmarking presented by GNF, most notably the comparisons to the Peach Bottom turbine trip experiments, demonstrate that for a core loaded with older BWR fuel under conditions similar to those expected during AOO analyses, TRACG adequately predicts the key parameters. In addition, assessments are also presented using plant data from Hatch MSIV closure, Nine Mile Point 2 pump upshift test, and the Leibstadt loss of feedwater event. Thus, a range of fuel generations have been included in the assessment cases. Finally, the independent assessment efforts of the staff focused on evaluating TRACG's ability to predict modern fuel for limiting transients, while not showing exact agreement with diverse methods, provides the staff with enough confidence in TRACG to conclude that it is

acceptable for AOO analyses. Issues discovered with the PIRT18 model do not significantly affect these conclusions because it has been shown that this model does not impact the primary result ($\Delta\text{CPR}/\text{ICPR}$) of AOO analyses. Should GNF wish to apply TRACG to RIA analyses using this PIRT18 model, further justification will need to be provided. Most importantly, GNF will be required to demonstrate how the MCNP code can reliably predict point estimates for BWR lattice k-infinity values.

5.6 Statistical Methodology

In the subject report GENE requests review and approval by the NRC of:

1. The uncertainties documented in Section 5.0.
2. The statistical methodology for analyzing AOOs described in Section 7.0.

This evaluation is limited to these two sections.

The general overall analysis approach in the subject report follows the code, scaling applicability and uncertainty (CSAU) analysis methodology (Reference 3). This methodology consists of 14 steps that are addressed in the TRACG application in the subject report. The first few steps in the CSAU methodology identify and rank the physical phenomena important to judging the performance of the safety systems and margins in the design. The phenomena are compared to the modeling capability of the code to assess whether the code has the necessary models to simulate the phenomena. Most importantly, the range of the identified phenomena covered in experiments is compared to the corresponding range of the intended application to assure that the code has been qualified for the highly ranked phenomena over the appropriate range.

5.6.1 Model Uncertainties and Biases

This section quantifies the overall biases and uncertainties of the individual models associated with each high and medium ranked phenomenon in TRACG. The biases and uncertainties are computed and evaluated by comparing calculated results to: (1) separate effects test facility test data, (2) integral test facility data, (3) component qualification test data, and (4) BWR plant data. The sensitivity of $\Delta\text{CPR}/\text{ICPR}$, the basic figure of merit for AOO transients, to the estimated magnitude of the uncertainty of each phenomenon is quantified for a typical BWR/4 plant for a turbine trip without bypass transient.

For each applicable phenomenon, Table 5-5 of Reference 1 summarizes quantitatively the bias and uncertainty associated with the parameters. For those parameters where there is sufficient and appropriate test data to compare to calculation, a statistical estimate is made of the bias and variance of the distribution. The distributions are tested for normality via the Anderson-Darling statistic and accepted as normal at the 5 percent level. For those phenomena where the descriptive statistics are explicitly shown, all distributions met this acceptance criterion except for some of the TRACG comparisons with respect to jet pump characteristics (Figures 5-19 and 5-21 of Reference 1). This non-normality appears, to some extent, to be most likely due to the relative small sample size with respect to the other phenomena.

For phenomena where data are not available, code comparisons are used to estimate the biases and variances. A parameter of particular importance for BWR AOO analysis and which falls into this category is the void coefficient. In the context of the TRACG three-dimensional transient neutron diffusion equations using one neutron energy group and up to six delayed neutron precursor groups, the nodal reactivity is computed in terms of the infinite multiplication factor, migration area, the fast group removal cross-section and fast group diffusion coefficient. These parameters are correlated to the void coefficient in terms of the moderator density. The infinite multiplication factor's dependence is also related to a history-weighted moderator density and nodal exposure.

The dominant component in the biases and uncertainties in the void coefficient is attributed to the biases and uncertainties in the infinite lattice eigenvalues calculated with the lattice physics code TGBLA. The TGBLA code is used to generate the cross section fits that are evaluated in TRACG. The biases and uncertainties associated with the TGBLA computed infinite multiplication factors are estimated by comparing the TGBLA results to those computed with the continuous energy Monte Carlo code MCNP (Reference 13).

GENE has evaluated the performance of MCNP against a set of critical experiments spanning a range of temperatures and fuel types; in particular Babcock and Wilcox UO₂ experiments. The results indicate that the code performs very well in comparison to the experiments (Reference 14). Thus, the results of the Monte Carlo calculations are taken as the "true" value of k-infinity in estimating bias and uncertainty of the void coefficient.

The bias and uncertainty in the void coefficient are computed based on k-infinity calculations by TGBLA and MCNP. The void coefficient at each lattice - exposure - in-channel void fraction can be computed for both the TGBLA and MCNP generated k-infinity values. The bias at a lattice-exposure-in-channel void point in the TGBLA void coefficient is defined as the difference at that point between the void coefficient computed by TGBLA and MCNP. In the analysis of an AOO, the initial spatial distribution of composition and void fraction are fixed within each node. The value of the bias and the uncertainty at that node are defined as the average of the biases associated with the lattices. The uncertainty is then the root-mean-square deviation of the biases from the mean bias at each exposure - in-channel void point. To implement these in TRACG requires a transformation from in-channel void fraction to relative water density for application to the number densities in the nodal neutronic calculation and the normalization of the TGBLA - MCNP differences in k-effective.

The claim is made that the lattices are a random sample from "literally thousands that are available" (Reference 8). In principle, the sample size is too small to characterize such a large population, unless the variation in the parameters of interest is well represented and/or does not have a large span. The latter appears to be the case, since the GENE 8x8, 9x9 and 10x10 geometric designs are included, and the differences between product lines is less important than the isotopic composition and concentrations as specified by the exposure. Table 5-1 of Reference 1 gives the p-values for the Andersen-Darling statistic and demonstrates the normality at the 5 percent level at each exposure - in-channel void fraction point.

GENE has assessed the sensitivity of $\Delta\text{ICRP}/\text{ICPR}$ to an individual perturbation of each of the phenomena under consideration, and has demonstrated the effect to be small.

5.6.2 Combination of Uncertainties

Estimation of Design Limits

GENE has assessed the different basic methods for combining uncertainties, such as propagation of errors, Monte Carlo sampling methods in conjunction with the response surface technique and the evaluation of one-sided upper tolerance limits based on order statistics, or normal theory where applicable. Due to the limitation of the linearity assumption in the case of the propagation of errors, and the prohibitively large number of TRACG runs in the case of the response surface technique, GENE has chosen the estimation of one-sided upper tolerance intervals based on normal theory, when appropriate, and otherwise on order statistics. It is recognized that, especially in the case of order statistics, this results in more conservative design limits than one would obtain on the average from the other methods.

The methodology for combining the individual biases and uncertainties in the TRACG model and plant parameters in order to generate a probability density function of the code output of primary safety criteria parameters is based on Monte Carlo sampling. That is, the distributions given in Table 5-5 (Reference 1) are sampled at random; and for each sample of parameters an AOO transient is computed with TRACG. The histogram of the code output of primary safety criteria parameters forms the estimate of the probability density function and forms the basis for the design limits.

A histogram of at least 59 TRACG outputs is tested for normality. If normal, the 95/95 upper tolerance quantile value can be computed from normal theory. The interval is interpreted as containing 95 percent of all possible TRACG outcomes for the particular AOO with 95 percent confidence. If the normality test fails at 59 outcomes, the nonparametric method of order statistics is applied. The computation of a 95/95 upper tolerance quantile value in nonparametric statistical theory requires a sample size of at least 59 observations. Operationally the sample is ordered by value, from lowest to highest; and the 59th value becomes the upper 95/95 tolerance limit. The interpretation of the interval is that 95 percent of all possible TRACG outcomes for the particular AOO lie below the 59th outcome with 95 percent confidence. The interval based on normal theory is likely to be much more narrow than the one computed with nonparametric methods.

Determination of Operating Limit Minimum Critical Power Ratio (OLMCPR)

The approach to deriving an OLMCPR is to impose an uncertainty on the models and plant parameters judged of high importance in determining the progression of the transient computed with the TRACG code and based on the variation in the transient due to the uncertainties compute the probability of avoiding the boiling transition.

The general approach to accounting for statistical uncertainty in thermal-hydraulic test data and measurements of the core operating state is to evaluate an MCPR. The safety limit minimum critical power ratio (SLMCPR_{99.9}) is determined so that less than 0.1 percent of the rods in the core are expected to experience boiling transition at this value (i.e., 99.9 percent of the rods in the core are expected to avoid boiling transition if the limiting MCPR is greater than the SLMCPR_{99.9}).

The concept of an OLMCPR is introduced to assure that the safety limit is not exceeded during a transient. In principle, the OLMCPR can be computed for the limiting AOO by running a large number of TRACG transient calculations and randomly varying in each calculation the initial conditions, model parameters and plant parameter based on the distributions established in Section 5.0. These computations can, in principle, generate histograms of rod critical power ratios (CPRs) for a core under transient conditions.

Central to evaluating $SLMCPR_{99.9}$ is the computation of the number of rods subject to boiling transition (NRSBT) which is based on the experimental critical power ratio (ECPR) distribution from data obtained at GENE's ATLAS test facility. Operationally, the probability that some rod "i" operating at $MCPR_i$ is in boiling transition is given by the integral of the ECPR distribution from $MCPR_i$ to $+\infty$. It should be noted that the distribution of the random variable ECPR is based on experimentally measured values, while MCPR is computed at thermal-hydraulic conditions based on TRACG calculations. Strictly speaking, only if ECPR and MCPR have the same distribution can a probability based on an observation of MCPR be computed with the probability density function of ECPR. For the analysis at hand, this discrepancy in the numerical value of the probability that a rod is in boiling transition is likely to be very small. GENE has done extensive sensitivity analysis of $\Delta CPR/ICPR$ to variations in the parameters deemed important and demonstrated very low sensitivity. Furthermore, the standard deviation of these parameters is generally on the order of a few percent, thus indicating that the difference in the distributions is small. In addition, the MCPR values of interest lie in the tail of the normal distribution and the small differences between MCPR and ECPR contribute little to the probability that a rod is in boiling transition.

The expected number of rods subject to boiling transition can be computed by summing the probability that a rod is subject to boiling transition for all the rods in the core. The OLMCPR is then determined from the limiting MCPR value in the core when the NRSBT equals 0.1 percent.

The drawback to the above approach is the large number of TRACG transient calculations required for a sufficiently high confidence in the results. The currently approved approach to determining OLMCPR is divided into two distinct steps. First the $SLMCPR_{99.9}$ is determined. The OLMCPR is then established by adding to $SLMCPR_{99.9}$ the maximum change in MCPR ($\Delta CPR_{95/95}$) expected for the most limiting transient event. The transient uncertainty in ΔCPR for computing $\Delta CPR_{95/95}$ is obtained by Monte Carlo trials combining model uncertainty with uncertainties in the plant parameters such as core power and scram speed.

The proposed approach uses TRACG for computing the thermal-hydraulic conditions during a transient and builds on the currently approved methodology for establishing the OLMCPR. The approach is based on the following computations. For each type of AOO and for each class of BWR plant type and each fuel type the "generic" transient bias and uncertainty in $\Delta CPR/ICPR$ is determined based on TRACG runs using nominal initial conditions, random variations in the models and plant parameters. Since an OLMCPR is to be established for a specific plant/cycle/event, a TRACG transient calculation is performed for such a specific plant/cycle/event starting from nominal initial conditions. This results in a nominal $\Delta CPR/ICPR$ for this specific event. Based on these (i.e., "specific" nominal $\Delta CPR/ICPR$ and a "generic" $\Delta CPR/ICPR$ uncertainty), a MCPR can be computed for each rod in the specific core. As in the previous described methodologies, the value of NRSBT for each rod is computed as an integral from the rod MCPR to infinity over the ECPR probability density distribution. The initial

minimum CPR value corresponds to the OLMCPR when the mean value of NRSBT is equal to 0.1 percent.

5.6.3 Summary of Findings

In the subject report, GNF has documented the quantification of uncertainties as applied to realistic nominal results of TRACG analyses such that less than 0.1 percent of the fuel rods are expected to experience a boiling transition for the most severe AOO. The approach follows the accepted CSAU analysis methodology by which the physical phenomena important to judging the performance of the safety systems and margins in the design are elicited by the Delphi Method. GNF has quantified the uncertainties and biases in models associated with these identified and highly ranked phenomena based on experimental data and computation with validated codes. The process is acceptable and the quantities are reasonable. These together with the computed sensitivity estimates of $\Delta\text{CPR}/\text{ICPR}$ with respect to variation in the model parameters indicate smoothness and stability in the solution to TRACG transient computations within the uncertainties in the models. Moreover, random sampling from the estimated uncertainty distributions in the model parameters is likely to be adequate in light of "the curse of dimensionality."

The objective of estimating the uncertainties associated with the TRACG models is to determine the OLMCPR so as to demonstrate acceptable margins to design limits. The proposed methodology groups the TRACG statistical studies by event/BWR type/fuel type; thereby establishing a generic bias and uncertainty. Subsequently, any, for example, BWR/4 type plant loading GENE14 fuel can utilize the generic bias and uncertainty of the group for a specific transient event. The separation of analysis of the transient behavior under uncertainty into a generic transient bias and uncertainty in $\Delta\text{CPR}/\text{ICPR}$ and a nominal $\Delta\text{CPR}/\text{ICPR}$ for the specific plant/cycle/event under consideration is reasonable and avoids running on the order of 100 TRACG transient calculations for each AOO.

5.7 Code User Experience

The TRACG code uses an input deck which closely emulates the input deck of the original TRAC base code it grew out of. Therefore, a knowledgeable user of TRAC can readily understand the structure and design of the TRACG input decks. An appendix to the model description document facilitates the transfer between codes by outlining the major changes between the TRAC-BF1 and TRACG codes. The user's manual for TRACG contains less guidance than the original TRAC base code user's manual. Significant changes to the input deck design are in the areas where GENE has expanded or refined the original code to more easily model BWR systems or components or to include proprietary modeling in the code.

TRACG maintains the execution structure for control blocks of the original TRAC code. This structure will only allow the execution of the control blocks in the numerical order they are entered into the code. This limitation requires the renumbering of control blocks if additional control blocks are needed after the original deck is created. Renumbering the control blocks and changing the associated variables in the blocks can be a source of user error. Additionally, this limitation can introduce difficulty if a feedback loop exists in the control system. To reduce the impact of this limitation, a small time step size must be used. While the user manual gives some general guidance on the maximum time step size, it is not very clear on this issue.

Instead, it mentions that the automatic control algorithm will respond to the numerical instability caused by reducing the time step size. Additional guidance on this issue would be very helpful to the user.

In TRACG the user creates an initial input deck which is then run under the steady state option of the code until steady state conditions are achieved. During this steady state calculation procedure, the code will determine the correct flow regimes for the components and use the constitutive relations for these flow regimes. This prevents the user from using options to change the relations. Steady state conditions are determined by the user through inspection of the time rates of change of the thermal and fluid variables. This can be a source of error if the user identifies a state which may not be changing significantly at the time step chosen but is not the actual steady state condition.

GENE has developed standard input for the classes of BWR systems this code will be used to analyze. This standard input was developed after sensitivity studies to ensure that the modeling parameters chosen would not bias the analysis results. These standard input sets will reduce the user introduced error in the code results.

6.0 CONDITIONS AND LIMITATIONS

The following are conditions and limitations on use of the TRACG code for analysis of AOO events.

1. Use of the GEXL14 correlation is acceptable provided that when the NRC approves the critical boiling length correlation uncertainty it is applied in TRACG.
2. Should the applicant want to apply TRACG to stability analyses beyond the limited application discussed in Reference 13, the methodology is to be submitted for staff review for that purpose.
3. TRACG is not acceptable for application to ATWS analyses without specific staff review for that purpose, beyond previously accepted use for bench marking ODYN (Reference 14).
4. The PIRT18 model will have to be reassessed and better justified before TRACG can be applied to RIA analyses. Most importantly, GNF will be required to demonstrate how the MCNP code can reliably predict point estimates for BWR lattice k-infinity values.
5. Should the code be applied to transients requiring a condenser, a separate model will be needed or the ability to adequately model the condenser must be demonstrated.

7.0 CONCLUSIONS

The staff supports the efforts of applicants to integrate codes for analysis of accidents and transients rather than manual transfer of information between the codes. Integrating the thermal-hydraulic, fuel rod performance, and other codes, permits a smoother and more accurate prediction of the performance of the system under accident conditions.

The TRACG code has had the GEXL heat transfer correlation installed. Based on reviews of that correlation, the staff has concluded that it is acceptable provided the NRC approved critical boiling length correlation uncertainty is applied.

The staff has reviewed the theoretical development of the TRACG code, validation presented by GNF, and information generated during our own analytical assessment of TRACG. The staff finds that the information presented on the theoretical development of the kinetics solver and its associated models is adequate to support the conclusion that these models are correctly derived and account for the important phenomena involved in AOO analyses. The bench marking presented by GNF, most notably the comparisons to the Peach Bottom turbine trip experiments, demonstrate that for a core loaded with older BWR fuel under conditions similar to those expected during AOO analyses, TRACG adequately predicts results. Finally, the independent assessment efforts of the staff, which focused on evaluating TRACG's ability to predict fuel behavior for limiting transients, while not showing exact agreement with diverse methods, provides the staff with enough confidence in TRACG to conclude that it is acceptable for AOO analyses. Issues discovered with the so-called PIRT18 model do not significantly affect these conclusions because it has been shown that this model does not impact the primary result ($\Delta\text{CPR}/\text{ICPR}$) of AOO analyses. Should GNF wish to apply TRACG to RIA analyses using this PIRT18 model, further justification will need to be provided. Most important, GNF will need to demonstrate that a Monte Carlo code can reliably predict point answers.

GNF has documented the quantification of uncertainties as applied to realistic nominal results of TRACG analyses such that less than 0.1 percent of the fuel rods are expected to experience a boiling transition for the most severe AOO. The approach follows the accepted CSAU analysis methodology by which the physical phenomena important to judging the performance of the safety systems and margins in the design are elicited by the Delphi Method. GNF has quantified the uncertainties and biases in models associated with these identified and highly ranked phenomena based on experimental data and computation with validated codes. The process is acceptable and the quantities are reasonable. These together with the computed sensitivity estimates of $\Delta\text{CPR}/\text{ICPR}$ with respect to variation in the model parameters indicate smoothness and stability in the solution to TRACG transient computations within the uncertainties in the models.

GENE has developed standard input for the classes of BWR systems this code will be used to analyze. This standard input was developed after sensitivity studies to ensure that the modeling parameters chosen would not bias the analysis results. These standard input sets will reduce the user introduced error in the code results.

8.0 REFERENCES

1. NEDE-32906P, Rev. 0, "TRACG Application for Anticipated Operational Occurrences (AOO) Transient Analyses," January 2000.
2. NEDE-32176P, Rev. 2, "TRACG Model Description," December 1999.
NEDE-32177P, Rev. 2, "TRACG Qualification," January 2000.
NEDC-32956P, Rev. 0, "TRACG02A User's Manual," February 2000.

3. Boyack, B., et al, Quantifying Reactor Safety Margins: Application of Code Scaling, Applicability, and Uncertainty Evaluation Methodology to a Large-Break, Loss-of-Coolant Accident," NUREG/CR-5249, December 1989.
4. Nuclear Regulatory Commission, Office of Nuclear Regulatory Research, Regulatory Guide 1.157, "Best-Estimate Calculations of Emergency Core Cooling System Performance," May 1989.
5. NUREG/CR-3633, "TRAC-BD1/MOD1: An Advanced Best Estimate Program for Boiling Water Reactor Transient Analysis, Volumes 1-4," Idaho National Engineering Laboratory, April 1984.
6. Nuclear Regulatory Commission, Office of Nuclear Regulatory Research, Draft Regulatory Guide, DG-1096, "Transient and Accident Analysis Methods," December 2000.
7. Nuclear Regulatory Commission, Draft Standard Review Plan, Section 15.0.2, "Review of Analytical Computer Codes," December 2000.
8. Letter NRC to GENE, "Request for Additional Information," July 2001.
9. Letter GENE to NRC, "Responses to RAIs," August 2001.
10. Jones, Robert C., (NRC) letter to R. A. Pinelli (Chairman, BWR Owner's Group), "Acceptance for Referencing of Topical Report NEDO-32465, *BWR Owner's Group Reactor Stability Detect and Suppress Solutions Licensing Basis Methodology and Reload Applications (TAC M92882)*," March 4, 1996.
11. Essig, Thomas H., (NRC) letter to J. F. Quirk (GENE), "Safety Evaluation by the Office of Nuclear Reactor Regulation of NEDC-24154P, Supplement 1," November 17, 1998.
12. Duderstadt, J. and Hamilton, L., Nuclear Reactor Analysis, Chapter 6, John Wiley and Sons, 1976.
13. Briemeister, J. G., Ed., "MCNP - A General Monte Carlo Code for Neutron, Photon and Electron Transport, Version 3A/3B/4," LA-7396-M, Los Alamos National Laboratory, 1986/Rev. 1988 and 1991.
14. S. Sitaraman, "MCNP: Light Water Reactor Critical Benchmarks," NEDO-32028, March 1992.

Attachments: Figure 1 through Figure 8

Principal Contributors: R. Landry
A. Uises
Y. Orechwa

Date: October 22, 2001

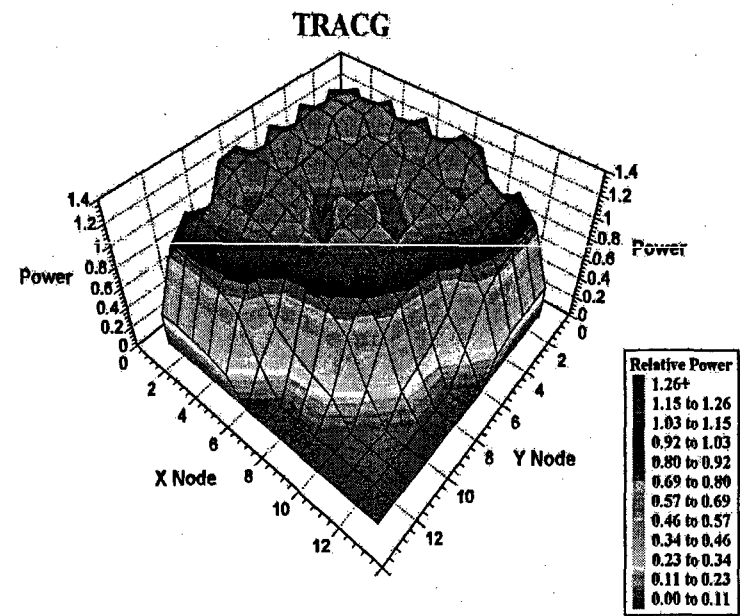
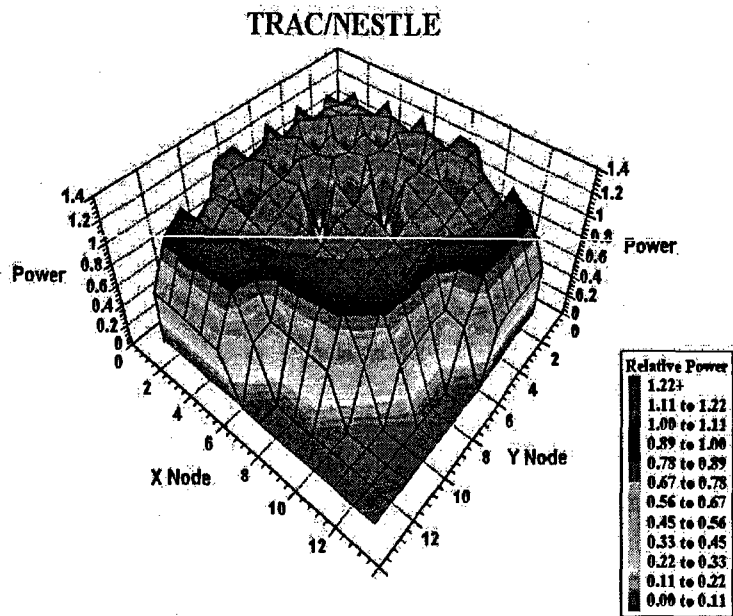


Figure 1 Comparison of Radial Power Distributions for two Methods used in the Analysis

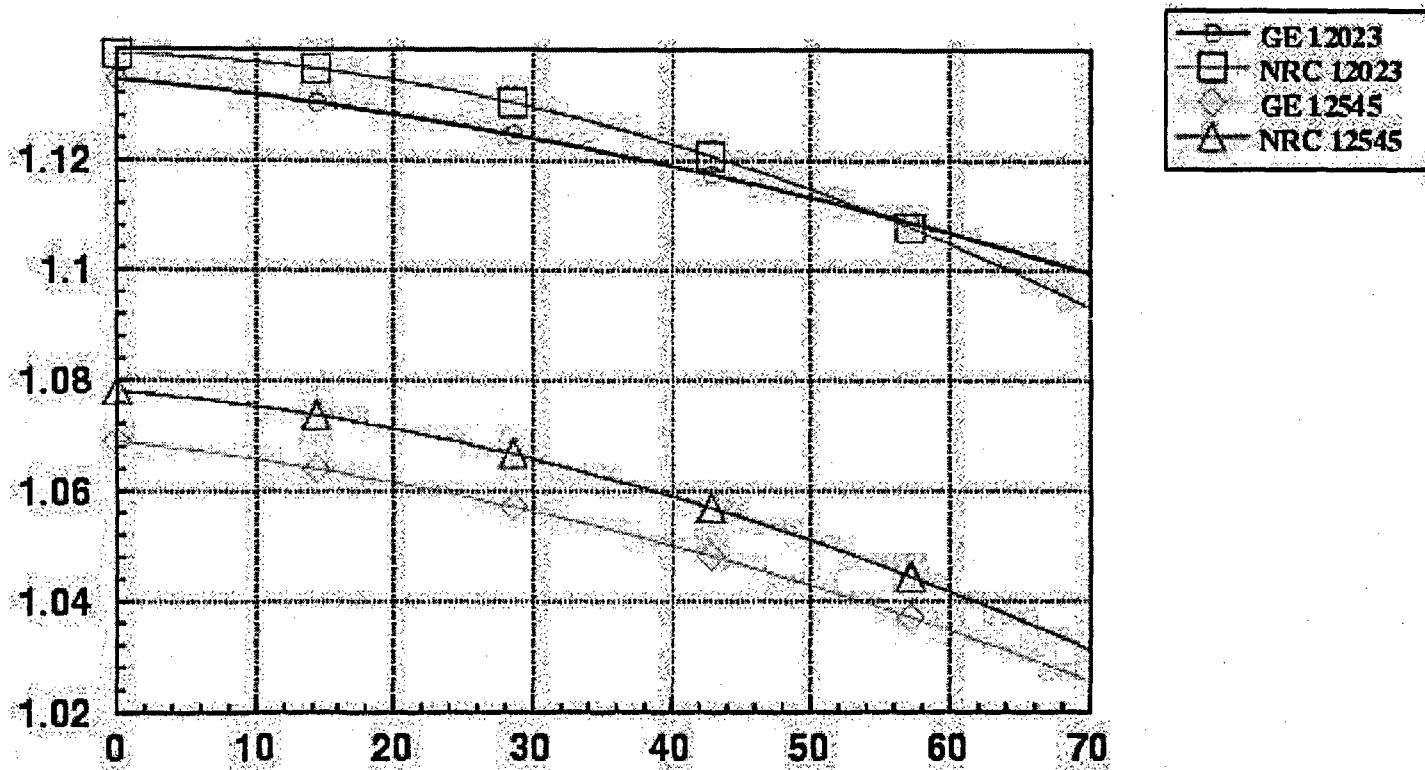


Figure 2 Comparison of Void Reactivity between NRC and GENE Methods for Sample Core

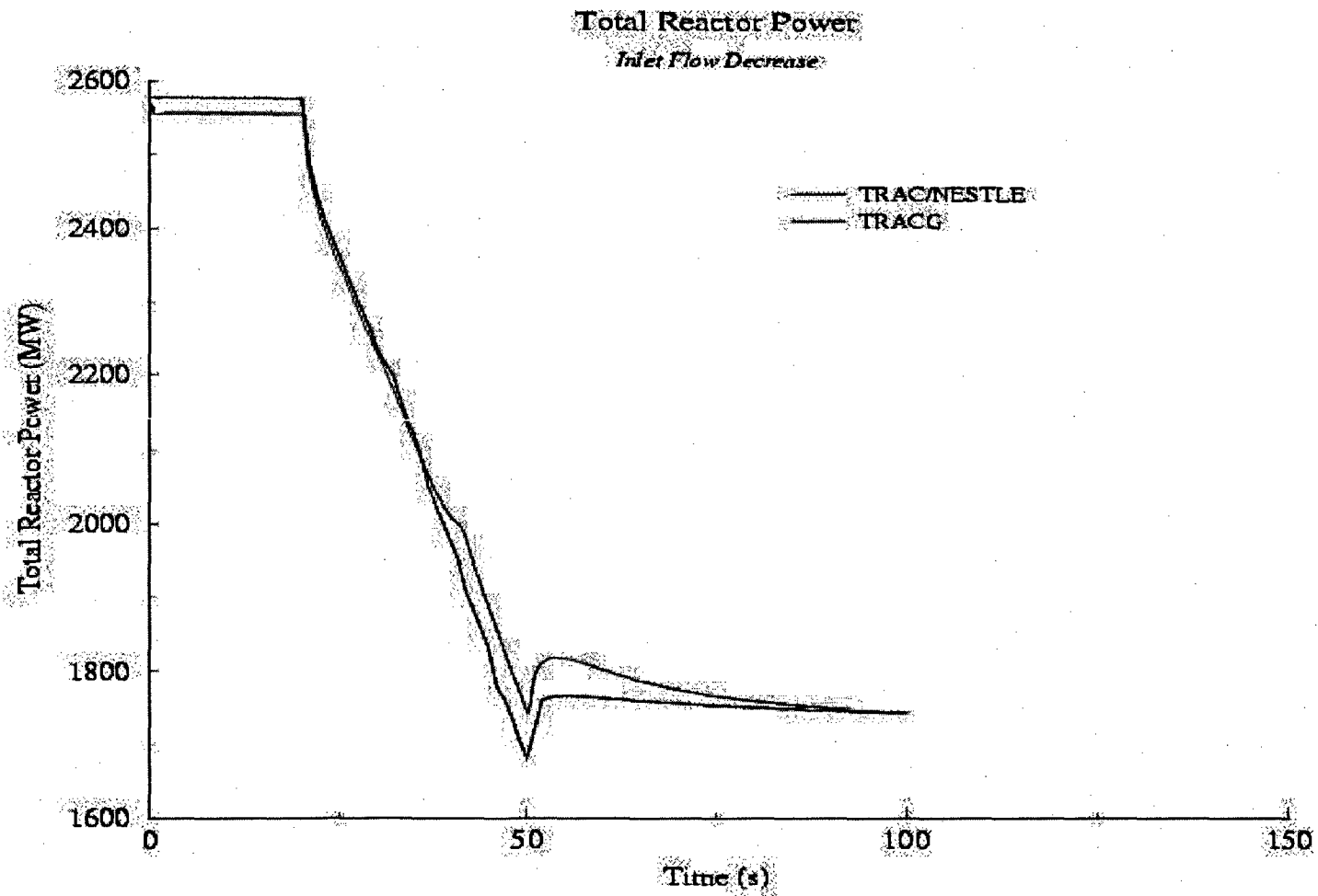


Figure 3 Total Power for a Inlet Flow Ramp

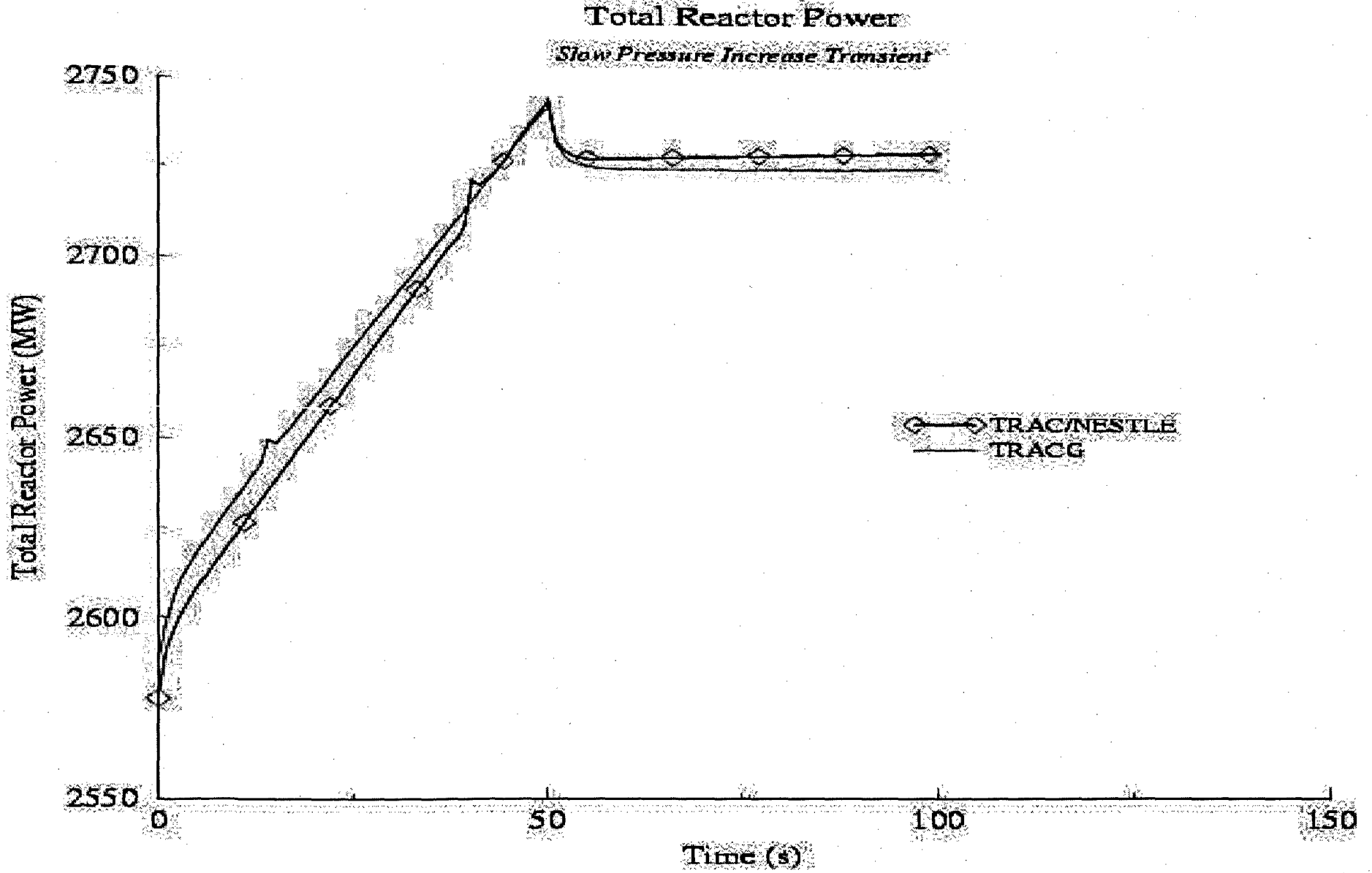


Figure 4 Total Reactor Power for Slow Pressure Increase Transient

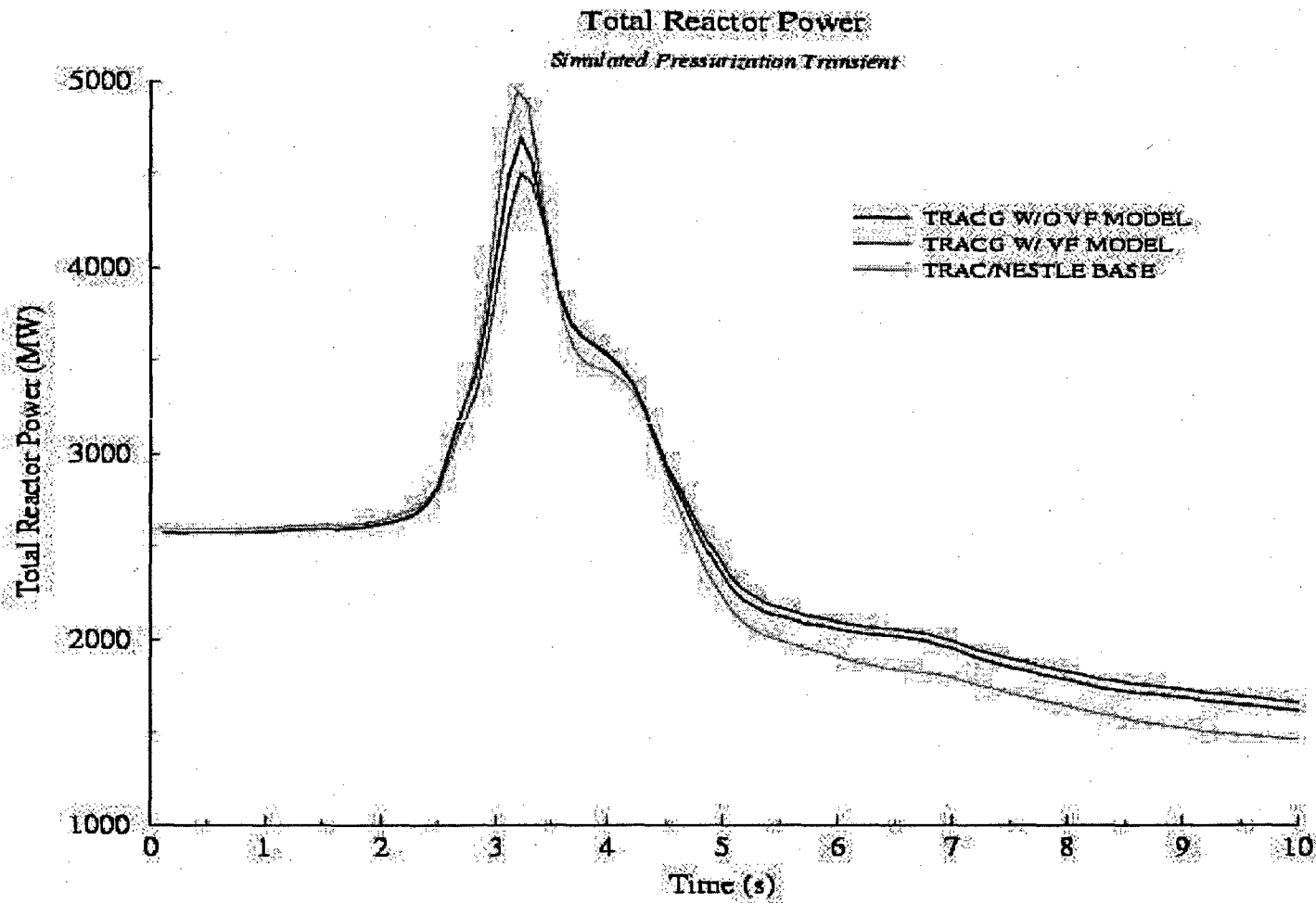


Figure 5 Total Reactor Power for Simulated Pressurization Transient

Void Reactivity Prediction for GNF Lattice

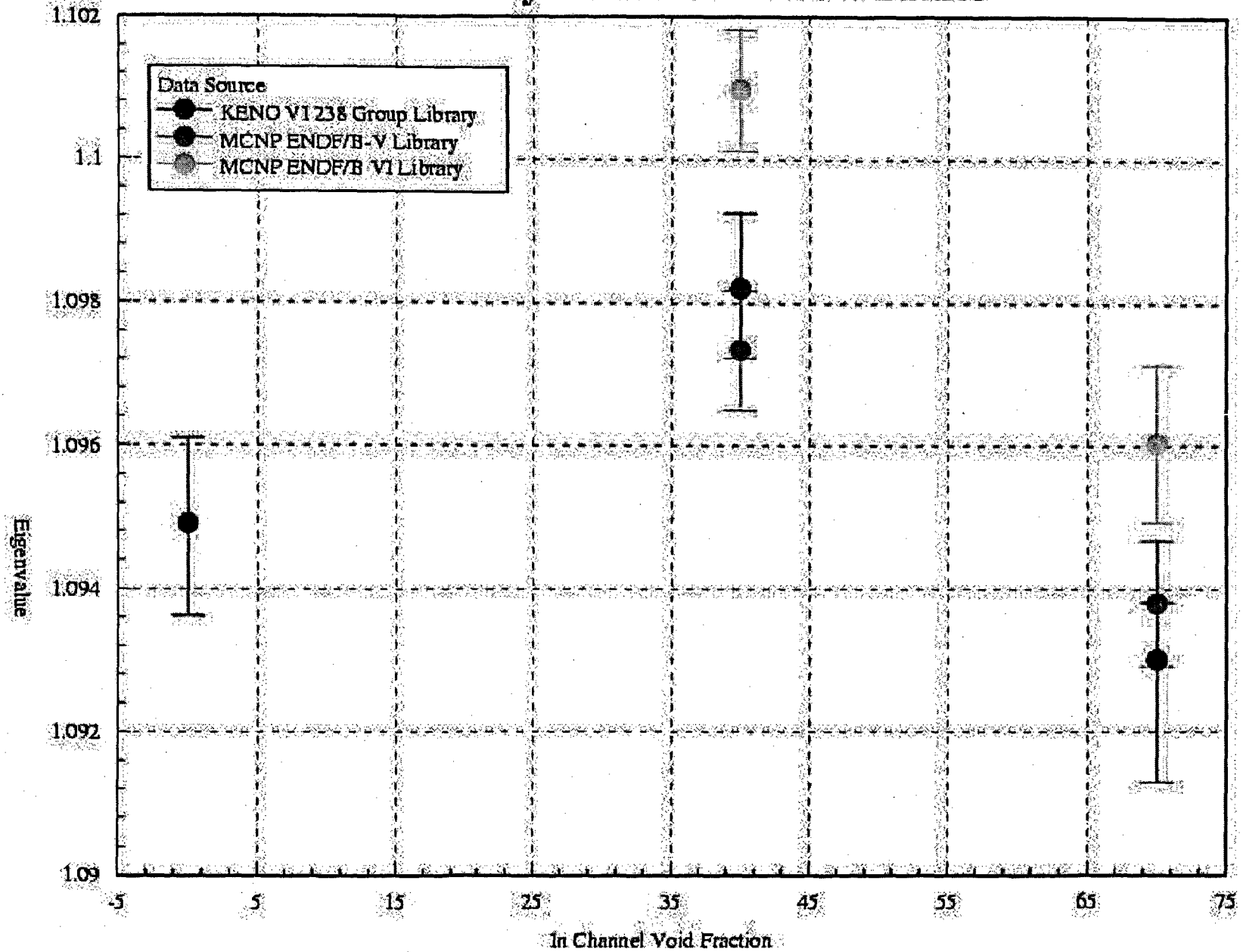


Figure 6 Comparison of Different Monte Carlo Evaluations of the Same GNF Lattice

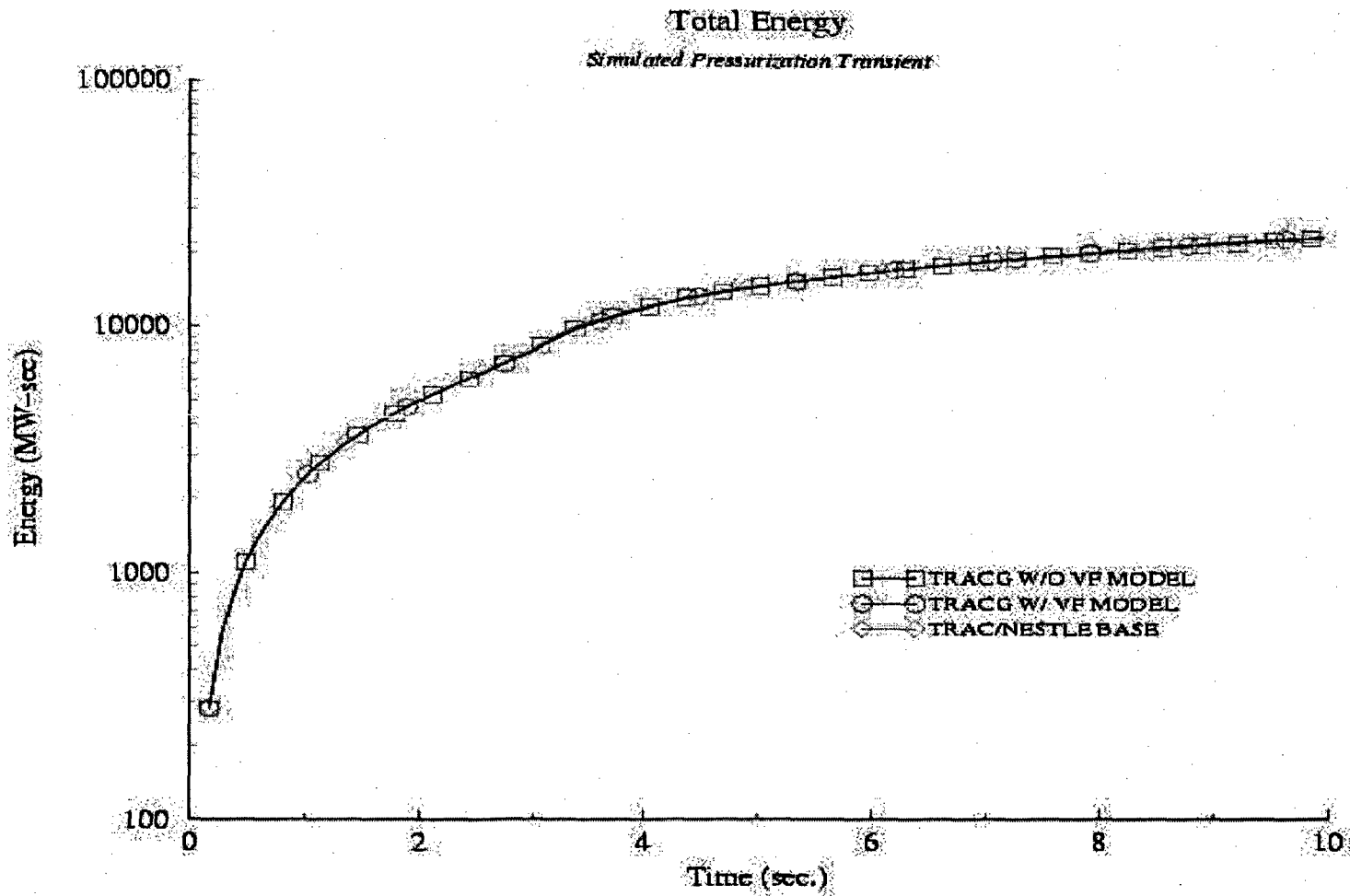


Figure 7 Energy released during simulated MSIV closure event.

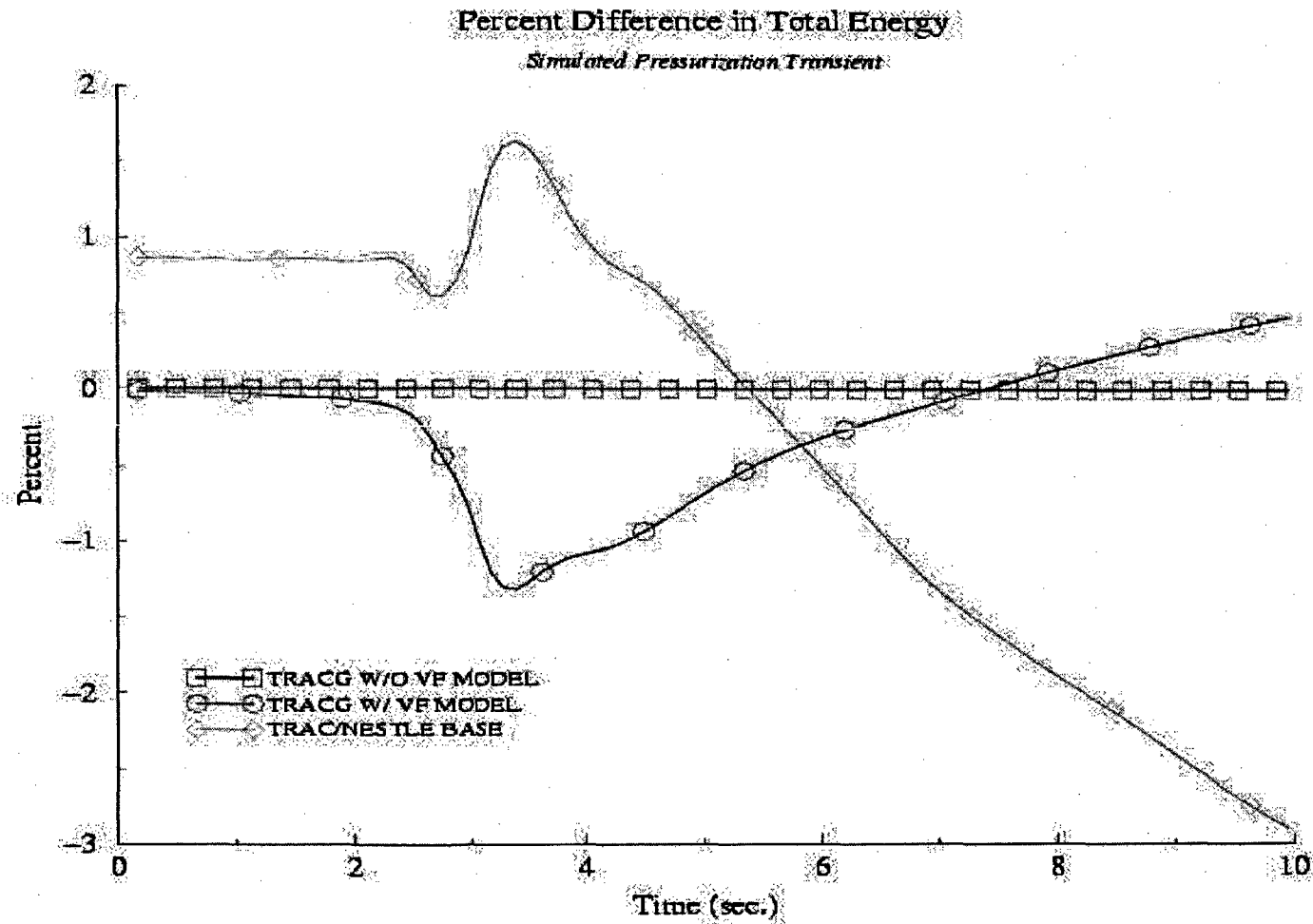


Figure 8 Relative differences between TRACG and TRAC/NESTLE results for MSIV closure simulation.

ACKNOWLEDGMENTS

The TRACG Transient Application is the result of the technical contributions from many individuals. At the General Electric Company (GE), L.A. Klebanov, T. Nakanishi, U. Öberg, and J.C. Shaug, with support from J. Haces (ENUSA), L. Prieto (ENUSA), M. Trueba (ENUSA), have made significant contributions to the development of the TRACG Transient Application. The advice and careful review from J.L. Casillas, Y.K. Cheung, E.C. Eckert, W. Marquino and R.W. Schrum, is highly appreciated. Also, J.M. Healzer has provided valuable counsel.

CONTENTS

		Page
1.0	Introduction	1-1
1.1	Background	1-1
1.2	Summary	1-1
1.3	Scope of Review	1-3
2.0	Licensing Requirements and Scope of Application	2-1
2.1	10CFR50 Appendix A	2-1
2.2	Standard Review Plan Guidelines (NUREG 800)	2-1
2.3	Current Implementations and Practices	2-2
2.4	Proposed Application Methodology	2-3
	2.4.1 Conformance with CSAU Methodology	2-3
	2.4.2 Advantages of TRACG Compared to the Current Process	2-4
2.5	Implementation Requirements	2-5
2.6	Review Requirements For Updates	2-5
	2.6.1 Updates to TRACG Code	2-5
	2.6.2 Updates to TRACG Model Uncertainties	2-5
	2.6.3 Updates to TRACG Statistical Method	2-6
	2.6.4 Updates to Event Specific Uncertainties	2-6
2.7	AOO Scenario Specification	2-6
2.8	Nuclear Power Plant Selection	2-7
3.0	Phenomena Identification, Ranking	3-1
4.0	Applicability of TRACG to AOOs	4-1
4.1	Model Capability	4-1
4.2	Model Assessment Matrix	4-7
5.0	Model Uncertainties and Biases	5-1
5.1	Model Parameters and Uncertainties	5-1
5.2	Effects of Nodalization	5-36
5.3	Effects of Scale	5-36
5.4	Sensitivity Analysis	5-37
6.0	Application Uncertainties and Biases	6-1
6.1	Input	6-1
6.2	Initial Conditions	6-2
6.3	Plant Parameters	6-4

NEDO-32906-A, Revision 1

7.0	Combination of Uncertainties	7-1
7.1	Traditional Bounding Analysis	7-1
7.2	Statistical Treatment of Overall Computational Uncertainty	7-1
7.3	Comparison of Approaches for Combining Uncertainties	7-2
7.3.1	Propagation of Errors	7-3
7.3.2	Response Surface Technique	7-3
7.3.3	Order Statistics Method - Single Bounding Value (GRS)	7-3
7.3.4	Normal Distribution One-Sided Upper Tolerance Limit	7-6
7.4	Recommended Approach for Combining Uncertainties	7-6
7.5	Implementation of Statistical Methodology	7-9
7.5.1	Conformance with Design Limits	7-9
7.5.2	Determination of OLMCPR	7-10
7.6	Statistical Analysis for Qualification Events	7-25
7.6.1	Peach Bottom Turbine Trip Test Statistical Analysis	7-25
7.6.2	Nine Mile Point-2 Pump Upshift Statistical Analysis	7-28
7.6.3	Leibstadt Loss of Feedwater Statistical Analysis	7-30
8.0	Demonstration Analysis	8-1
8.1	Baseline Analysis	8-1
8.1.1	Baseline Analysis of Pressurization Transients	8-4
8.1.2	Baseline Analysis of Depressurization Transients	8-13
8.1.3	Baseline Analysis of Core Flow Transients	8-16
8.1.4	Baseline Analysis of Cold Water Transients	8-22
8.1.5	Baseline Analysis of RPV Level Transients	8-25
8.2	Initial Condition and Plant Parameter Review	8-28
8.2.1	Initial Conditions and Allowable Operating Range	8-28
8.2.2	Initial Conditions Uncertainty	8-41
8.2.3	Plant Parameters	8-48
8.2.4	Summary of Initial Conditions and Plant Parameter	8-49
8.3	Fuel Rod Thermal-Mechanical Performance	8-50
8.4	Statistical Analysis for Licensing Events	8-51
8.4.1	Uncertainty Screening	8-52
8.4.2	Statistical Results	8-60
9.0	Technical Specification Modifications	9-1
10.0	References	10-1
Attachment A	NRC RAIs and Associated Responses	A-1

LIST OF FIGURES

Figure	Page
Figure 5-1. Void Coefficient Normalized %Bias and %Standard Deviation.....	5-4
Figure 5-2. FRIGG OF64 Void Fraction Data.....	5-8
Figure 5-3. FRIGG OF64 Void Fraction Data.....	5-8
Figure 5-4. FRIGG OF64 Void Fraction Data - Fully Developed Nucleate Boiling.....	5-9
Figure 5-5. Test 14, Average Impact of PIRT22.....	5-10
Figure 5-6. Test 03, Average Impact of PIRT22.....	5-10
Figure 5-7. FRIGG OF64 Void Fraction Data - Subcooled Boiling.....	5-11
Figure 5-8. Void Fraction Sensitivity to PIRT23.....	5-12
Figure 5-9. Sensitivity of Fuel Center to Fluid Temperature Difference for 8x8 Fuel.....	5-13
Figure 5-10. Sensitivity of Fuel Center to Fluid Temperature Difference for 9x9 Fuel.....	5-14
Figure 5-11. Uncertainty in Normalized Total DMH.....	5-15
Figure 5-12. Normalized In-Channel Direct Moderator Heating.....	5-15
Figure 5-13. Normalized Direct Moderator Heating in Bypass and Water Rods.....	5-16
Figure 5-14. Normality Test for the Total DMH Residual Errors.....	5-17
Figure 5-15. All CCFL Data - Relative Error.....	5-18
Figure 5-16. TRACG Comparison to 1/6 Scale Jet Pump.....	5-25
Figure 5-17. Statistics for TRACG Comparison to 1/6 Scale Jet Pump.....	5-25
Figure 5-18. TRACG Comparison to Full-Scale One Nozzle Jet Pump.....	5-26
Figure 5-19. Statistics for TRACG Comparison to Full-Scale One-Nozzle Jet Pump.....	5-26
Figure 5-20. TRACG Comparison to Full-Scale Five-Nozzle Jet Pump.....	5-27
Figure 5-21. Statistics for TRACG Comparison to Full-Scale Five-Nozzle Jet Pump.....	5-27
Figure 5-22. Jet Pump Sensitivity to Inlet Loss for One-Nozzle Jet Pump.....	5-28
Figure 5-23. Jet Pump Sensitivity to Inlet Loss for Five-Nozzle Jet Pump.....	5-28
Figure 5-24. TRACG Comparison to 1/6 Scale Jet Pump for Reverse Drive Flow.....	5-29
Figure 5-25. Statistics for TRACG Comparison to 1/6 Scale Jet Pump for Reverse Drive Flow.....	5-30
Figure 5-26. Jet Pump Sensitivity to Nozzle Loss for 1/6 Scale Jet Pump.....	5-30
Figure 5-27. Error in Prediction of Carry Under for 2-Stage Separator.....	5-31
Figure 7-1. Schematic Process for Combining Uncertainties.....	7-5
Figure 7-2. NRSBT Determination with Ideal Process.....	7-12
Figure 7-3. GETAB SLMCPR NRSBT Determination.....	7-14

Figure 7-4. OLMCPR Method with 95/95 Δ CPR.....	7-14
Figure 7-5. GESAM Calculation Procedure for Analytical Determination of SLMCPR.....	7-15
Figure 7-6. Generic Δ CPR/ICPR Uncertainty Development.....	7-17
Figure 7-7. NRSBT Determination with Proposed Process.....	7-17
Figure 7-8. GESAM Calculation Procedure for Analytical Determination of OLMCPR.....	7-19
Figure 7-9. Comparison of GESAM/TRACG Transient MCPR to TRACG MCPR.....	7-22
Figure 7-10. Transformation of GESAM ICPR Distribution to Transient MCPR.....	7-23
Figure 7-11. PB TT Test 1 Statistical Peak Power Response.....	7-25
Figure 7-12. PB TT Test 1 Statistical Dome Pressure Response.....	7-26
Figure 7-13. PB TT Test 2 Statistical Peak Power Response.....	7-26
Figure 7-14. PB TT Test 2 Statistical Dome Pressure Response.....	7-27
Figure 7-15. PB TT Test 3 Statistical Peak Power Response.....	7-27
Figure 7-16. PB TT Test 3 Statistical Dome Pressure Response.....	7-28
Figure 7-17. NMP-2 Pump Upshift Statistical Peak Power Response.....	7-29
Figure 7-18. NMP-2 Pump Upshift Statistical Core Flow Response.....	7-29
Figure 7-19. Leibstadt Loss of Feedwater Statistical Wide Range Level Response.....	7-30
Figure 8-1. TRACG BWR/4 Vessel Modeling.....	8-2
Figure 8-2. TRACG Core Map and Channel Grouping.....	8-3
Figure 8-3. TRACG Power and Flow Response for TTNB Event.....	8-4
Figure 8-4. TRACG CPR Response for TTNB Event.....	8-5
Figure 8-5. TRACG Pressure and Relief Valve Response for TTNB Event.....	8-5
Figure 8-6. TRACG Vessel Inlet and Exit Flow for TTNB Event.....	8-6
Figure 8-7. TRACG Power and Flow Response for FWCF Event.....	8-7
Figure 8-8. TRACG CPR Response for FWCF Event.....	8-8
Figure 8-9. TRACG Pressure and Relief Valve Response for FWCF Event.....	8-8
Figure 8-10. TRACG Vessel Inlet and Exit Flow for FWCF Event.....	8-9
Figure 8-11. TRACG Power and Flow Response for MSIVF Event.....	8-10
Figure 8-12. TRACG Pressure and Relief Valve Response for MSIVF Event.....	8-11
Figure 8-13. TRACG Vessel Inlet and Exit Flow for MSIVF Event.....	8-11
Figure 8-14. TRACG Power and Flow Response for PRFO Event.....	8-13
Figure 8-15. TRACG CPR Response PRFO Event.....	8-14
Figure 8-16. TRACG Pressure and Bypass Valve Response for PRFO Event.....	8-14
Figure 8-17. TRACG Vessel Inlet and Exit Flow for PRFO Event.....	8-15
Figure 8-18. TRACG Power and Flow Response for 2PTR Event.....	8-16

Figure 8-19. TRACG CPR Response 2PTR Event	8-17
Figure 8-20. TRACG Pressure Response for 2PTR Event	8-17
Figure 8-21. TRACG Vessel Inlet and Exit Flow for 2PTR Event.....	8-18
Figure 8-22. TRACG Power and Flow Response for RFCF Event	8-19
Figure 8-23. TRACG CPR Response for RFCF Event.....	8-20
Figure 8-24. TRACG Recirculation Response for RFCF Event.....	8-20
Figure 8-25. TRACG Vessel Inlet and Exit Flow for RFCF Event.....	8-21
Figure 8-26. TRACG Power and Flow Response for LFWH Event.....	8-22
Figure 8-27. TRACG CPR Response LFWH Event.....	8-23
Figure 8-28. TRACG Pressure and Feed Temperature Response for LFWH Event	8-23
Figure 8-29. TRACG Vessel Inlet and Exit Flow for LFWH Event.....	8-24
Figure 8-30. TRACG Power and Flow Response for LOFW Event.....	8-25
Figure 8-31. TRACG Downcomer Water Level Response for LOFW Event	8-26
Figure 8-32. TRACG Pressure Response for LOFW Event	8-26
Figure 8-33. TRACG Vessel Inlet and Exit Flow for LOFW Event.....	8-27
Figure 8-34. Typical Power/Flow Map	8-30
Figure 8-35. EOC Axial Power Shape	8-30
Figure 8-36. MOC Nominal Rod Pattern.....	8-31
Figure 8-37. MOC Black and White Rod Pattern.....	8-31
Figure 8-38. EOC High Worth Scram Rods	8-31
Figure 8-39. TTNB Sensitivity to Individual Uncertainties.....	8-52
Figure 8-40. Void Fraction Response Comparing Base to - 1 σ Interfacial Shear	8-53
Figure 8-41. FWCF Sensitivity to Individual Uncertainties	8-54
Figure 8-42. MSIVF Sensitivity to Individual Uncertainties.....	8-55
Figure 8-43. RFCF Sensitivity to Individual Uncertainties	8-56
Figure 8-44. Rod Heat Flux Response Comparing Base to +1 σ Fuel Heat Transfer	8-57
Figure 8-45. LFWH Sensitivity to Individual Uncertainties.....	8-58
Figure 8-46. LOFW Sensitivity to Individual Uncertainties.....	8-59
Figure 8-47. Channel 29 Δ CPR/ICPR Normality for TTNB	8-60
Figure 8-48. Channel 29 Δ CPR/ICPR Descriptive Statistics for TTNB	8-61
Figure 8-49. Channel 29 % Δ CPR/ICPR Descriptive Statistics for TTNB	8-61
Figure 8-50. Channel 27 % Δ CPR/ICPR Descriptive Statistics for TTNB	8-62
Figure 8-51. Channel 29 Δ CPR/ICPR Normality for FWCF.....	8-63
Figure 8-52. Channel 29 Δ CPR/ICPR Descriptive Statistics for FWCF	8-64

Figure 8-53. Channel 29 % Δ CPR/ICPR Descriptive Statistics for FWCF..... 8-64

Figure 8-54. Channel 27 % Δ CPR/ICPR Descriptive Statistics for FWCF..... 8-65

Figure 8-55. Peak Pressure Normality for MSIVF 8-66

Figure 8-56. Peak Pressure Descriptive Statistics for MSIVF..... 8-67

Figure 8-57. Δ Peak Pressure Descriptive Statistics for MSIVF 8-67

Figure 8-58. Channel 29 Δ CPR/ICPR Normality for RFCF..... 8-68

Figure 8-59. Channel 29 Δ CPR/ICPR Descriptive Statistics for RFCF 8-69

Figure 8-60. Channel 29 % Δ CPR/ICPR Descriptive Statistics for RFCF 8-69

Figure 8-61. Channel 27 % Δ CPR/ICPR Descriptive Statistics for RFCF 8-70

Figure 8-62. Channel 29 Δ CPR/ICPR Normality for LFWH..... 8-71

Figure 8-63. Channel 29 Δ CPR/ICPR Descriptive Statistics for LFWH..... 8-72

Figure 8-64. Channel 29 % Δ CPR/ICPR Descriptive Statistics for LFWH 8-72

Figure 8-65. Channel 27 % Δ CPR/ICPR Descriptive Statistics for LFWH 8-73

Figure 8-66. Minimum Wide Range Level Normality for LOFW 8-74

Figure 8-67. Minimum Wide Range Level Descriptive Statistics for LOFW 8-75

Figure 8-68. % Change in Minimum Wide Range Level Descriptive Statistics for LOFW 8-75

Figure 9-1. BOC to EOC High Worth Scram Rods..... 9-1

LIST OF TABLES

Table	Page
Table 2-1 CODE SCALING, APPLICABILITY AND UNCERTAINTY EVALUATION METHODOLOGY	2-4
Table 3-1 PHENOMENA THAT GOVERN BWR/2-6 AOO TRANSIENT	3-3
Table 4-1 BWR PHENOMENA AND TRACG MODEL CAPABILITY MATRIX	4-2
Table 4-2 QUALIFICATION ASSESSMENT MATRIX FOR BWR/2-6 AOO TRANSIENT PHENOMENA	4-8
Table 5-1 NORMALITY TEST P-VALUES FOR THE VOID COEFFICIENT RESIDUAL ERRORS	5-6
Table 5-2 BIAS AND UNCERTAINTY FOR 9x9 AND 10x10 SEO AND LTPs	5-21
Table 5-3 BIAS AND UNCERTAINTY FOR 9x9 AND 10x10 SPACERS	5-21
Table 5-4 BIAS AND UNCERTAINTY FOR 9x9 AND 10x10 UPPER TIE PLATES	5-22
Table 5-5 HIGH AND MEDIUM RANKED MODEL PARAMETERS	5-35
Table 6-1 KEY PLANT INITIAL CONDITIONS	6-3
Table 6-2 ANALYTICAL SCRAM SPEEDS	6-5
Table 7-1 METHODS FOR COMBINED UNCERTAINTY	7-2
Table 7-2 COMPARISONS OF METHODS FOR COMBINING UNCERTAINTIES	7-8
Table 7-3 IMPACT OF CRITICAL ICPR UNCERTAINTIES ON Δ CPR/ICPR	7-20
Table 8-1 TTNB KEY TRANSIENT PARAMETERS	8-6
Table 8-2 FWCF KEY TRANSIENT PARAMETERS	8-9
Table 8-3 MSIVF KEY TRANSIENT PARAMETERS	8-12
Table 8-4 PRFO KEY TRANSIENT PARAMETERS	8-15
Table 8-5 2PTR KEY TRANSIENT PARAMETERS	8-18
Table 8-6 RFCF KEY TRANSIENT PARAMETERS	8-21
Table 8-7 LFWH KEY TRANSIENT PARAMETERS	8-24
Table 8-8 LOFW KEY TRANSIENT PARAMETERS	8-27
Table 8-9 ALLOWABLE OPERATING RANGE CHARACTERIZATION BASIS	8-29
Table 8-10 TTNB ALLOWABLE OPERATING RANGE RESULTS	8-32
Table 8-11 TTNB ALLOWABLE OPERATING RANGE CHARACTERIZATIONS	8-33
Table 8-12 FWCF ALLOWABLE OPERATING RANGE RESULTS	8-34
Table 8-13 FWCF ALLOWABLE OPERATING RANGE CHARACTERIZATIONS	8-34
Table 8-14 MSIVF ALLOWABLE OPERATING RANGE RESULTS	8-35

Table 8-15 MSIVF ALLOWABLE OPERATING RANGE CHARACTERIZATIONS 8-35

Table 8-16 PRFO ALLOWABLE OPERATING RANGE RESULTS 8-36

Table 8-17 2PTR ALLOWABLE OPERATING RANGE RESULTS 8-36

Table 8-18 RFCF ALLOWABLE OPERATING RANGE RESULTS 8-37

Table 8-19 RFCF ALLOWABLE OPERATING RANGE CHARACTERIZATIONS 8-38

Table 8-20 LFWH ALLOWABLE OPERATING RANGE RESULTS 8-39

Table 8-21 LFWH ALLOWABLE OPERATING RANGE CHARACTERIZATIONS 8-39

Table 8-22 LOFW ALLOWABLE OPERATING RANGE RESULTS 8-40

Table 8-23 LOFW ALLOWABLE OPERATING RANGE CHARACTERIZATIONS 8-40

Table 8-24 INITIAL CONDITION UNCERTAINTY CHARACTERIZATIONS 8-41

Table 8-25 TTNB INITIAL CONDITION UNCERTAINTY RESULTS 8-42

Table 8-26 TTNB INITIAL CONDITION UNCERTAINTY CHARACTERIZATIONS 8-42

Table 8-27 FWCF INITIAL CONDITION UNCERTAINTY RESULTS 8-43

Table 8-28 FWCF INITIAL CONDITION UNCERTAINTY CHARACTERIZATIONS 8-43

Table 8-29 MSIVF INITIAL CONDITION UNCERTAINTY RESULTS 8-44

Table 8-30 MSIVF INITIAL CONDITION UNCERTAINTY CHARACTERIZATIONS 8-44

Table 8-31 PRFO INITIAL CONDITION UNCERTAINTY RESULTS 8-45

Table 8-32 2PTR INITIAL CONDITION UNCERTAINTY RESULTS 8-45

Table 8-33 RFCF INITIAL CONDITION UNCERTAINTY RESULTS 8-45

Table 8-34 RFCF INITIAL CONDITION UNCERTAINTY CHARACTERIZATIONS 8-46

Table 8-35 LFWH INITIAL CONDITION UNCERTAINTY RESULTS 8-46

Table 8-36 LFWH INITIAL CONDITION UNCERTAINTY CHARACTERIZATIONS 8-47

Table 8-37 LOFW INITIAL CONDITION UNCERTAINTY RESULTS 8-47

Table 8-38 LOFW INITIAL CONDITION UNCERTAINTY CHARACTERIZATIONS 8-48

Table 8-39 SCRAM SPEED UNCERTAINTY RESULTS 8-48

Table 8-40 TTNB FUEL THERMAL-MECHANICAL RESULTS 8-51

ABSTRACT

This report discusses the application of TRACG, the General Electric (GE) proprietary version of the Transient Reactor Analysis Code, to analyses of Anticipated Operational Occurrences (AOOs) for boiling water reactors. Realistic calculations with TRACG can be used together with statistical quantification of uncertainties to support licensing evaluations for these transient events.

1.0 INTRODUCTION

1.1 Background

TRACG is a General Electric (GE) proprietary version of the Transient Reactor Analysis Code (TRAC). TRACG uses advanced realistic one-dimensional and three-dimensional methods to model the phenomena that are important in evaluating the operation of BWRs. Realistic analyses performed with TRACG have been used previously to support licensing applications in different areas, including transients otherwise known as an Anticipated Operational Occurrence (AOO). GE currently performs licensing calculations for transient events using other NRC-approved computer codes and methods [15, 29].

TRAC was originally developed for pressurized water reactor (PWR) analysis by Los Alamos National Laboratory, the first PWR version of TRAC being TRAC-P1A [3]. The development of the BWR version of TRAC started in 1979 in close cooperation between GE and Idaho National Engineering Laboratory. The objective of this cooperation was the development of a version of TRAC capable of simulating BWR LOCAs. The main tasks consisted of improving the basic models in TRAC for BWR applications and in developing models for specific BWR phenomena and components. This work culminated in the middle 1980's with the development of TRACB04 at GE [4 through 11] and TRACG-BD1/MOD1 at INEL [12]. Due to the joint development, these versions were very similar. In the earlier stages, General Electric (GE), the United States Nuclear Regulatory Commission (NRC) and the Electric Power Research Institute (EPRI) jointly funded the development of the code. A detailed description of these earlier versions of TRAC for BWRs is contained in References 12 through 14.

1.2 Summary

This document demonstrates the acceptable use of TRACG analysis results for licensing BWR/2-6 power plants within the applicable licensing bases. GE has provided information to support *the use of TRACG as an alternative to previously approved methods of analyzing BWR AOOs and demonstrating compliance with licensing limits*. AOO events are analyzed to establish the reactor

system response, including the calculation of the Operating Limit Minimum Critical Power Ratio (OLMCPR). This application specifically addresses TRACG capabilities to ensure that acceptable fuel design limits and reactor coolant pressure boundary design conditions are not exceeded during an AOO. This application report demonstrates that TRACG analyses can be used as an alternate AOO analysis process for licensing calculations. This document describes the quantification of uncertainties as applied to the realistic nominal results of TRACG analyses such that less than 0.1% of the fuel rods are expected to experience a boiling transition for the most severe AOO.

The transient analysis of these events statistically accounts for the uncertainties and biases in the models and plant parameters using a Monte Carlo method. The uncertainties and biases considered include the following:

Some of these uncertainties are plant, fuel type, and event dependent. Therefore, periodic changes in the statistical analysis will be required as these factors change. Demonstration of the statistical analysis and criteria to be used to change this analysis is provided in this report.

The overall analysis approach followed is consistent with the Code Scaling Applicability and Uncertainty (CSAU) analysis methodology [22] and Regulatory Guide 1.157 [23]. Conformance with CSAU methodology is demonstrated in the subsequent sections. The sensitivity of each event analyses to the initial input parameters is established in this report. Values for these parameters will be included in the core analyses reports, including the supplement reload licensing submittal for reload cores.

1.3 Scope of Review

NEDE-32176P Rev. 2 TRACG Model Description and NEDE-32177 Rev. 2 TRACG Qualification LTRs are incorporated by reference as part of the review scope.

2.0 LICENSING REQUIREMENTS AND SCOPE OF APPLICATION

2.1 10CFR50 Appendix A

The *General Design Criteria for Nuclear Power Plants* are stipulated in Appendix A to Part 50 of 10CFR. Anticipated Operational Occurrences are classified as transient events of moderate frequency. The Standard Review Plan for events in this classification states that the “acceptance criteria are based on meeting the requirements of the following regulations” and then defines the acceptance criteria “as it relates” to the general design criteria (GDC). NRC approval of licensing methods used for AOO analysis implies that the methods are capable of assessing an AOO transient response “as it relates” to the GDC.

2.2 Standard Review Plan Guidelines (NUREG 800)

The NRC guidelines for review of anticipated operation occurrences (AOOs) are identified in Section 15 of the Standard Review Plan (SRP) [7].

The AOO scenarios (incidents of moderate frequency) that can be analyzed using TRACG are listed with the corresponding SRP section.

Section	Event
15.1.1 - 15.1.4	Decrease in feedwater temperature, increase in feedwater flow, increase in steam flow, and inadvertent opening of a steam generator relief or safety valve.
15.2.1 - 15.2.5	Loss of external load; turbine trip; loss of condenser vacuum; closure of main steam isolation valve (BWR); and steam pressure regulator failure (closed).
15.2.6	Loss of non-emergency AC power to the station auxiliaries.
15.2.7	Loss of normal feedwater flow.
15.3.1 - 15.3.2	Loss of forced reactor coolant flow, including trip of pump motor and flow controller malfunctions.
15.4.4 - 15.4.5	Startup of an inactive loop or recirculation loop at an incorrect temperature, and flow controller malfunction causing an increase in BWR core flow rate.
15.5.1 - 15.5.2	Inadvertent operation of ECCS and chemical and volume control system malfunction that increases reactor coolant inventory.
15.6.1	Inadvertent opening of a PWR pressurizer pressure relief valve or a BWR pressure relief valve.

In addition to the events given above, there are others such as the rod withdrawal errors (Section 15.4.1.3) and fuel misloading errors (Section 15.4.7) that are currently analyzed with the steady-state three-dimensional core simulator PANACEA [27]. Control rod drop accidents (Section 15.4.9) are currently considered using a generic approach that does not require reassessment every fuel cycle. At this time, GE does not intend to change how these events are considered for licensing purposes. GE has used TRACG to perform realistic calculations for control rod drop accidents but this application is not included in the scope of the current submittal.

2.3 Current Implementations and Practices

The following criteria in the *Specified Acceptable Fuel Design Limits* (SAFDLs) have been defined [28] to meet the requirements of GDC 10, 15, 17 and 26:

- Pressure in the reactor coolant and main steam systems should be maintained below 110% of the design values.
- Fuel cladding integrity shall be maintained by ensuring that the minimum CPR (MCPR) remains above the MCPR safety limit based on acceptable correlations.
- An incident of moderate frequency should not generate a more serious plant condition without other faults occurring independently.
- An incident of moderate frequency, in combination with any single active component failure, or single operator error, shall be considered and is an event for which an estimate of the number of potential fuel failures shall be provided for radiological dose calculations.

The licensing basis analysis of AOOs must be performed with an approved model and analysis assumptions. The ODYN code [15] is cited in the SRP [7] as an acceptable model. TRACG has model capabilities that exceed those in ODYN and has been qualified against a wider range of data.

The following are examples of acceptable analysis assumptions:

- The reactor is initially at 102% of the rated (licensed) core thermal power (to account for a 2% power measurement uncertainty), and the primary flow is at the nominal design flow less the flow measurement uncertainty. (This assumption is not applied for scenarios where it will yield non-conservative results.)
- Conservative scram characteristics are assumed (i.e., maximum time delay and a 0.8 multiplier on the predicted reactivity insertion rate).
- The core burnup is selected to yield the most limiting combination of moderator temperature coefficient, void coefficient, Doppler coefficient, axial power profile, and radial power distribution.
- Subsequently, the NRC has approved the use of a procedure (Option B) for a statistical determination of the normalized CPR change, delta CPR divided by initial CPR ($\Delta\text{CPR}/\text{ICPR}$) for pressurization transients, such that there is a 95% probability with a 95% confidence (95/95) that the event will not cause the critical power ratio to fall below the MCPR Safety

Limit [30]. Utilities using Option B must demonstrate that their plant's scram speed probability distribution is consistent with that used in the statistical analysis. This is accomplished through an approved technical specification, which consists of testing at the 5% significance level and allows adjustment of the Operating Limit MCPR (OLMCPR) if the scram speed is outside the assumed distribution. The use of realistic analysis codes, in conjunction with a statistical basis for accounting for uncertainties in its application, is consistent with currently approved practice.

2.4 Proposed Application Methodology

The methodology for this application of TRACG to BWR/2-6 AOs retains the essential statistical basis approved by the NRC for ODYN and addresses all the elements of the NRC-developed Code Scaling, Applicability and Uncertainty (CSAU) evaluation methodology [22].

This report demonstrates application of a nominal calculation with TRACG, with the calculation of appropriate uncertainties and validation by comparison to plant test data. Using the results from the realistic model and nominal values for plant parameters, the uncertainty is determined by perturbing major model and plant parameters to calculate the one-sided upper tolerance limit for critical safety parameters. Confirmation is shown by comparison to full-scale plant data from tests. TRACG has been qualified against a wider range of data than the approved ODYN methodology.

2.4.1 Conformance with CSAU Methodology

The proposed application methodology using TRACG for BWR AOO transient analyses addresses all the elements of the NRC-developed CSAU evaluation methodology [22]. The CSAU report describes a rigorous process for evaluating the total model and plant parameter uncertainty for a nuclear power plant calculation. The rigorous process for applying realistic codes and quantifying the overall model and plant parameter uncertainties appears to represent the best available practice. While the CSAU methodology was developed for application to loss-of-coolant accidents (LOCAs), there are no technical reasons that prevent CSAU methodology from being applied to other event scenarios such as anticipated operational occurrences (AOOs). A statistical process very similar to the CSAU methodology was applied by the NRC in the safety evaluation of the current US ODYN based licensing methodology for AOs [30].

The CSAU methodology as documented in Reference 22 consists of 14 steps, as outlined in Table 2-1, which also shows where these steps are addressed for the current TRACG application.

In the currently approved process, the ODYN model uncertainty was quantified by comparison against the Peach Bottom turbine trip tests, and an estimate based on the propagation of individual model uncertainties was used for confirmation.

In the CSAU process, the reverse is true. The model uncertainty is derived from the propagation of individual model uncertainties through code calculations; experimental comparisons are used as a check on the derived uncertainty. In either case, both techniques of obtaining the total uncertainty are employed.

Table 2-1

CODE SCALING, APPLICABILITY AND UNCERTAINTY EVALUATION METHODOLOGY

CSAU Step	Description	Addressed In
1	Scenario Specification	Section 2.7
2	Nuclear Power Plant Selection	Section 2.8
3	Phenomena Identification and Ranking	Section 3.0
4	Frozen Code Version Selection	Reference [1]
5	Code Documentation	Reference [1]
6	Determination of Code Applicability	Section 4.0 Reference [2]
7	Establishment of Assessment Matrix	Section 4.2
8	Nuclear Power Plant Nodalization Definition	Section 5.2
9	Definition of Code and Experimental Accuracy	Reference [2]
10	Determination of Effect of Scale	Section 5.3
11	Determination of the Effect of Reactor Input Parameters and State	Section 6.0
12	Performance of Nuclear Power Plant Sensitivity Calculations	Section 7.0, 8.0
13	Determination of Combined Bias and Uncertainty	Section 7.0, 8.0
14	Determination of Total Uncertainty	Section 7.0, 8.0

2.4.2 Advantages of TRACG Compared to the Current Process

TRACG has many advantages over the current processes used for AOO transient analyses. These advantages include:

- A single code is used in the analysis of short-term and long-term transient response. TRACG is not only capable of simulating core response, but also of determining the response of individual (including limiting) channels, including transient critical power response. As many as seven codes will be replaced by this single code.

2.5 Implementation Requirements

The implementation of TRACG into actual licensing analysis is contingent on completion of the following implementation requirements:

- Review and approval by the NRC of:
 1. The uncertainties documented in Section 5.0.
 2. The statistical process for analyzing AOOs described in Section 7.0.
- A generic analysis by event, BWR type, and fuel type to determine specific biases and uncertainties to be applied to the specific analysis that will be transmitted to the NRC for information.
- Plant-specific implementation using best-estimate modeling to consider sensitivities due to initial condition and plant parameters, as described in Sections 6.2 and 6.3.

Specific operating limits derived or comparison with acceptance criterion (peak pressure, water level, and fuel thermal/mechanical) will be based on application of the statistical application processes described in Section 7.0.

2.6 Review Requirements For Updates

In order to effectively manage the future viability of TRACG for AOO licensing calculations, GE proposes the following requirements for upgrades to the code to define changes that (1) require NRC review and approval and (2) that will be on a notification basis only.

2.6.1 Updates to TRACG Code

Modifications to the basic models described in Reference 1 may not be used for AOO licensing calculations without NRC review and approval.

Updates to the TRACG nuclear methods to ensure compatibility with the NRC-approved steady-state nuclear methods (e.g., PANAC11) may be used for AOO licensing calculations without NRC review and approval as long as the Δ CPR/ICPR, peak vessel pressure, and minimum water level shows less than 1 sigma deviation difference compared to the method presented in this LTR. A typical AOO in each of the event scenarios will be compared and the results from the comparison will be transmitted for information.

Changes in the numerical methods to improve code convergence may be used in AOO licensing calculations without NRC review and approval.

Features that support effective code input/output may be added without NRC review and approval.

2.6.2 Updates to TRACG Model Uncertainties

New data may become available with which the specific model uncertainties described in Section 5.0 may be reassessed. If the reassessment results in a need to change specific model uncertainty, the

specific model uncertainty may be revised for AOO licensing calculations without NRC review and approval as long as the process for determining the uncertainty is unchanged.

The nuclear uncertainties (void coefficient, Doppler coefficient, and scram coefficient) may be revised without review and approval as long as the process for determining the uncertainty is unchanged. In all cases, changes made to model uncertainties done without review and approval will be transmitted for information.

2.6.3 Updates to TRACG Statistical Method

Revisions to the TRACG statistical method described in Section 7.0 may not be used for AOO licensing calculations without NRC review and approval.

2.6.4 Updates to Event Specific Uncertainties

Event specific Δ CPR/ICPR, peak pressure, and water level biases and uncertainties will be developed for AOO licensing applications based on generic groupings by BWR type and fuel type. These biases and uncertainties do not require NRC review and approval. The generic uncertainties will be transmitted to the NRC for information.

2.7 AOO Scenario Specification

The transient scenarios are those associated with anticipated operational occurrences (AOOs) in BWR/2, BWR/3, BWR/4, BWR/5, and BWR/6 type plants. The following AOO transient events groups are specifically included:

1. Pressurization events, including: turbine trip without bypass, load rejection without bypass, feedwater controller failure increasing flow, downscale failure of pressure regulator, main steam line isolation valve closure without position scram. This grouping includes all events in SRP Section 15.2.1 - 15.2.5 which apply to BWRs. The feedwater controller failure increasing flow is in Section 15.1.1 - 15.1.4 but can also be considered a pressurization transient. The loss of auxiliary power is in SRP Section 15.2.6.
2. Depressurization events, including: upscale failure of pressure regulator, relief valve opening. The upscale failure of pressure regulator is in SRP Section 15.1.1 - 15.1.4. The inadvertent relief valve opening is in Section 15.6.1.
3. Core flow transients, including: pump trips, startup of idle pumps, pump runup or rundown, flow control valve actuations. This grouping includes all events in SRP Section 15.3.1 - 15.3.5 and 15.4.4 - 15.4.5 which apply to BWRs.
4. Cold water events, including: loss of feedwater heating and inadvertent high pressure coolant injection. The loss of feedwater heating (decrease in feedwater temperature) is in SRP Section 15.1.1 - 15.1.4. This grouping includes all events in SRP Section 15.5.1 - 15.5.2 which apply to BWRs.
5. Level transient events such as partial or complete loss of feedwater. This grouping includes all events in SRP Section 15.2.7 that apply to BWRs.

These events are described in plant UFSARs. A detailed description of selected limiting events is described in Section 8.0.

2.8 Nuclear Power Plant Selection

The included plant types are BWR/2s, BWR/3s, BWR/4s, BWR/5s, and BWR/6s. Both jet pump and non-jet pump designs are included. For the jet pump designs, the recirculation flow control systems include motor-generator designs, flow control valve designs, and variable speed pump designs.

Advanced BWRs (ABWRs) and other non-US internal pump designs have been analyzed using TRACG but GE is not requesting review and approval for licensing application to these designs at this time. The Simplified BWR (SBWR) has been previously analyzed using TRACG, but GE is not requesting review and approval for licensing application to the SBWR at this time.

3.0 PHENOMENA IDENTIFICATION, RANKING

The critical safety parameters for AOO transients are minimum critical power ratio (MCPR), fuel thermal-mechanical margins, downcomer water level and peak reactor pressure vessel (RPV) pressure. These are the criteria used to judge the performance of the safety systems and the margins in the design. The values of the critical safety parameters are determined by the governing physical phenomena. To delineate the important physical phenomena, it has become customary to develop phenomena identification and ranking tables (PIRTs). PIRTs are ranked with respect to their impact on the critical safety parameters. For example, the MCPR is determined by the reactor short-term response to transients. The coupled core neutronic and thermal-hydraulic characteristics govern the neutron flux, reactor pressure, core flow and downcomer water level transients

All processes and phenomena that occur during a transient do not equally influence plant behavior. The most cost efficient, yet sufficient, analysis reduces all candidate phenomena to a manageable set by identifying and ranking the phenomena with respect to their influence on the critical safety parameters. The phases of the events and the important components are investigated. The processes and phenomena associated with each component are examined. Cause and effect are differentiated. After the processes and phenomena have been identified, they are ranked with respect to their effect on the critical safety parameters for the event.

The phenomena identification and ranking tables (PIRTs) represent a consensus of GE expert opinions. PIRTs are developed with only the importance of the phenomena in mind and are independent of whether or not the model is capable of handling the phenomena and whether or not the model will show a strong sensitivity to the phenomena. For example, two phenomena may be of high importance yet tend to cancel each other in many AOO transient events so that there is little sensitivity to either phenomenon. Both phenomena are of high importance because the balance between these competing phenomena is important.

Table 3-1 was developed to identify the phenomena that govern BWR/2-6 AOO transient responses. The transient events have been categorized into five distinct groups: (1) pressurization events; (2) depressurization events; (3) core flow increase or decrease events; (4) cold water insertion events; and (5) water level transient events (like loss of feedwater). For each event type, the phenomena are listed and ranked for each major component in the reactor system. The ranking of the phenomena is done on a scale of high importance to low importance or not applicable, as defined by the following categories:

- *High importance (H)*: These phenomena have a significant impact on the primary safety parameters and should be included in the overall uncertainty evaluation. An example of such a parameter would be the *void coefficient* for a pressurization event (C1AX in Table 3-1). The void coefficient determines the amount of reactivity change due to void collapse during the transient.
- *Medium importance (M)*: These phenomena have insignificant impact on the primary safety parameters and may be excluded in the overall uncertainty evaluation. An example of such a parameter would be the *nucleate boiling wall heat transfer* for a depressurization event (C1 in

Table 3-1). The nucleate boiling heat transfer coefficient is so large that it is not the limiting thermal resistance.

- *Low importance (L) or not applicable (N/A)*: These phenomena have no impact on the primary safety parameters and need not be considered in the overall uncertainty evaluation. An example of such phenomenon would be *lower plenum stratification* during a pressurization event (A10 in Table 3-1). The pressurization event happens so quickly that even if there were significant thermal stratification in the lower plenum, it could not impact the critical parameters before the event was over.

The PIRT serves a number of purposes. First, the phenomena are identified and compared to the modeling capability of the code to assess whether the code has the necessary models to simulate the phenomena. Second, the identified phenomena are cross-referenced to the qualification basis to determine what qualification data are available to assess and qualify the code models and to determine whether additional qualification is needed for some phenomena. As part of this assessment, the range of the PIRT phenomena covered in the tests is compared with the corresponding range for the intended application to establish that the code has been qualified for the highly ranked phenomena over the appropriate range.

Finally, uncertainties in the modeling of the highly ranked PIRT phenomena are carefully evaluated, and then combined through a statistical process, to arrive at the total model uncertainty. In this third stage, one may find that some highly ranked phenomena do not contribute significantly to the overall uncertainty even when conservative values for the individual phenomena uncertainties are used. It is at this stage that one can determine how individual uncertainties influence the total uncertainty so that the effort can be focused on establishing the uncertainties for those phenomena that have the greatest impact on the critical safety parameters. These uncertainties will be more fully developed later in this report and their impact on the critical safety parameters will be quantified for each of the transient scenarios.

[Redacted]										

		Phenomena							Ranking
		1	2	3	4	5	6	7	
[Redacted]									
[Redacted]									
[Redacted]									
[Redacted]									

No.	Phenomenon	1	2	3	4	5	6	7	8	Remarks

4.0 APPLICABILITY OF TRACG TO AOOs

The objective of this section is to demonstrate the applicability of TRACG for the analysis of anticipated transient events in BWRs. To accomplish this purpose, the capability of the TRACG models to treat the highly ranked phenomena and the qualification assessment of the TRACG code for AOO applications is examined in the next two subsections.

4.1 Model Capability

The capability to calculate an event for a nuclear power plant depends on four elements:

- Conservation equations, which provide the code capability to address global processes.
- Correlations and models, which provide code capability to model and scale particular processes.
- Numerics, which provide code capability to perform efficient and reliable calculations.
- Structure and nodalization, which address code capability to model plant geometry and perform efficient and accurate plant calculations.

Consequently, these four elements must be considered when evaluating the applicability of the code to the event of interest for the nuclear power plant calculation. The key phenomena for each event are identified in generating the PIRTs for the intended application, as indicated in Section 3.0. The capability of the code to simulate these key phenomena is specifically addressed, documented, and supported by qualification in Reference 2.

Important BWR phenomena have been identified and TRACG models have been developed to address these phenomena as indicated in Table 4-1. Not all phenomena are important for AOO transient analyses.

4.2 Model Assessment Matrix

The qualification assessment of TRACG models are summarized in Table 4-2. The models are identified so that they may be easily correlated to the model description and qualification reports. For each model, the relevant elements from the Model Description LTR [1] and the Qualification LTR [2] are identified.

For each of the governing BWR phenomena, TRACG qualification has been performed against a wide range of data. In this section, the qualification basis is related to the phenomena that are important for the intended application. This is a necessary step to confirm that the code has been adequately qualified for the intended application.

The complete list of phenomena is cross-referenced to the model capabilities in Table 4-1. Similarly, as shown in Table 4-2, the complete list of phenomena is cross-referenced to the qualification assessment basis. Data from separate effects tests, component tests, integral system tests and plant tests as well as plant data have been used to qualify the capability of TRACG to model the phenomena.

Table 4-2 (Continued)

ID	REGION or PHENOMENA DESCRIPTION	Pressurization	Depressurization	Flow Increase or Decrease	Cold Water Insertion	Level Transient (Loss of FW)	Critical Safety Parameter	Critical Parameters: 1 = CPR 2 = Level 3 = Fuel thermal mechanical 4 = Pressure Comments	Qualification Basis Reference to Section Number in the <i>TRACG Qualification</i> LTR NEDE-32177 R2, [Reference 2]			
									Separate Effects Qualification	Component Performance Qualification	Integral System Qualification	Plant Data Qualification

Table 4-2 (Continued)

ID	REGION or PHENOMENA DESCRIPTION	Pressurization	Depressurization	Flow Increase or Decrease	Cold Water Insertion	Level Transient (Loss of FW)	Critical Safety Parameter	Critical Parameters: 1 = CPR 2 = Level 3 = Fuel thermal mechanical 4 = Pressure Comments	Qualification Basis Reference to Section Number in the <i>TRACG Qualification</i> LTR NEDE-32177 R2, [Reference 2]			
									Separate Effects Qualification	Component Performance Qualification	Integral System Qualification	Plant Data Qualification

Table 4-2 (Continued)

ID	REGION or PHENOMENA DESCRIPTION	Pressurization	Depressurization	Flow Increase or Decrease	Cold Water Insertion	Level Transient (Loss of FW)	Critical Safety Parameter	Critical Parameters: 1 = CPR 2 = Level 3 = Fuel thermal mechanical 4 = Pressure Comments	Qualification Basis Reference to Section Number in the <i>TRACG Qualification</i> LTR NEDE-32177 R2, [Reference 2]			
									Separate Effects Qualification	Component Performance Qualification	Integral System Qualification	Plant Data Qualification

Table 4-2 (Continued)

ID	REGION or PHENOMENA DESCRIPTION	Pressurization	Depressurization	Flow Increase or Decrease	Cold Water Insertion	Level Transient (Loss of FW)	Critical Safety Parameter	Critical Parameters: 1 = CPR 2 = Level 3 = Fuel thermal mechanical 4 = Pressure Comments	Qualification Basis Reference to Section Number in the <i>TRACG Qualification</i> LTR NEDE-32177 R2, [Reference 2]			
									Separate Effects Qualification	Component Performance Qualification	Integral System Qualification	Plant Data Qualification

5.0 MODEL UNCERTAINTIES AND BIASES

Overall model biases and uncertainties for a particular application are assessed for each high and medium ranked phenomena by using a combination of comparisons of calculated results to: (1) separate effects test facility data, (2) integral test facility test data, (3) component qualification test data and (4) BWR plant data. Where data is not available, cross-code comparisons or engineering judgment are used to obtain approximations for the biases and uncertainties. For some phenomena that have little impact on the calculated results, it is appropriate to simply use a nominal value or to conservatively estimate the bias and uncertainty.

The phenomena for BWR AOO transients have already been identified and ranked, as indicated in Section 3.0. For the high and medium ranked phenomena, the bases used to establish the nominal value, bias and uncertainty for that parameter are documented in Section 5.1. Also, the basis for the selection of the probability density function used to model the uncertainty is provided in Section 5.1.

5.1 Model Parameters and Uncertainties

This section discusses the uncertainties associated with each item from Table 3-1 that has been identified as having an impact on one or more critical safety parameters. The items are presented by ID, description, and highest ranking (M for Medium and H for High). The results are summarized in Table 5-3.

Figure 5-1. Void Coefficient Normalized %Bias and %Standard Deviation
[NOTE: Multiply these plotted values by $\Gamma(\alpha)$ from Equation 5.2 to remove the normalization.]

Figure 5-2. FRIGG OF64 Void Fraction Data

Figure 5-3. FRIGG OF64 Void Fraction Data

Figure 5-4. FRIGG OF64 Void Fraction Data - Fully Developed Nucleate Boiling

Figure 5-5. Test 14, Average Impact of PIRT22

Figure 5-6. Test 03, Average Impact of PIRT22

Figure 5-7. FRIGG OF64 Void Fraction Data - Subcooled Boiling

Figure 5-8. Void Fraction Sensitivity to PIRT23

Figure 5-9. Sensitivity of Fuel Center to Fluid Temperature Difference for 8x8 Fuel

Figure 5-10. Sensitivity of Fuel Center to Fluid Temperature Difference for 9x9 Fuel

Figure 5-11. Uncertainty in Normalized Total DMH

Figure 5-12. Normalized In-Channel Direct Moderator Heating

Figure 5-13. Normalized Direct Moderator Heating in Bypass and Water Rods

Figure 5-14. Normality Test for the Total DMH Residual Errors

Figure 5-15. All CCFL Data - Relative Error

Table 5-2

BIAS AND UNCERTAINTY FOR 9x9 AND 10x10 SEO AND LTPs

Table 5-3

BIAS AND UNCERTAINTY FOR 9x9 AND 10x10 SPACERS

Table 5-4

BIAS AND UNCERTAINTY FOR 9x9 AND 10x10 UPPER TIE PLATES

Figure 5-16. TRACG Comparison to 1/6 Scale Jet Pump

Figure 5-17. Statistics for TRACG Comparison to 1/6 Scale Jet Pump

Figure 5-18. TRACG Comparison to Full-Scale One Nozzle Jet Pump

Figure 5-19. Statistics for TRACG Comparison to Full-Scale One-Nozzle Jet Pump

Figure 5-20. TRACG Comparison to Full-Scale Five-Nozzle Jet Pump

Figure 5-21. Statistics for TRACG Comparison to Full-Scale Five-Nozzle Jet Pump

Figure 5-22. Jet Pump Sensitivity to Inlet Loss for One-Nozzle Jet Pump

Figure 5-23. Jet Pump Sensitivity to Inlet Loss for Five-Nozzle Jet Pump

Figure 5-24. TRACG Comparison to 1/6 Scale Jet Pump for Reverse Drive Flow

Figure 5-25. Statistics for TRACG Comparison to 1/6 Scale Jet Pump for Reverse Drive Flow

Figure 5-26. Jet Pump Sensitivity to Nozzle Loss for 1/6 Scale Jet Pump

Figure 5-27. Error in Prediction of Carry Under for 2-Stage Separator

5.4 Sensitivity Analysis

Sensitivity studies have been performed for each class of AOO, varying each highly ranked model parameter from -1σ to $+1\sigma$. These results are shown in Section 8.0, under each type of transient. These studies serve to identify the parameters that have the largest impact on the calculated safety parameters.

6.0 APPLICATION UNCERTAINTIES AND BIASES

6.1 Input

Specific inputs for each transient event are specified via internal procedures, which are the primary means used by GE to control application of engineering computer programs. The specific code input will be developed in connection with the application LTR and the development of the application specific procedure. This section will be limited to a more general discussion of how input is treated with respect to quantifying their impact on the calculated results. As such, it serves as a basis for the development of the application specific procedures.

Code inputs can be divided into four broad categories: (1) geometry inputs; (2) model selection inputs; (3) initial condition inputs; and (4) plant parameters. For each type of input, it is necessary to specify the value for the input. If the calculated result is sensitive to the input value, then it is also necessary to quantify the uncertainty in the input.

The geometry inputs are used to specify lengths, areas and volumes. Uncertainties in these quantities are due to measurement uncertainties and manufacturing tolerances. These uncertainties usually have a much smaller impact on the results than do other uncertainties associated with the modeling simplifications. When this is not the case, the specific uncertainties can usually be quantified in a straightforward manner. For example, consider the 2% channel flow area uncertainty that is considered as part of the Safety Limit MCPR (SLMCPR). This uncertainty is determined from the manufacturing tolerances on the inner dimensions of the channel box and the outer diameter of the fuel and water rods. It is known that neglecting this uncertainty causes the calculated SLMCPR value to be non-conservative by no more than 0.0015. Even though channel flow area is considered to be *important*, the impact associated with the uncertainty in this parameter is small.

Individual geometric inputs are the building blocks from which the spatial nodalization is built. Another aspect of the spatial nodalization includes modeling simplifications such as the lumping together of individual elements into a single model component. For example, several similar fuel channels may be lumped together and simulated as one fuel channel group. An assessment of these kinds of simplifications, along with the sensitivities to spatial nodalization, is included in the *TRACG Qualification* [2].

Model selection inputs are used to select the features of the model that apply for the intended application. Once established, these inputs are fully specified in the procedure for the application and will not be changed.

A distinction has been made in this document between *initial conditions* and *plant parameters*. Obviously, when specified in absolute units, the initial rated conditions for a nuclear power plant are specific to the plant and thus have in some documents been considered as plant parameters. In this document we consider *initial conditions* to be those key plant inputs that determine the overall steady-state nuclear and hydraulic conditions prior to the transient. These inputs are essential to determining that the steady-state condition of the plant has been established. Initial conditions parameters and the uncertainties associated with them are addressed in Section 6.2.

The name *plant parameter*, on the other hand, is reserved for such things as protection system setpoints, valve capacities and stroke times, and scram characteristics that influence the characteristics of the transient response but which do not (when properly prescribed) have an impact on steady-state operation. Plant parameters and the uncertainties associated with them are addressed in Section 6.3.

6.2 Initial Conditions

Initial conditions are those conditions that define a steady-state operating condition. Initial conditions for a particular transient scenario are specified in the procedure for the application. For example, the procedure may specify that the calculation be performed at the end-of-cycle exposure at 100% of rated power and flow using a power and exposure distribution that has been obtained from a prescribed process. The absolute values of these inputs will vary from plant to plant and from cycle to cycle. For example, the rated power and flow values for the plant are usually fixed (unless the plant has been relicensed to higher rated values), but the cycle exposure will change with each cycle.

Initial conditions may vary due to the allowable operating range or due to uncertainty in the measurement at a give operating condition. The plant Technical Specifications and Operating Procedures provide the means by which controls are instituted and the allowable initial conditions are defined. At a given operating condition, the plant's measurement system has inaccuracies that also must be accounted for as an uncertainty. The key plant initial conditions are identified in Table 6-1.

The analyses performed must maintain consistency with the allowed domains of operation. The impact of the initial condition on the results are characterized in the following manner:

- The results are sensitive to the initial condition and a basis for the limiting initial condition can not be established. Future plant analyses (e.g., the reload licensing analyses) will consider the full allowable range of the initial condition.
- The results are sensitive to the initial condition and a basis for the limiting initial condition can be established. Future plant analyses (e.g., the reload licensing analyses) will consider the parameter to be at its limiting initial condition.
- The results are not sensitive to the initial condition and a nominal initial condition will be assumed for the parameter.

Each initial condition is monitored through the use of plant sensors or simulated prediction. Because of instrument or simulation uncertainty, the plant condition may vary from the indicated value. The results are characterized in the following manner:

- The results are sensitive to the uncertainty in the initial condition and the uncertainty in the initial condition will be included in the statistical analysis.
- The results are not sensitive to the uncertainty in the initial condition and the uncertainty does not need to be accounted for.

The impact of the total uncertainty in initial conditions must also be quantified for the critical safety parameters such as $\Delta\text{CPR}/\text{ICPR}$, peak vessel pressure and water level. Some of these uncertainties

6.3 Plant Parameters

A *plant parameter* is defined as a plant-specific quantity such as a protection system setpoint, valve capacity or stroke time, or a scram characteristic, etc. *Plant parameters* influence the characteristics of the transient response and have essentially no impact on steady-state operation, whereas *initial conditions* are what define a steady-state operating condition.

For each plant parameter, a conservative value corresponding to the *analytic limit* is defined. The analytic limit (AL) is the value used for the transient licensing analyses. In many cases, the value used for the AL can be related to a plant technical specification (Tech Spec), since most of the plant parameter values that are important for AOO transient responses are related to processes that are controlled by the plant Tech Specs. These parameters may be periodically measured at the plants to assure compliance with the Tech Specs. Performance and uncertainties for the processes that the Tech Specs are designed to control are based on manufacturing specifications, performance data, as well as required surveillance. A Tech Spec value will usually be in terms of a maximum or minimum acceptable value that bounds the entire population of values that are measured at the plant.

The Tech Spec values may be used to define the analytic limits used for the licensing analyses. The original licensing basis specified bounding Tech Spec values for most of the plant parameters (see Table 1-1 in Volume 3 of Reference 15). This is one acceptable way by which conservatism can be added to a "best estimate" methodology. Another option for establishing plant parameters is to establish an uncertainty in the parameter. For example, the NRC has accepted for *Option B*, a faster scram speed when used together with considerations of the uncertainties in the scram speeds. This approach is supported by surveillance procedures at the plant, whereby the scram times are measured. The uncertainty in the scram times is then accounted for in the AOO analyses as part of the statistical methodology.

GE procedures define the critical Operating Parameters for Licensing (OPL) for transient analysis. GE and the utilities utilize this procedure. It serves as a guide for generating plant parameter data to be used for licensing. This procedure addresses Tech Spec items as well as other items that are important to the severity of transients.

The reactor scram is the most effective plant system for mitigating the severity of a transient. The plant Tech Specs provide surveillance requirements to ensure control rod operability and scram times. For most BWR/3 - BWR/5 plants, an additional surveillance is performed to demonstrate that the scram speed is within statistical basis of the faster *Option B* scram.

Table 6-2
ANALYTICAL SCRAM SPEEDS

7.0 COMBINATION OF UNCERTAINTIES

A proven Monte Carlo technique is used to combine the individual biases and uncertainties into an overall bias and uncertainty. The Monte Carlo sample is developed by performing random perturbations of model and plant parameters over their individual uncertainty ranges. Using the histogram generated by the Monte Carlo sampling technique, a probability density function is generated for code output of the primary safety criteria parameters.

In order to determine the total uncertainty in predictions with a computer code, it is necessary to combine the uncertainties due to model uncertainties (CSAU Step 9), scaling uncertainties (CSAU step 10), and plant condition or state uncertainties (CSAU Step 11). Various methods have been used to combine the effects of uncertainties in safety analysis. This section briefly summarizes different methods for combining uncertainties. All these approaches are within the framework of the CSAU methodology, since the CSAU methodology does not prescribe the approach to use. The method for combining uncertainties that is used for application to TRACG analyses is the same approach that has been successfully used in analyses of AOO transient scenarios and accident scenarios for the SBWR [16] and for ABWRs [17].

7.1 Traditional Bounding Analysis

A commonly used approach in traditional conservative analysis is to combine the uncertainties linearly, by taking bounding models for the phenomena and by setting plant parameters to limits expected to produce the most limiting plant response. Separate calculations may be required to obtain bounding results for different response parameters, because it may not be possible to define a single 'worst case' that will result in all key response or output parameters being calculated at their upper bounds. In any case, an advantage of this approach is that it requires no more than one computer run for each output parameter of interest. The most significant disadvantages with this method are that it is very conservative, in extreme cases can give unrealistic results; and no statistical quantification of the margins to design limits is possible. This bounding approach has historically been used for analyses of LOCA following 10CFR50 Appendix K [18] and NRC Regulatory Guides prior to 1.157.

7.2 Statistical Treatment of Overall Computational Uncertainty

A more realistic and rigorous approach has been introduced to the licensing process. In this approach the most realistic plant calculations are performed for the evaluation of the primary safety criteria using realistic models and nominal input for the plant parameters. An uncertainty is then added to the calculated primary safety parameters to account for modeling uncertainty, uncertainty in plant operation and state, and other factors such as effect of scale on the calculations. A statistical approach is used to determine the added uncertainty on top of the nominal calculation. Such an approach was adopted for the analysis of pressurization transients [30]. Nominal results were evaluated with the one-dimensional ODYN code, to which an adder was applied to account for uncertainty in modeling the plant transient response, and uncertainties in the plant initial power and scram speed, while bounding inputs and assumptions were used for other parameters. Similarly, a hybrid methodology was introduced for LOCA calculations with SAFER [20, 21]. In these calculations, nominal inputs together with realistic models plus a statistically based evaluation of the uncertainty adder were used for some parameters, while conservative inputs were used for other parameters. The NRC-developed CSAU methodology [22] and NRC Regulatory Guide 1.157 [23] complete the transition to realistic

methods. Realistic models and input are used for all processes and inputs, and the design calculation accounts for uncertainties in all major models and plant parameters.

NRC Regulatory Guide 1.157, for use of best-estimate models for LOCA analysis, defines acceptable model features and application procedures. The Guide states that a one-sided upper tolerance limit (OSUTL) can be calculated at the 95% probability level for the primary safety parameters. In addition, the statistical methodology should be provided and justified. The Regulatory Guide finds the CSAU methodology acceptable for this purpose.

7.3 Comparison of Approaches for Combining Uncertainties

Several options exist to perform the statistical combination of the uncertainties. Neither the CSAU methodology report [22] nor NRC Regulatory Guide 1.157 [23] specifies how this should be done. Some possible options are summarized in Table 7-1.

These options are discussed and compared in the following paragraphs. Justification for use of the Monte Carlo method will be developed.

Table 7-1
METHODS FOR COMBINED UNCERTAINTY

Method	Description
Propagation of Errors	Uncertainties in the calculated safety parameters to individual phenomena are evaluated from single perturbations and the overall uncertainty is determined as the square root of the sum of the squares of the individual uncertainties.
Response Surface Technique	Response surface for the safety parameter is generated from parameter perturbations. Statistical upper bound is determined from the Monte Carlo method using a response surface.
Order Statistics Method - Single Bounding Value (GRS Method)	Monte Carlo method using random perturbations of all important parameters. Sample size defined to yield desired statistical confidence. Statistical upper bound is determined from most limiting perturbation (for first order statistics).
Normal Distribution One Side Upper Tolerance Limit	Monte Carlo method using random perturbations of all important parameters. Normality of output distribution established by statistical checks. Statistical upper bound is determined from sample variance from all perturbations.

7.3.1 Propagation of Errors

In the propagation of errors method, the uncertainties are combined by taking the square root of the sum of the squares (SRSS) of the individual uncertainties. In this approach, the effects of individual phenomena on key response parameters are determined, and then combined using SRSS. For this approach, a relatively small number of computer runs is required. The number of runs required is directly related to the number of input parameters for which uncertainty ranges have been established. This approach is justifiable if the effects on the calculated responses of the phenomena, whose uncertainties are being accounted for, are independent of each other. For complex processes requiring complex code calculations, independence rarely exists and is difficult to impossible to demonstrate. A secondary requirement for this approach is that all input and output parameters can be modeled by a normal distribution.

7.3.2 Response Surface Technique

In this method, individual model and plant parameters are perturbed and the sensitivity of the primary safety parameter to these perturbations is determined. The process begins by examining each model and plant parameter uncertainty. Using test data and expert knowledge, each parameter is assigned a probability density function (i.e., normal, log normal, exponential, uniform, etc.). The probability density function (PDF) describes the method by which the uncertainty would vary from the expected value. The range for each PDF is determined from the standard deviation, if known, or by the maximum and minimum value of the parameter. As an example, the parameter governing void fraction uncertainty is distributed normally with a nominal (mean) value of 1.00 and a standard deviation of 0.02. According to conventional response surface techniques, a large number of transient simulations per each event scenario would be needed due to the large number of parameters to be varied. At least two cases would be required (in addition to the nominal calculations) for each important plant and model parameter to quantify the responses to $\pm 2\sigma$ perturbations. Additional cases would be needed to quantify curvature if the output responses did not vary linearly with the input perturbations. Furthermore, many cases would have to be made, where several parameters are perturbed simultaneously to account for covariances. A response surface would be fit to all these cases, and Monte Carlo analysis would be performed with the response surface to determine the 95% fractile. This method is advantageous when few parameters are involved, but is impractical when a large number of parameters are involved due to the prohibitively large number of perturbations needed to account for non-linearities and covariances.

The PIRTs in Section 3.0 identify over 30 highly ranked phenomena. Assuming one input parameter per phenomena and not even considering other uncertainties associated with initial conditions and plant parameters, a large number of calculations are required. To run the base case, the $\pm 2\sigma$ perturbations, cases to quantify the curvature, and cases to evaluate covariances would require over 200 transient simulations even using efficient Box techniques. However, an important advantage is that single parameter perturbations provide useful insight by identifying the most sensitive parameters.

7.3.3 Order Statistics Method - Single Bounding Value (GRS)

The Monte Carlo method that has been used in Germany by Gesellschaft für Anlagen-und Reaktorsicherheit (GRS) [24] requires only a modest number of calculations, and automatically includes the effects of interactions between perturbations to different parameters. In this GRS method, Monte Carlo trials are used to vary all uncertain model and plant parameters randomly and

simultaneously, each according to its uncertainty and assumed probability density function (PDF), and then a method based on the order statistics of the output values is used to derive upper tolerance bounds (one-sided, upper tolerance limits OSUTLs).

Monte Carlo sampling of each parameter according to its assigned PDF yields the value of that parameter to be used for a particular trial. Given such a trial set of input parameters, the calculation process determines the corresponding output parameter of interest. Therefore, while void coefficient might be set at a -1.5σ value, inter-facial shear might be set to a value of $+2.0\sigma$, each according to its own probability model. In this manner, the effects of interactions between all model parameters are captured in a single calculation. Once all of the trials have been completed, the desired output parameter (e.g., $\Delta\text{CPR}/\text{ICPR}$) is extracted from each of the trials and the set of parameter values is then used to construct an OSUTL for that particular output parameter. Figure 7-1 illustrates this process.

Individual TRACG overlay files containing all the perturbed parameter values are created for each separate trial. For each trial, this overlay file is appended to the end of the base transient input file and the TRACG calculation is performed to determine the output parameter value as a function of time for this particular transient and set of inputs. The process is repeated n times to define the sample values of the output parameter of interest for the particular transient under consideration. Similar samples for other parameters, for the same transient, can be generated at the same time without additional TRACG calculations.

An OSUTL is a function $U = U(x_1, \dots, x_n)$ of the data x_1, \dots, x_n (which will be the values of an output parameter of interest in a set of Monte Carlo trials), defined by two numbers $0 < \alpha, \beta < 1$, so that the proportion of future values of the quantity of interest that will be less than U is $100\alpha\%$, with confidence at least $100\beta\%$ --- this is called an OSUTL with $100\alpha\%$ -content and (at least) $100\beta\%$ confidence level.

The order statistics method, originally developed by Samuel Wilks, produces OSUTLs that are valid irrespective of the probability distribution of the data, requiring only that they be a sample from a continuous PDF. Given values of α and β , the OSUTL can be defined as the largest of the data values, provided the sample size $n \geq \log(1 - \beta) / \log \alpha$ [25]. For 95%-content and 95% confidence level, the minimum sufficient sample size is $n=59$.

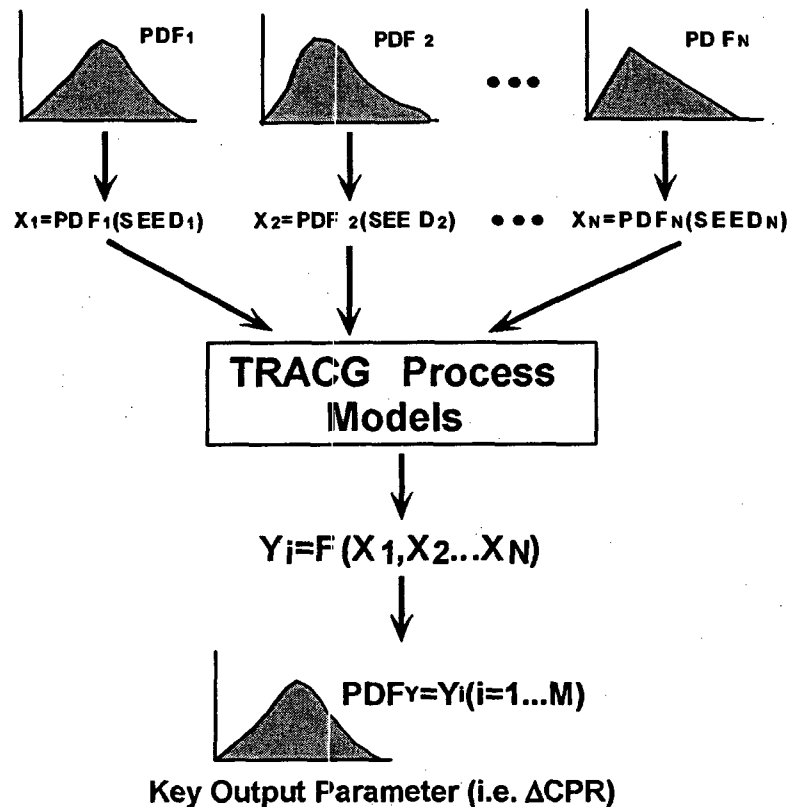


Figure 7-1. Schematic Process for Combining Uncertainties

The order statistics method is generally applicable, irrespective of the probability distribution of the data, and requires only that these be like outcomes of independent random variables with a common probability distribution.

If the method is implemented as described above, whereby the sample size (59) was chosen so that the sample maximum is the upper tolerance bound sought (95% content with 95% confidence), then this bound, as a random quantity, has variability that is typical of the maximum of a sample of that size, which can be substantial, and occasionally may yield an apparently conservative bound.

To mitigate this variability, one can choose a suitably larger sample size so that the bound sought is now given by the second or third largest sample value. For example, the 95% content with 95% confidence tolerance bound is the third largest observation in a sample of size 124: just for the sake of illustration, in normal (that is, Gaussian) populations its variability is about one half of the variability of the maximum in a sample of size 59; and in the more heavily-tailed Student's *t* distribution with 4 degrees of freedom, the variability of the third largest in a sample of size 123 is about one third of the variability of the maximum in a sample of size 59.

The following table summarizes the sample sizes that are required, when the bound is the largest, the second largest, or the third largest order statistic, all for 95% content and 95% confidence:

<u>Order Statistic</u>	<u>Sample Size</u>
Largest	59
2 nd Largest	93
3 rd Largest	124

7.3.4 Normal Distribution One-Sided Upper Tolerance Limit

If the data the tolerance bound will be derived from can reasonably be regarded as a sample from a normal (that is, Gaussian) probability distribution, then this normal distribution one-sided upper tolerance limit (ND-OSUTL) is of the form

$$ND - OSUTL_{\alpha,\beta} \equiv \bar{y} + z_{\alpha,\beta} \cdot s \quad (7-2)$$

where \bar{y} denotes the average of the outcomes of the TRACG trials, and s denotes their standard deviation, and the factor $z_{\alpha,\beta}$ is chosen to guarantee 100 α %-content and 100 β % confidence level. Since this factor $z_{\alpha,\beta}$ depends on the assumption of normality for the data, one must first ascertain whether the data does indeed conform with the Gaussian model, typically using one or several goodness-of-fit tests: for example, Ryan-Joiner's, Shapiro-Wilk's, or Anderson-Darling's. The values of $z_{\alpha,\beta}$ are tabulated in many statistical textbooks [25] as *factors for one-sided normal tolerance limits*. For example, for a sample of size $n=59$, and a 95% content and a 95% confidence level, $z_{95,95} = 2.024$: as the sample size n increases, this factor approaches 1.645, the 95th percentile of the standard normal distribution. Unlike the order statistics method, this ND-OSUTL method does not require specific minimum sample sizes; but it does require normality. If the data are unlikely to have originated from a normal population, then one should use the order statistics method.

An example in Section 8.4.2.1 shows that the calculated values of Channel 29 Δ CPR/ICPR for the TTNB event may be regarded as a sample from a normal population, to which this ND-OSUTL method can be applied. Although the illustrations are presented only for Δ CPR/ICPR, the same approach can in principle be used to determine the total uncertainty in other calculated results such as centerline temperature, clad strain, vessel pressure, and downcomer water level, again provided the requirement of normality is met.

7.4 Recommended Approach for Combining Uncertainties

- The OSUTL for each output parameter of interest (summarized in Table 7-2) can be defined over the entire duration of the transient. That is, it is not limited to using only the peak values for the output variables over the duration of the event analyzed or the values at a particular point in time.

Table 7-2

COMPARISONS OF METHODS FOR COMBINING UNCERTAINTIES

Method for Combining Uncertainties	Advantages	Disadvantages
Propagation of Errors	Relatively small number computer runs, when the number of input variables is small. The number of cases is linearly related to the number of input parameter uncertainties considered.	Approximate because it involves linearization. Necessary either to demonstrate independence of effects of individual uncertainties on responses, or else must include covariances explicitly.
Response Surface	Very precise statistical characterization of results with a large number of Monte Carlo Trials using response surface. Different distributions can be specified for each input uncertainty. Independence of the effect of individual input parameters on response is not necessary.	Number of computer runs depends on the response surface model and increases exponentially with the number of input parameter uncertainties considered. Interactions between input parameters have to be established and considered in the development of the response surface.
Order Statistics (GRS)	The number of random trials is independent of the number of input parameters considered. The method requires no assumption about the PDF of the output parameter. It is not necessary to perform separate calculations to determine the sensitivity of the response to individual input parameters. It is not necessary to make assumptions about the effect on the output of interactions of input parameters.	Since the tolerance limits are based on order statistics, they will vary from one set of TRACG trials to another, and these differences may be substantial, especially for small sets of TRACG trials, and particularly if the tolerance bound is the sample extremum.
Normal Distribution One-sided Upper Tolerance Limit (ND-OSUTL)	The number of random trials is independent of the number of input parameters considered. Only a relatively small number of random trials is needed for a precise statistical characterization of the results. It is not necessary to perform separate calculations to determine the sensitivity of the response to individual input parameters. It is not necessary to make assumptions about the effect on the output of interactions of input parameters.	The normality of the PDF for the output variable must be demonstrated.

The advantage of the order statistics method is that it does not depend on the PDF of the output variable, and the disadvantage is that the OSUTLs, because they are based on order statistics, will

vary from one set of TRACG trials to another, and these differences may be substantial, especially for small sets of TRACG trials, and particularly if the tolerance bound is the sample maximum. The ND-OSUTL method, on the other hand, provides an OSUTL that typically is less sensitive to the particular values in the sample of TRACG trial values, but depends on the output variable being normally distributed.

7.5 Implementation of Statistical Methodology

The purpose of this section is (1) to describe the process by which the statistical results will be used to determine the Operating Limit Minimum Critical Power Ratio (OLMCPR), and (2) establish that fuel thermal/mechanical performance, peak vessel pressure, and minimum water level have acceptable margins to design limits. The application to the latter three is straightforward, and is discussed in the next section. The determination of the OLMCPR is more involved, and is detailed in the subsequent sections.

7.5.1 Conformance with Design Limits

7.5.2 Determination of OLMCPR

7.5.2.1 OLMCPR Method Background

To conservatively account for statistical uncertainty in thermal-hydraulic test data and measurements of the core operating state, a minimum allowable (lower limit) MCPR is evaluated. The Safety Limit Minimum Critical Power Ratio (SLMCPR_{99.9}) is determined so that less than 0.1% of the rods in the core will be expected to experience boiling transition at this value. In other words, 99.9% of the fuel rods in the core will be expected to avoid boiling transition if the limiting MCPR in the core is greater than the SLMCPR_{99.9}.

To assure that the safety limit is not exceeded as a result of transient events, the concept of an Operating Limit MCPR (OLMCPR) is introduced. The OLMCPR is established to satisfy the thermal-hydraulic design criterion that fuel assemblies be operated under planned, steady-state conditions such that the envelope of initial conditions used in the safety analysis is not exceeded. The OLMCPR is currently established by adding the maximum change in MCPR (Δ CPR) expected from the most limiting transient event (including uncertainties) to the SLMCPR_{99.9}. Conformance to the SLMCPR_{99.9} can be demonstrated by assuring that normal operating MCPR values are greater than the OLMCPR.

In principle, the OLMCPR could be calculated directly such that, for the limiting AOO, less than 0.1% of the rods in the core would be expected to experience boiling transition. The process involved is shown in Figure 7-2, which depicts a histogram of rod CPR values (A). While the CPR value is usually associated with a fuel bundle, it actually refers to the limiting rod in the bundle. Each rod in

the bundle has a CPR value that is determined by the local power distribution and relative position of the rod within the bundle (R-Factor). The lowest CPR rod is used to characterize the bundle CPR.

The CPR for a given rod has an associated probability distribution function (PDF), which reflects the uncertainties in its determination. The PDF for the limiting rods is shown in Figure 7-2 (B). The variability in the rod CPR is due to uncertainties in the initial conditions [i.e., uncertainties in the measurements of parameters at the reactor operating state (core power) and in the modeling of derived parameters (power distribution)].

During a transient, the histogram of rod CPRs shifts to the left (to lower CPR values). This histogram is shown as A' in the figure for the 'nominal' transient at the point where the minimum value is reached during the transient. The limiting rod will have an associated PDF B', which includes both the uncertainties in the initial conditions (B) and 'transient uncertainties'. The latter includes uncertainties in the modeling of the transient, both the physical models (included in the PIRT) and plant parameters (scram speed variability). Ideally, this transient distribution would be generated as follows:

- Run a large number of TRACG transient calculations (in the order of 100 calculations is sufficient to give high confidence in the result). In each calculation, randomly vary the initial conditions, model parameters and plant parameters using the PDF for each parameter. Obtain a histogram of rod CPR values at the time of minimum CPR. Compile the statistics for the cases.

For each transient histogram of rod CPRs, the Number of Rods Subject to Boiling Transition (NRSBT) can be calculated from the intersection of the histogram with the Experimental Critical Power Ratio (ECPR) distribution shown on the left side of Figure 7-2.

The ECPR is given by:

$$ECPR = \frac{\text{(Critical Power Predicted by GEXL Correlation)}}{\text{(Measured Critical Power)}} \quad (7-8)$$

The ECPR values are *normally* distributed about a mean value, $ECPR_0$ (note that $ECPR_0 = 1$). The probability density function for the ECPR values is given by the normal distribution. The probability that some rod "i" operating at $MCPR_i$ is in Boiling Transition (BT) is given by:

$$P_i = P(z_i) = \frac{1}{\sqrt{2\pi}} \int_{z_i}^{\infty} e^{-\frac{1}{2}u^2} du \quad (7-9)$$

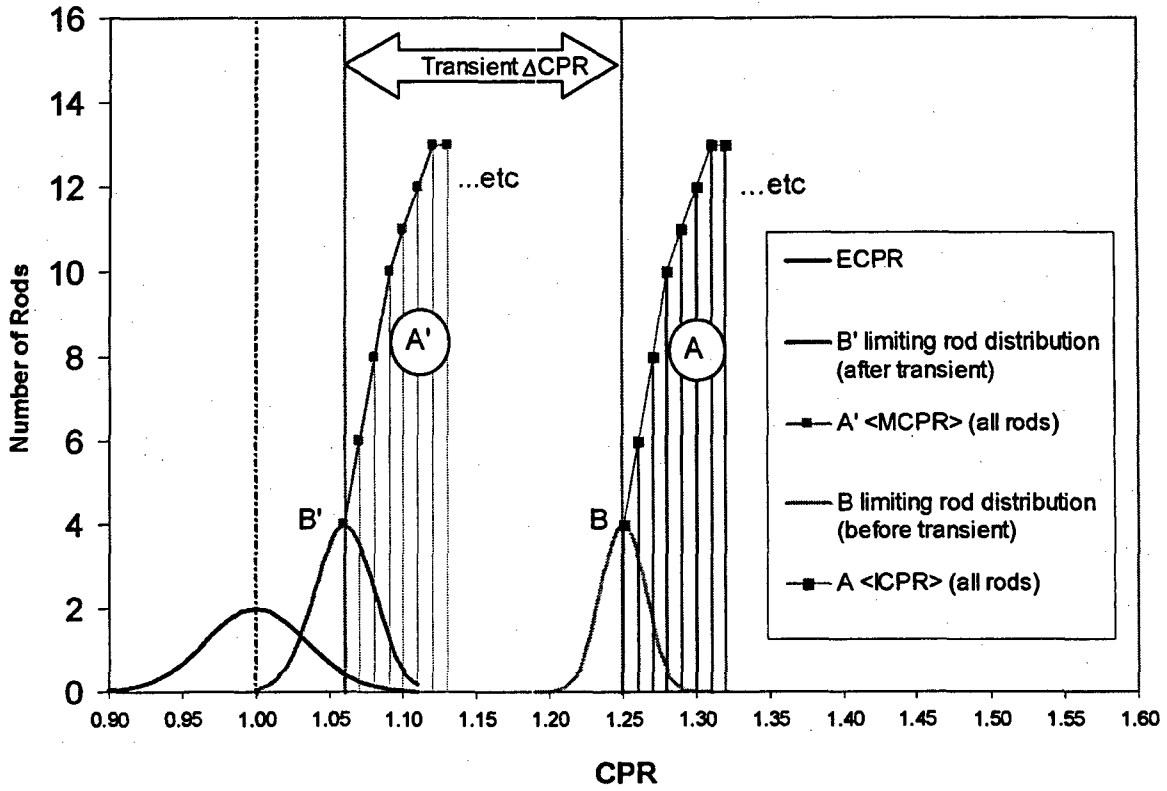


Figure 7-2. NRSBT Determination with Ideal Process

The *expected* Number of Rods Subject to Boiling Transition (NRSBT or $\overline{\text{NRSBT}}$) can be found by summing the probability that a rod is subject to boiling transition for all the rods in the core.

$$\text{NRSBT (\%)} = \frac{100}{N_{\text{rod}}} \times \sum_{i=1}^{N_{\text{rod}}} [P_i \times (1 \text{ Rod})] \quad (7-10)$$

For a given core operating state, the expected NRSBT is the sum of the product of a probability and one (1) rod, for each rod in the core. The calculation of NRSBT would be performed for each of the transient trials, enabling the determination of the mean value of NRSBT.

The OLMCPR is determined from the limiting MCPR value in the core when the NRSBT equals 0.1%.

7.5.2.2 Currently Approved SLMCPR Process

In the current process, the OLMCPR determination is divided into two distinct steps. As stated in the previous section, first the Safety Limit Minimum Critical Power Ratio (SLMCPR_{99.9}) is determined so that less than 0.1% of the rods in the core will be expected to experience boiling transition at this value. In other words, 99.9% of the fuel rods in the core will be expected to avoid boiling transition if the limiting MCPR in the core is greater than the SLMCPR_{99.9}. The OLMCPR is then established by adding the maximum change in MCPR ($\Delta\text{CPR}_{95/95}$) expected from the most limiting transient event to the SLMCPR_{99.9}. This process is illustrated in Figures 7-3 and 7-4.

As in the previous section, the value of NRSBT is determined from the intersection of the rod CPR histogram with the ECPR PDF. A number of trials are made with variation in the initial conditions to generate a number of rod CPR histograms. The variation in CPR for the limiting rod is characterized by the PDF B. From these trials, a mean value of NRSBT is established. The SLMCPR is determined from the limiting MCPR value in the core when the NRSBT equals 0.1%. Note that these MCPR values will be in the range corresponding to the minimum CPR during a transient, rather than in the operating range. This process is performed by the GESAM Engineering Computer Program (ECP). The GESAM Monte Carlo process is shown Figure 7-5.

Specifically, the Safety Limit MCPR accounts for uncertainties in the following parameters:

- Feedwater flow
- Steam dome pressure
- Feedwater temperature
- Core flow
- Core Inlet Temperature
- Channel flow area
- Two-phase friction factor multiplier
- Channel friction factor multiplier
- TIP readings
- R-factor
- GEXL correlation prediction error

The first three factors are used in the calculation of the total core power. The TIP readings determine the local power distribution uncertainties. A change in a core-wide variable such as the core thermal power, inlet temperature or total core flow will effectively bias the operating MCPRs of the *entire population* of bundles in the core.

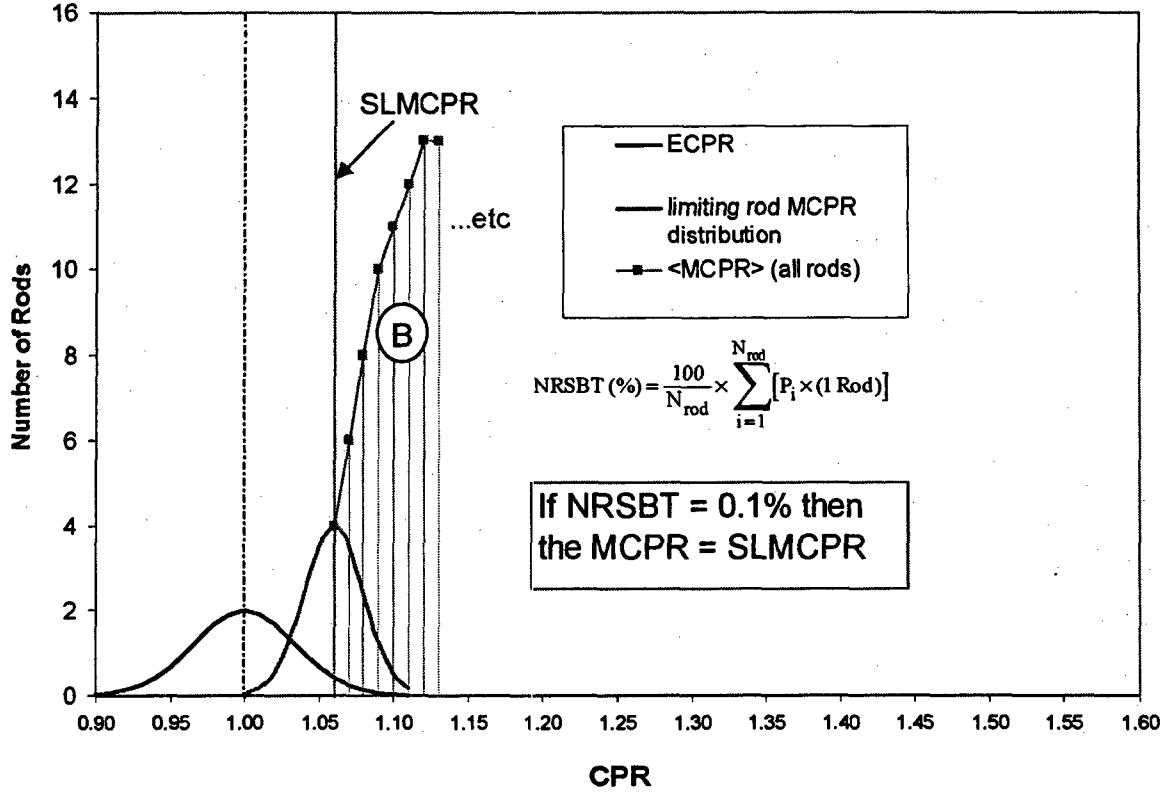


Figure 7-3. GETAB SLMCPR NRSBT Determination

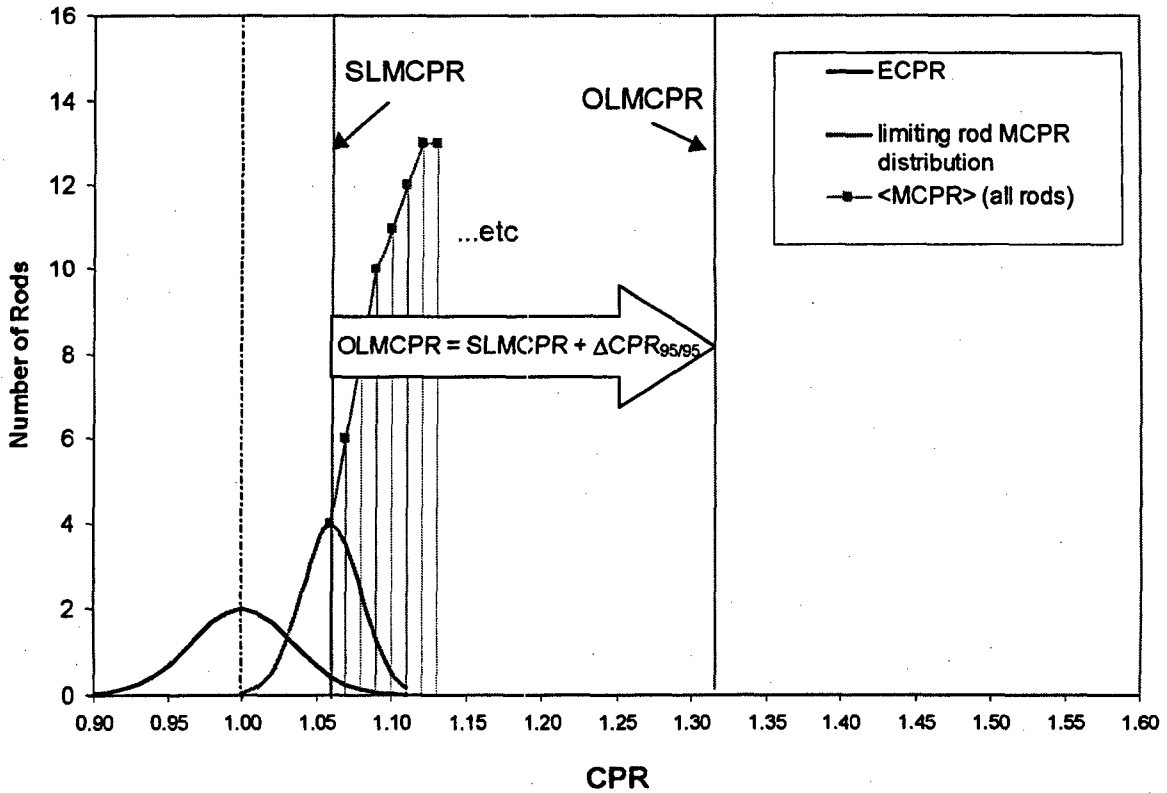


Figure 7-4. OLMCPR Method with 95/95 ΔCPR

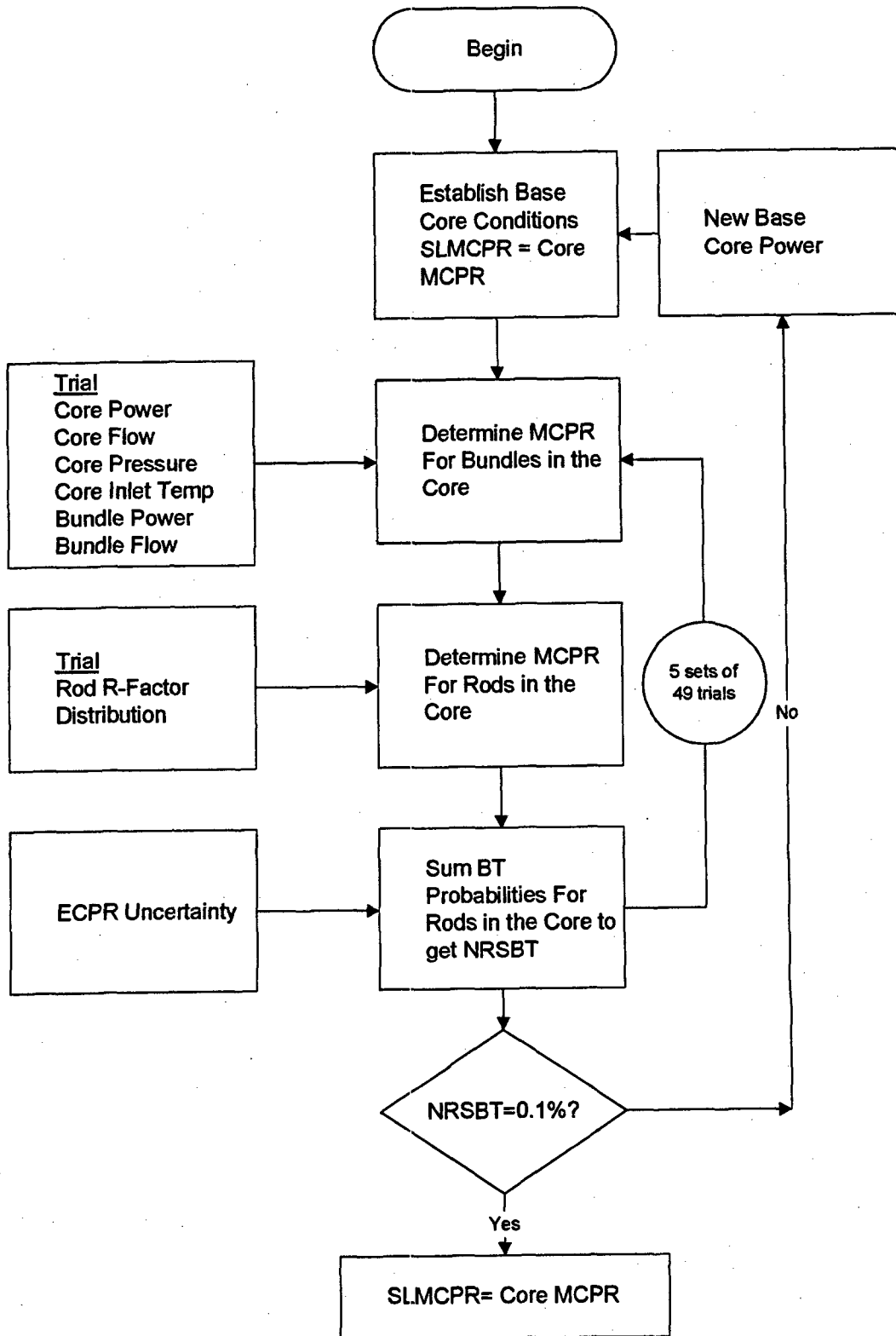


Figure 7-5. GESAM Calculation Procedure for Analytical Determination of SLMCPR

The plant process computer also uses the TIP and LPRM readings to predict individual bundle CPRs. The process computer has uncertainties in its use of these instrument readings along with uncertainty in the simulator's ability to predict bundle power, which also serves to bias the operating MCPRs of *individual bundles*. The power distribution in the limiting bundles is very important in determining the SLMCPR because these bundles are the biggest contributors to NRSBT.

The second part of the process is illustrated in Figure 7-4. Starting with an initial condition in the operating MCPR range, calculations are made for the limiting transient. Typically, the MCPR during the transient is calculated only for the limiting bundle in the core. This is the bundle with the lowest CPR rod at the initial conditions. It is assumed that the change in CPR ($\Delta\text{CPR}/\text{ICPR}$) is the same or less for other rods/bundles, such that they will not become limiting during the transient. The transient uncertainty in $\Delta\text{CPR}/\text{ICPR}$ is obtained by Monte Carlo trials combining model uncertainty with uncertainties in plant parameters such as core power and scram speed. Because of the approximations in the process, the transient $\Delta\text{CPR}/\text{ICPR}$ is evaluated at a 95% probability/95% confidence level. The OLMCPR is obtained by linearly adding the transient $\Delta\text{CPR}_{95/95}$ to the Safety Limit CPR.

This approach has been previously reviewed and approved by the NRC [32].

7.5.2.3 Proposed Approach

- It would be too cumbersome to perform on the order of 100 TRACG transient calculations for each AOO.
- TRACG does not have the capability to simulate the effects of the TIP/LPRM uncertainties on the local power distribution or to calculate rod by rod R-factors and CPRs.

For these reasons, the ideal process will be approximated as shown in Figures 7-6 and 7-7. The steps are as follows:

Figure 7-6. Generic Δ CPR/ICPR Uncertainty Development

Figure 7-7. NRSBT Determination with Proposed Process

7.5.2.4 Validation of Assumptions Used in Proposed Approach

Calculations were made to demonstrate that the value of the transient $\Delta\text{CPR}/\text{ICPR}$ calculated by TRACG is insensitive to variations in the initial conditions.

Figure 7-8. GESAM Calculation Procedure for Analytical Determination of OLMCPR

Table 7-3

IMPACT OF CRITICAL ICPR UNCERTAINTIES ON $\Delta\text{CPR}/\text{ICPR}$

***Boldface applied to direction that will decrease the ICPR.**

The other assumption to be validated is that a constant value of $\Delta\text{CPR}/\text{ICPR}$ can be applied to rods at different initial values of CPR. The transient MCPR distribution will be obtained by transforming the ICPR distribution using Equation 7-11.

To further validate this assumption, a specific set of calculations was performed. Benchmark calculations were made with TRACG for a turbine trip without bypass event that included the uncertainties in core power and channel pressure drop as initial conditions, as well as the model uncertainties. These uncertainties (core power and channel pressure drop) were chosen because they are the only SLMCPR compatible uncertainties that are also varied in the TRACG statistical analysis. MCPR distributions during the transient were generated for two fuel bundles in the core (Channels 27 and 29) through 98 transient calculations (Figure 7-6). The two channels are very close in the ICPR values and have identical $\Delta\text{CPR}/\text{ICPR}$ values. These TRACG calculations serve as the reference.

7.5.2.5 Example of Application Process

Figure 7-10 is an example of the application of this process for the limiting rod starting from a set of 98 GESAM ICPR trials with all uncertainties applied. Of the 118 TRACG trials for the TTNB event (Section 8.4.2.1), 98 are used to generate a Δ CPR/ICPR distribution. The 98 TRACG random Δ CPR/ICPR trials (Hot Channel 29) are applied to the ICPR distribution of the limiting bundle to get the transient MCPR distribution. The intersection of the transient MCPR with the GEXL CPR uncertainty is the basis for determining the NRSBT.

Figure 7-9. Comparison of GESAM/TRACG Transient MCPR to TRACG MCPR

Figure 7-10. Transformation of GESAM ICPR Distribution to Transient MCPR

7.5.2.6 Scram Speed Dependent OLMCPR

7.5.2.7 High Worth Scram Rods for Pressurization Event OLMCPR

7.6 Statistical Analysis for Qualification Events

Although, the models can be evaluated and the code uncertainty can be determined purely based on an evaluation of the impact of the uncertainties, the TRACG performance is also demonstrated on available qualification plant events. This demonstration includes a statistical analysis that has a purpose of showing whether the plant data is within the uncertainty of the code.

7.6.1 Peach Bottom Turbine Trip Test Statistical Analysis

Statistical analyses were performed for the three Peach Bottom turbine trip tests described in Section 7.1 of the Qualification LTR [2]. The analysis includes random variation (59 trials) of the model uncertainties described in Section 5.0 which have High or Medium PIRT ranking for pressurization events. The analysis also considers the uncertainty in core power. The key outputs from these cases are core neutron flux and dome pressure. These are chosen since they are the critical parameters that effect $\Delta\text{CPR}/\text{ICPR}$ and peak pressure. Figures 7-11 through 7-16 present the TRACG results as compared to the test data. Bands are set to ± 2 sigma. The bands are determined by calculating the standard deviation for the output variable at each time step in the 59 trials.

Figure 7-11. PB TT Test 1 Statistical Peak Power Response

Figure 7-12. PB TT Test 1 Statistical Dome Pressure Response

Figure 7-13. PB TT Test 2 Statistical Peak Power Response

Figure 7-14. PB TT Test 2 Statistical Dome Pressure Response

Figure 7-15. PB TT Test 3 Statistical Peak Power Response

Figure 7-16. PB TT Test 3 Statistical Dome Pressure Response

7.6.2 Nine Mile Point-2 Pump Upshift Statistical Analysis

Statistical analyses were performed for the Nine Mile Point-2 pump upshift described in Section 7.1 of the Qualification LTR [2]. The analysis includes random variation (59 trials) of the model uncertainties described in Section 5.1 which have High or Medium PIRT ranking for flow events. The analysis also considers the uncertainty in core power. The key outputs from this case are core neutron flux and core flow. These are chosen since they are the critical parameters that affect $\Delta\text{CPR}/\text{ICPR}$. Figures 7-17 and 7-18 present the TRACG results as compared to the test data. Bands are set to ± 2 sigma. The bands are determined by calculating the standard deviation for the output variable at each time step in the 59 trials.

Figure 7-17. NMP-2 Pump Upshift Statistical Peak Power Response

Figure 7-18. NMP-2 Pump Upshift Statistical Core Flow Response

7.6.3 Leibstadt Loss of Feedwater Statistical Analysis

Statistical Analyses were performed for the Leibstadt loss of feedwater flow startup test described in Section 7.1 of the Qualification LTR [2]. The analysis includes random variation (59 trials) of the model uncertainties described in Section 5.1 which have High or Medium PIRT ranking for pressurization events. The key output from this case is wide range level. Figure 7-19 presents the TRACG results as compared to the test data. Bands are set to ± 2 sigma. The bands are determined by calculating the standard deviation for the output variable at each time step in the 59 random trials.

Figure 7-19. Leibstadt Loss of Feedwater Statistical Wide Range Level Response

8.0 DEMONSTRATION ANALYSIS

The analyses provided in this Section form the bases for future application of TRACG. The analyses provided are a demonstration of the process.

Plant operating limits can not be derived directly from the demonstration analyses. The implementation of TRACG will require repetition of the statistical analysis for a grouping of similar plants with similar events and similar fuels (for example TTNB for BWR4/5 plants with RPT and GE13 fuel). The results of the statistical analysis will be applicable to the grouping. A specific application will require a nominal analysis. The nominal results will be combined with the statistical uncertainties for the grouping.

The TRACG performance is demonstrated on one or more limiting licensing basis events in each of the scenarios specified in Section 2.5. In some scenarios the events are not evaluated with respect to the uncertainties since the initial condition is more limiting than the transient condition. This demonstration includes:

1. a TRACG analysis for a representative plant (the analysis will be performed with an analysis procedure equivalent to that applied in plant USAR evaluations),
2. a demonstration of the sensitivity of the transient to initial conditions and plant parameters,
3. a demonstration of the sensitivity of the transient to the individual model uncertainties, and
4. a statistical analysis in accordance with the process defined in Section 7.5.

The overall statistical application of TRACG was validated in Section 7.6, where it was shown that sample data falls within the statistical tolerance bands on the predictions or is conservative.

8.1 Baseline Analysis

A baseline analysis was performed for each of the event scenarios. A typical BWR/4 type plant is used for all the baseline cases. The plant has 560 bundles and a rated thermal power of 2558 MWth. The vessel modeling is illustrated in Figure 8-1. The plant is loaded with fresh and exposed GE13 9x9 fuel and contains exposed GE9B 8x8 fuel. Figure 8-2 illustrates the TRACG core map and channel grouping.

Figure 8-1. TRACG BWR/4 Vessel Modeling

	1	2	3	4	5	6	7	8	9	10	11	12	13	
1									20	20	20	20	20	52
2								20	21	21	21	21	21	50
3					20	20	20	21	21	21	22	21	22	48
4				20	21	21	21	21	21	22	23	22	23	46
5			20	21	21	21	22	21	22	21	22	24	25	44
6			20	21	21	22	23	22	23	25	26	25	24	42
7			20	21	22	23	22	24	25	24	27	24	27	40
8		20	21	21	21	22	24	25	26	27	26	25	26	38
9	20	21	21	21	22	23	25	26	27	24	25	24	25	36
10	20	28	21	22	21	25	24	29	24	25	24	24	24	34
11	20	21	22	23	22	26	27	26	25	24	30	24	30	32
12	20	21	21	22	24	25	24	25	24	24	24	30	24	30
13	20	21	22	23	25	24	27	26	25	24	30	24	24	28
	1	3	5	7	9	11	13	15	17	19	21	23	25	

Fuel Type	Group #	Vessel Ring	Number of Channels	Avg Radial Peaking
GE9 (8x8)	20	3	76	0.38
GE9 (8x8)	21	2	136	0.80
GE13 (9x9)	22	2	72	1.24
GE9 (8x8)	23	2	32	1.12
GE9 (8x8)	24	1	100	1.07
GE13 (9x9)	25	1	64	1.38
GE9 (8x8)	26	1	32	1.22
GE13 (9x9)	27	1	24	1.41
GE13 (9x9)	28	2	4	0.72
GE13 (9x9)	29	1	4	1.41
GE13 (9x9)	30	1	16	1.32

Figure 8-2. TRACG Core Map and Channel Grouping

Channel groups were created based on core position, fuel type, orifice geometry, and peaking factor. Out of the 11 groups, a four bundle hot group (single bundle in quarter core) and a multi-bundle, hot group were created for CPR analysis. Channel group 29 is the single hot channel, whereas channel 27 is the multi-channel, hot group. For cases where a significant distribution in the radial power distribution existed, the channels were re-grouped to accurately represent the average and hot bundles.

The following events are analyzed with this model:

1. Pressurization event: turbine trip without bypass (TTNB), feedwater controller failure (FWCF), and main steam line isolation valve closure with the backup (flux) scram (MSIVF);
2. Depressurization events: upscale failure of pressure regulator (PRFO);

3. Core flow transient: two recirculation pump trip (2PTR) and recirculation flow controller failure (RFCF);
4. Cold water transient: loss of feedwater heating (LFWH).
5. Level transient: complete loss of feedwater flow (LOFW);

8.1.1 Baseline Analysis of Pressurization Transients

8.1.1.1 Turbine Trip No Bypass (TTNB) Baseline Analysis

The TTNB event is characterized by the fast closure of the turbine stop valves (TSV). The sudden closure of the stop valves causes a rapid pressurization of the steam lines and reactor vessel, resulting in a rapid power excursion. The event is heightened by the assumed failure of the pressure relief function provided by the turbine bypass valves. The turbine stop valve position switches initiate a reactor scram and recirculation pump trip (RPT). Power is mitigated with the help of negative reactivity due to the scram and due to void production as the RPT reduces core flow and as the heat flux rises. The safety/relief valves actuate as the steamline pressure rises to the setpoint. This action limits the pressure rise. The event is modeled at 100% power and 100% flow with an EOC nominal power shape. The key parameters are presented in Figures 8-3 through 8-6 and Table 8-1 for the TTNB event.

Figure 8-3. TRACG Power and Flow Response for TTNB Event

Figure 8-4. TRACG CPR Response for TTNB Event

Figure 8-5. TRACG Pressure and Relief Valve Response for TTNB Event

8.1.1.2 Feedwater Controller Failure (FWCF) Baseline Analysis

The FWCF event is characterized by the feedwater flow controller failing to the maximum demand value. This causes an increase in the feedwater flow. The water level rises until the high level trip setpoint (L8) is reached. When L8 is reached, a high level turbine trip is initiated, the feedwater pumps are tripped off, recirculation pumps are tripped off, and a reactor scram is initiated. The turbine trip causes a rapid pressurization event that results in a power excursion similar, but less severe than the TTNB. Power is mitigated with the help of negative reactivity due to the scram and due to void production as the RPT reduces core flow and as the heat flux rises. The safety/relief valves actuate as the steamline pressure rises to the setpoint. This action limits the pressure rise. The event is modeled at 100% power and 100% flow with an EOC nominal power shape. The key parameters are presented in Figures 8-7 through 8-10 and Table 8-2 for the FWCF event.

Figure 8-7. TRACG Power and Flow Response for FWCF Event

Figure 8-8. TRACG CPR Response for FWCF Event

Figure 8-9. TRACG Pressure and Relief Valve Response for FWCF Event

8.1.1.3 MSIV Closure Flux Scram (MSIVF) Baseline Analysis

The MSIV closure is characterized by closure of the main steam isolation valves. The closure causes a rapid pressurization event that leads to a power excursion. The reactor scram is conservatively assumed to occur on high flux rather than the earlier isolation valve position. Power is mitigated with the help of negative reactivity due to the scram and due to void production as the heat flux rises. The safety/relief valves actuate as the steamline pressure rises to the setpoint. This action limits the pressure rise. This is the limiting event for vessel overpressure protection. The primary output is peak pressure response. The event is modeled at 100% power and 100% flow with an EOC nominal power shape. The key parameters are presented in Figures 8-11 through 8-13 and Table 8-3 for the MSIVF event.

Figure 8-11. TRACG Power and Flow Response for MSIVF Event

Figure 8-12. TRACG Pressure and Relief Valve Response for MSIVF Event

Figure 8-13. TRACG Vessel Inlet and Exit Flow for MSIVF Event

8.1.2 Baseline Analysis of Depressurization Transients

8.1.2.1 Pressure Regulator Failed Open (PRFO) Baseline Analysis

The PRFO event is characterized by failure of the pressure regulator to the controller upper limit. The turbine control valves and bypass valves respond by opening, increasing steam flow, and dropping turbine inlet pressure. The depressurization causes the RPV water level to swell causing a Level 8 turbine trip. Reactor scram is automatically initiated by turbine trip. The event is modeled at 100% power and 100% flow with an EOC nominal core power shape. The key parameters are presented in Figures 8-14 through 8-17 and Table 8-4 for the PRFO event.

Figure 8-14. TRACG Power and Flow Response for PRFO Event

Figure 8-15. TRACG CPR Response PRFO Event

Figure 8-16. TRACG Pressure and Bypass Valve Response for PRFO Event

8.1.3 Baseline Analysis of Core Flow Transients

8.1.3.1 Two Recirculation Pump Trip (2PTR) Baseline Analysis

The 2PTR event is initiated by the inadvertent simultaneous opening of the recirculation pump motor line breakers. An abrupt reduction in core flow increases the core void fraction and thereby increases water level and reduces reactor power. An automatic reactor scram is not initiated for this event. The event is modeled at 100% power and 100% flow with an EOC nominal power shape. The key parameters are presented in Figures 8-18 through 8-21 and Table 8-5 for the 2PTR event.

Figure 8-18. TRACG Power and Flow Response for 2PTR Event

Figure 8-19. TRACG CPR Response 2PTR Event

Figure 8-20. TRACG Pressure Response for 2PTR Event

8.1.3.2 Recirculation Flow Controller Failure (RFCF) Baseline Analysis

The RFCF event is characterized by an upscale failure of the recirculation motor/generator speed controller in one loop. The B loop fluid coupler velocity is assumed to increase at a rate of 25%/sec. The pump speed increases to maximum in about 3 seconds. The APRM high neutron flux trip is assumed to be disabled so that an automatic scram is not initiated for this event (will discuss further in Section 8.2). The event is modeled at 50% power and 40% flow at MOC. The key parameters are presented in Figures 8-22 through 8-25 and Table 8-6 for the RFCF event.

Figure 8-22. TRACG Power and Flow Response for RFCF Event

Figure 8-23. TRACG CPR Response for RFCF Event

Figure 8-24. TRACG Recirculation Response for RFCF Event

8.1.4 Baseline Analysis of Cold Water Transients

8.1.4.1 Loss of Feedwater Heating (LFWH) Baseline Analysis

The LFWH event is characterized by the reduction in core inlet subcooling caused by a reduction in feedwater heating. The increase of inlet subcooling increases moderation and causes an increase in power. An automatic reactor scram does not occur for this event. The event assumes a 30 second feedwater heater time constant. The event is modeled at 100% power and 100% flow at representative MOC conditions. The key parameters are presented in Figures 8-26 through 8-29 and Table 8-7 for the LFWH event.

Figure 8-26. TRACG Power and Flow Response for LFWH Event

Figure 8-27. TRACG CPR Response LFWH Event

Figure 8-28. TRACG Pressure and Feed Temperature Response for LFWH Event

8.1.5 Baseline Analysis of RPV Level Transients

8.1.5.1 Loss of Feedwater (LOFW) Baseline Analysis

The Loss of Feedwater Flow (LOFW) event is characterized by a rapid water level reduction after all FW flow is tripped. Low water level scram occurs early in the event. Low water level setpoint logic initiates automatic reactor scram, trips the recirculation pumps and initiates high pressure makeup with the Reactor Core Isolation Cooling (RCIC) system. This system mitigates the level reduction and maintains reactor water level above the top-of-active fuel (TAF). The baseline analysis of this event is modeled at 100% power and 100% flow with an EOC nominal power shape. The key parameters are presented in Figures 8-30 through 8-33 and Table 8-8 for the LOFW event.

Figure 8-30. TRACG Power and Flow Response for LOFW Event

Figure 8-31. TRACG Downcomer Water Level Response for LOFW Event

Figure 8-32. TRACG Pressure Response for LOFW Event

8.2 Initial Condition and Plant Parameter Review

8.2.1 Initial Conditions and Allowable Operating Range

As described in Section 6.2, the impact of the initial condition on the results are characterized in the following manner:

Figure 8-34. Typical Power/Flow Map

Figure 8-35. EOC Axial Power Shape

Figure 8-36. MOC Nominal Rod Pattern

Figure 8-37. MOC Black and White Rod Pattern

Figure 8-38. EOC High Worth Scram Rods

Based on the analysis results, all trends could be characterized. Where applicable, the application procedure will require analysis at the limiting initial condition.

8.2.1.3 MSIVF Allowable Operating Range Results

A summary of the results of the sensitivity analysis for the MSIVF transient is provided in Table 8-14.

Table 8-14

MSIVF ALLOWABLE OPERATING RANGE RESULTS

The characterization of these results is described in Table 8-15.

Table 8-15

MSIVF ALLOWABLE OPERATING RANGE CHARACTERIZATIONS

Based on the analysis results, all trends could be characterized. Where applicable, the application procedure will require analysis at the limiting initial condition.

Table 8-19

RFCF ALLOWABLE OPERATING RANGE CHARACTERIZATIONS

8.2.1.7 LFWH Allowable Operating Range Results

A summary of the results of the sensitivity analysis for the FWCF transient is provided in Table 8-20.

8.2.1.8 LOFW Allowable Operating Range Results

A summary of the results of the sensitivity analysis for the LOFW transient is provided in Table 8-22.

Table 8-22

LOFW ALLOWABLE OPERATING RANGE RESULTS

The characterization of these results is described in Table 8-23.

Table 8-23

LOFW ALLOWABLE OPERATING RANGE CHARACTERIZATIONS

Based on the analysis results, all trends could be characterized. The nominal initial condition may be assumed for all parameters.

8.2.2 Initial Conditions Uncertainty

As described in Section 6.2, the initial condition is monitored through the use of plant sensors or on-line calculations based on plant sensors. Because of instrument or simulation uncertainty, the plant condition may vary from the indicated value. The results are characterized in the following manner:

Table 8-24

INITIAL CONDITION UNCERTAINTY CHARACTERIZATIONS

With the exception of core power, the results from the allowable operating range evaluations, documented in Section 8.2.1, are used for the characterization.

Table 8-25

TTNB INITIAL CONDITION UNCERTAINTY RESULTS

The characterization of these results is described in Table 8-26.

Table 8-26

TTNB INITIAL CONDITION UNCERTAINTY CHARACTERIZATIONS

Table 8-27

FWCF INITIAL CONDITION UNCERTAINTY RESULTS

The characterization of these results is described in Table 8-28.

Table 8-28

FWCF INITIAL CONDITION UNCERTAINTY CHARACTERIZATIONS

8.2.2.3 MSIVF Initial Condition Uncertainty Results

A summary of the results of the core power sensitivity analysis for the MSIVF transient is provided in Table 8-29.

Table 8-29

MSIVF INITIAL CONDITION UNCERTAINTY RESULTS

The characterization of these results is described in Table 8-30.

Table 8-30

MSIVF INITIAL CONDITION UNCERTAINTY CHARACTERIZATIONS

8.2.2.4 PRFO Initial Condition Uncertainty Results

A summary of the results of the core power sensitivity analysis for the PRFO transient is provided in Table 8-31.

Table 8-31

PRFO INITIAL CONDITION UNCERTAINTY RESULTS

Results are not sufficiently sensitive to any of the initial conditions uncertainties to yield a positive $\Delta\text{CPR}/\text{ICPR}$.

8.2.2.5 2PTR Initial Condition Uncertainty Results

A summary of the results of the core power sensitivity analysis for the 2PTR transient is provided in Table 8-32.

Table 8-32

2PTR INITIAL CONDITION UNCERTAINTY RESULTS

Results are not sufficiently sensitive to any of the initial conditions uncertainties to yield a positive $\Delta\text{CPR}/\text{ICPR}$.

8.2.2.6 RFCF Initial Condition Uncertainty Results

A summary of the results of the core power sensitivity analysis for the RFCF transient is provided in Table 8-33.

Table 8-33

RFCF INITIAL CONDITION UNCERTAINTY RESULTS

The characterization of these results is described in Table 8-34.

Table 8-34

RFCF INITIAL CONDITION UNCERTAINTY CHARACTERIZATIONS

8.2.2.7 LFWH Initial Condition Uncertainty Results

A summary of the results of the core power sensitivity analysis for the LFWH transient is provided in Table 8-35.

Table 8-35

LFWH INITIAL CONDITION UNCERTAINTY RESULTS

The characterization of these results is described in Table 8-36.

Table 8-36

LFWH INITIAL CONDITION UNCERTAINTY CHARACTERIZATIONS

8.2.2.8 LOFW Initial Condition Uncertainty Results

A summary of the results of the core power sensitivity analysis for the FWCF transient is provided in Table 8-37.

Table 8-37

LOFW INITIAL CONDITION UNCERTAINTY RESULTS

The characterization of these results is described in Table 8-38.

Table 8-38

LOFW INITIAL CONDITION UNCERTAINTY CHARACTERIZATIONS

8.2.3 Plant Parameters

As described in Section 6.3, critical plant parameters will be set at a bounding value (for example the APRM flux scram setpoint will be set to the maximum value in the analysis). This process is described in the procedure that defines the critical Operating Parameters for Licensing (OPL) for transient analysis. For BWR/2 through BWR/5 plants, the scram speed is assumed to vary with the statistical distribution described in Table 6-2. Only the OLMCPR defining pressurization events will assume the statistical scram speed. Table 8-39 shows the sensitivity of the TTNB and FWCF event to scram speed.

Table 8-39

SCRAM SPEED UNCERTAINTY RESULTS

The scram speed uncertainty is added to the parameters in the statistical analysis.

8.2.4 Summary of Initial Conditions and Plant Parameter

The conclusions from the initial conditions and plant parameter analysis form the basis of the plant specific analysis process. The following can be concluded based on the initial condition and plant parameter analysis results:

Pressurization Events:

Depressurization Transients:

8.3 Fuel Rod Thermal-Mechanical Performance

For fast transients like TTNB, the heat flux is not as effective in determining the margin to centerline melt and 1% strain. The most limiting rated power case for the BWR/4 plant presented in this demonstration is a case with no RPT and with Tech Spec scram. The results of a calculation of peak centerline temperature and mid plain plastic strain are presented in Table 8-40. An additional case is analyzed scaling the nodal integrated powers by a factor of 1.5 in order to bound the 95/95 transient. A value of 1.5 was chosen since it is consistent with the change in the integral power peak for the worst case TTNB statistical trial (of 118 trials) described in Section 8.4.2.1.

Table 8-40

TTNB FUEL THERMAL-MECHANICAL RESULTS

8.4 Statistical Analysis for Licensing Events

A statistical analysis is performed for each of the event scenarios that result in a positive $\Delta\text{CPR}/\text{ICPR}$ and for the LOFW transient. The statistical analysis is provided as a demonstration of the statistical process. This analysis must be repeated or the application must be justified when the results are to be applied to other BWR types, other fuel types, or other plant hardware options (example Recirculation Pump Trip).

The statistical analysis is performed in two steps. First each High and Medium ranked parameter is evaluated at both the $+1\sigma$ and -1σ level (call this uncertainty screening). This allows for determination of the sensitivity of the results to the parameter. It allows for assessment of the reasonableness of the sensitivity. It also allows for quantification of the impact of parameters that are difficult to assign exact probability density functions. The second step is a random statistical evaluation. In this case each model parameter is varied randomly as described in Section 5.1.

8.4.1 Uncertainty Screening

8.4.1.1 TTNB Uncertainty Screening

Analysis has been performed at both the $+1\sigma$ and -1σ level. These results are presented in Figure 8-39.

Figure 8-39. TTNB Sensitivity to Individual Uncertainties

Figure 8-40. Void Fraction Response Comparing Base to - 1 σ Interfacial Shear

8.4.1.2 FWCF Uncertainty Screening

Analysis has been performed at both the $+1\sigma$ and -1σ level. These results are presented in Figure 8-41.

Figure 8-41. FWCF Sensitivity to Individual Uncertainties

8.4.1.3 MSIVF Uncertainty Screening

Analysis has been performed at both the $+1\sigma$ and -1σ level. These results are presented in Figure 8-42.

Figure 8-42. MSIVF Sensitivity to Individual Uncertainties

8.4.1.4 RFCF Uncertainty Screening

Analysis has been performed at both the $+1\sigma$ and -1σ level. These results are presented in Figure 8-43.

Figure 8-43. RFCF Sensitivity to Individual Uncertainties

Figure 8-44. Rod Heat Flux Response Comparing Base to +1 σ Fuel Heat Transfer

8.4.1.5 LFWH Uncertainty Screening

Analysis has been performed at both the $+1\sigma$ and -1σ level. These results are presented in Figure 8-45.

Figure 8-45. LFWH Sensitivity to Individual Uncertainties

8.4.1.6 LOFW Uncertainty Screening

Analysis has been performed at both the $+1\sigma$ and -1σ level. These results are presented in Figure 8-46.

Figure 8-46. LOFW Sensitivity to Individual Uncertainties

8.4.2 Statistical Results

Two sets of 59 random trials were performed for each of the event scenarios which resulted in a positive $\Delta\text{CPR}/\text{ICPR}$ and for the LOFW transient. The statistical parameters varied randomly are the model parameters in Section 5.1, 2% core power uncertainty, and scram speed (for the TTNBP and FWCF).

8.4.2.1 TTNB Statistical Analysis

The results of the statistical analysis for the TTNB event are presented in Figures 8-47 through 8-50.

Figure 8-47. Channel 29 $\Delta\text{CPR}/\text{ICPR}$ Normality for TTNB

Figure 8-48. Channel 29 Δ CPR/ICPR Descriptive Statistics for TTNB

Figure 8-49. Channel 29 % Δ CPR/ICPR Descriptive Statistics for TTNB

Figure 8-50. Channel 27 % Δ CPF/ICPR Descriptive Statistics for TTNB

8.4.2.2 FWCF Statistical Analysis

The results of the statistical analysis for the FWCF event are presented in Figures 8-51 through 8-54.

Figure 8-51. Channel 29 Δ CPR/ICPR Normality for FWCF

Figure 8-52. Channel 29 Δ CPR/ICPR Descriptive Statistics for FWCF

Figure 8-53. Channel 29 % Δ CPR/ICPR Descriptive Statistics for FWCF

Figure 8-54. Channel 27 % Δ CPR/ICPR Descriptive Statistics for FWCF

8.4.2.3 MSIVF Statistical Analysis

The results of the statistical analysis for the MSIVF event are presented in Figures 8-55 through 8-57.

Figure 8-55. Peak Pressure Normality for MSIVF

Figure 8-56. Peak Pressure Descriptive Statistics for MSIVF

Figure 8-57. Δ Peak Pressure Descriptive Statistics for MSIVF

Figure 8-58. Channel 29 Δ CPR/ICPR Normality for RFCF

Figure 8-59. Channel 29 Δ CPR/ICPR Descriptive Statistics for RFCF

Figure 8-60. Channel 29 % Δ CPR/ICPR Descriptive Statistics for RFCF

Figure 8-61. Channel 27 % Δ CPR/ICPR Descriptive Statistics for RFCF

8.4.2.5 LFWH Statistical Analysis

The results of the statistical analysis for the LFWH event are presented in Figures 8-62 through 8-65.

Figure 8-62. Channel 29 Δ CPR/ICPR Normality for LFWH

Figure 8-63. Channel 29 Δ CPR/ICPR Descriptive Statistics for LFWH

Figure 8-64. Channel 29 % Δ CPR/ICPR Descriptive Statistics for LFWH

Figure 8-65. Channel 27 % Δ CPR/ICPR Descriptive Statistics for LFWH

8.4.2.6 LOFW Statistical Analysis

Figure 8-66. Minimum Wide Range Level Normality for LOFW

Figure 8-67. Minimum Wide Range Level Descriptive Statistics for LOFW

Figure 8-68. % Change in Minimum Wide Range Level Descriptive Statistics for LOFW

9.0 TECHNICAL SPECIFICATION MODIFICATIONS

No Technical Specification or Technical Specification Bases revisions are required with the implementation of TRACG; however, Core Operating Limits Report (COLR) modifications will be required if the Selected Scram Rod option is implemented for pressurization event based OLM CPR.

The requirements for the Selected Scram Rod option are defined in the COLR as follows:

Requirements for Implementation of Selected Scram Rods

1. The plant is operating with the Selected Scram Rods in notch positions defined by Figure 9-1 (example).
2. All rods that are adjacent to the Selected Scram Rods are fully withdrawn.
3. The High Worth Scram Rods meet the Technical Specification scram speed requirements.

	1	2	3	4	5	6	7	8	9	10	11	12	13	14	15	16	17	18	19	20	21	22	23	24	25	26
1									+	+	+	+	+													
2																										
3					+		+		+	+	+		+		+											
4																										
5			+		+		+		+	+	3		+		+											
6											6															
7			+		+		+		+	+	+		+		+											
8																										
9	+		+		+		+		+	+	+		+		+											
10																										
11	+		+		+		+		+	+	+		+		+											
12																										
13	+		+		3		+		+	+	+		+		3											
14					6										6											
15	+		+		+		+		+	+	+		+		+											
16																										
17	+		+		+		+		+	+	+		+		+											
18																										
19			+		+		+		+	+	+		+		+											
20																										
21			+		+		+		+	+	3		+		+											
22											6															
23					+		+		+	+	+		+		+											
24																										
25									+	+	+		+		+											
26																										

Figure 9-1. BOC to EOC High Worth Scram Rods

10.0 REFERENCES

- [1] J. G. M. Andersen, et al., *TRACG Model Description*, NEDE-32176P, Rev. 2, December 1999.
- [2] J. G. M. Andersen, et al., *TRACG Qualification*, NEDE-32177P, Rev. 2, January 2000.
- [3] R. J. Pryor, et al., *TRAC-PIA, An Advanced Best Estimate Computer Program for PWR LOCA Analysis*, Los Alamos Scientific Laboratory, NUREG/CRA-0665, May 1979.
- [4] J. G. M. Andersen, K. H. Chu and J. C. Shaug, *BWR REFILL/REFLOOD Program Task 4.7 - Model Development, Basic Models for the BWR Version of TRAC*, GEAP-22051, NUREG/CR-2573, EPRI NP-2376, April 1983.
- [5] Y. K. Cheung, V. Parameswaran and J. C. Shaug, *BWR REFILL/REFLOOD Program Task 4.7 - TRAC BWR Component Models*, GEAP-22052, NUREG/CR-2574, EPRI NP-2377, April 1983.
- [6] Md. Alamgir, *BWR REFILL/REFLOOD Program Task 4.8 - TRAC-BWR Model Qualification for BWR Safety Analysis, Final Report*, GEAP-30157, NUREG/CR-2571, EPRI NP-2377, October 1983.
- [7] USNRC Standard Review plan - NUREG 0800
- [8] J. G. M. Andersen and C. L. Heck, *BWR Full Integral Simulation Test (FIST) Program, TRAC-BWR Model Development, Volume 1 - Numerical Methods*, GEAP-30875-1, NUREG/CR-4127-1, EPRI NP-3987-1, November 1985.
- [9] K. H. Chu, J. G. M. Andersen, Y. K. Cheung and J. C. Shaug, *BWR Full Integral Simulation Test (FIST) Program, TRAC-BWR Model Development, Volume 2 - Models*, GEAP-30875-2, NUREG/CR-4127-2, EPRI NP-3987-2, October 1985.
- [10] Y. K. Cheung, J. G. M. Andersen, K. H. Chu and J. C. Shaug, *BWR Full Integral Simulation Test (FIST) Program, TRAC-BWR Model Development, Volume 2 - Developmental Assessment for Plant Applications*, GEAP-30875-3, NUREG/CR-4127-3, EPRI NP-3987-3, October 1985.
- [11] W. A. Sutherland, Md. Alamgir J. A. Findlay and W. S. Hwang, *BWR Full Integral Simulation Test (FIST) Program, Phase II Test Results and TRAC-BWR Model Qualification*, GEAP-30876, NUREG/CR-4128, EPRI NP-3988, October 1985.
- [12] D. D. Taylor, et al., *TRAC-BD1/MOD1: An Advanced Best Estimate Program for Boiling Water Reactor Transient Analysis, Volumes 1-4*, NUREG/CR-3633, Idaho National Engineering Laboratory, April 1984.
- [13] J. A. Borkowski, et al., *TRAC-BF1/Mod1: An Advanced Best Estimate Program for BWR Accident Analysis*, NUREG/CR-4356, Idaho National Engineering Laboratory, August 1992.

- [14] J. A. Borkowski, et al., *TRAC-BF1/Mod1 Models and Correlations*, NUREG/CR-4391, Idaho National Engineering Laboratory, August 1992.
- [15] *Qualification of the One-Dimensional Core Transient Model for Boiling Water Reactors*, NEDO-24154-A and NEDE-24154-P-A, Volumes I, II and III, August 1986.
- [16] B. S. Shiralkar, et al., *SBWR Test and Analysis Program Description*, NEDC-32391P, Rev. C, August 1995.
- [17] Takashi Hara, et al., *TRACG Application to Licensing Analysis*, (ICONE-7311), 7th International Conference on Nuclear Engineering, Tokyo, April 19-23, 1999.
- [18] *Analytical Model for Loss-of-Coolant Analysis in Accordance with 10CFR50 Appendix K*, NEDE-20566-P, December 1975.
- [19] (Not used)
- [20] B. S. Shiralkar, et al., *The GESTR-LOCA and SAFER Models for the Evaluation of the Loss-of-Coolant Accident, Volume III: SAFER/GESTR Application Methodology*, NEDE-23785-1-PA, Rev. 1, October 1984.
- [21] J. A. Findlay, et al., *SAFER Model Evaluation of Loss-of-Coolant Accidents for Jet Pump and Non-Jet Pump Plants, Volume II : SAFER/GESTR Application Methodology for Non-Jet Pump Plants*, NEDO-30996P, June 1986.
- [22] B. Boyack, et al., *Quantifying Reactor Safety Margins: Application of Code Scaling, Applicability, and Uncertainty Evaluation Methodology to a Large-Break, Loss-of-Coolant Accident*, NUREG/CR-5249, December 1989.
- [23] Nuclear Regulatory Commission, Office of Nuclear Regulatory Research, *Regulatory Guide 1.157, Best-Estimate Calculations of Emergency Core Cooling System Performance*, May 1989.
- [24] H. Glaeser and R. Pochard, *Review on Uncertainty Methods for Thermal Hydraulic Computer Codes*, International Conference on New Trends in Nuclear System Thermohydraulics Proceedings, Volume I, Pisa, Italy, May 30 and June 2, 1994, 447-455.
- [25] H. A. David, *Order Statistics (2nd edition)*, John Wiley & Sons, New York, 1969.
- [26] (Not used)
- [27] *Steady State Nuclear Methods*, NEDO-30130-A, April 1985.

- [28] *General Electric Standard Application for Reactor Fuel (GESTAR II)*, NEDE-24011-P-A-13, August 1996.
- [29] F. Odar, et al., "Safety Evaluation for the General Electric Topical Report *Qualification of the One-Dimensional Core Transient Model for Boiling Water Reactors*, NEDO24154P, Volumes I, II, and III," Prepared by Reactor Systems Branch, DSI, June 1980.
- [30] "Safety Evaluation for the *Qualification of the One-Dimensional Core Transient Model for Boiling Water Reactors*, NEDO24154P, Volumes I, II, and III" Memo from Paul S. Check, NRC to T. Novak, Assistant Director for Operating Reactors, NRC, October 1980.
- [31] (Not used)
- [32] Acceptance for Referencing of Licensing Topical Reports, *Methodology and Uncertainties for Safety Limit MCPR Evaluations*, NEDC-32601P; *Power Distribution Uncertainties for Safety Limit MCPR Evaluation*, NEDC-32694P; Letter from F. Akstulewicz (NCR) to G. A. Watford (GE) dated March 11, 1999.
- [33 - 53] (Not used)

Attachment A

NRC RAIs and Associated Responses

RAI 1

Request:

As discussed in the September 1, 2000, conference call, the staff intends to run some comparative calculations between the TRACG kinetics model and NRC methods. Please prepare and provide relevant information about fuel designs and core layout as well as the input deck to allow the staff to develop a model and run comparative cases. What is needed is as follows:

1. Core design,
2. Assembly design information including radial and axial enrichment information,
3. Control rod positions.

Response:

The requested core design information for a core at zero exposure was provided at the meeting on September 11, 2000 in the separate document titled "Hypothetical Initial Core of GE12"^[1-1]. This document includes the information necessary to construct a nuclear model for the core such as core loading, control rod patterns and detailed nuclear design information for the fuel bundles.

A sample TRACG input deck that describes the channel hydraulic conditions initialized at rated power and flow is contained in the file TT . INP file. This input file has been designed so that boundary conditions to the core can be easily perturbed in order to test the response of the neutronics model. This input file together with other input files needed to execute TRACG are include in the attached ZIP file RAI1 . ZIP. The included files are summarized in Table 1-1.

Table 1-1 Summary of Files Contained in RAI1.ZIP

Description	File Name	Format
primary input file	TT.INP	ASCII
input overlay to increase flow by 20%	F UP.INP	ASCII
input overlay to decrease flow by 20%	F DN.INP	ASCII
input overlay to increase pressure by 20%	P UP.INP	ASCII
input overlay to decrease pressure by 20%	P DN.INP	ASCII
input file to GRIT graphics output code	TT.GRI	ASCII
sample command file to run a 5-sec null transient	TT.COM	ASCII
sample command file to invoke a transient input overlay	TT .COM	ASCII
neutronics transient input file	TT.TDT	ASCII
neutronics static restart file (input)	SS .TSS	VMS binary
neutronics dynamic restart file (input)	SS .TTR	VMS binary

The link below the table title for Table 1-1 can be used to access and view the ZIP file from a PC. Use FTP in binary form to transfer the ZIP file to the VMS machine before expanding it in order to avoid potential machine-dependent conflicts with file and record formats. All the files on the ZIP file

are *input* files so it will be most convenient if they are extracted into the VMS directory from which the TRACG code will be executed. How the various input files are used is described in Appendix A of the user's manual^[1-2]. Changes will be required in the COM files to specify the appropriate default directory name and to reference the locations where the TRACG and GRIT executables have been installed. The TT.COM file will execute a 5-second null transient that is useful for testing the installation. No input parameters are needed to run TT.COM. The other command file, TT_.COM, file can be used to run some simple perturbations to the core boundary conditions. A single command line parameter specifying the basename of the input overlay file should be provided when using TT_.COM. Four such overlay files have been provided for illustration purposes.

The rest of this response provides some descriptive information regarding the sample input model that has been provided.

The input setup contains a truncated vessel model for the regions from the lower plenum to the upper plenum as suggested by the NRC staff during our phone conversations. This simple setup facilitates testing of the neutronics model since the core hydraulic conditions can easily be altered by changing the boundary conditions. Although the vessel model contains two radial rings, the outer ring corresponding to the downcomer region outside the core is not connected in this setup to the inner ring since the recirculation system is not modeled. Thus the core flow is determined by a FILL component connected directly to the lower plenum. Similarly, the core pressure is controlled by a PIPE and BREK component connected directly to the upper plenum.

The 560 fuel bundles in the core are modeled hydraulically by 11 TRACG CHAN components. The CHAN groups are shown in Figure 1-1. The "IAT" values tabulated in the figure correspond to the different fuel assembly types defined by PANACEA. For each unique assembly type there is an associated bundle number that defines the detailed nuclear design. The detailed bundle design information for these bundles was provided previously in Reference [1-1].

The initial control blade positions for this core were also previously indicated in Reference [1-1]. Typically control blades are not moved during AOO transients except for the case of a scram where all the control blades will accelerate and move into the core from their initial position at some prescribed rate. For the sample problem, additional flexibility for moving groups of control blades has been provided by specifying 10 different groups of control blades so that particular groups can be selectively moved. The control blade groupings are shown in Figure 1-2. The four bundles surrounding each control blade position are indicated by the dark lines that denote the boundaries of the control cells. The numbers denote the control blade group associated with the control cell. If desired, control blades within each group can be moved by specifying "TROD" in the *neutronics transient input file* TT.TDT.

Figure 1-1 Channel Groups

Figure 1-2 Control Cells for the Control Blade Groups

The ARK edit for the PANACEA wrapup provided previously in Appendix B of Reference [1-1] indicates a number of other key core hydraulic parameters that can be used to cross check for consistency with the TRACG steady state conditions. These hydraulic parameters are compared in Table 1-3.

Some of the details for the 11 channel groups that comprise the core for the provided sample problem are shown in Table 1-4. The tabulated values represent a single bundle in the channel group. Much more detailed information will be available from the TRACG output file or graphics file when the code is executed for the sample problem. The user's manual that has been provided^[1-2] describes the inputs and provides an example of the types of outputs that can be obtained.

A transient calculation was performed for each of the four input overlay files identified in Table 1-1. Each file specifies either a 20% step increase or decrease in either core pressure or total core flow. The perturbations are performed individually and instantaneously at time zero without change in any other quantity. The calculated total core power responses for these four scenarios are shown in Figure 1-3. Please note the logarithmic scale for the relative power. These four scenarios are provided as illustrations of how to use the input deck that has been provided to perform transient calculations for scenarios of interest to the NRC staff.

Table 1-2 Steady State Core Flow Components at Rated Power and Flow

Table 1-3 Core Hydraulic Parameters for Steady State at Rated Power and Flow

Table 1-4 Steady State Conditions for the Channel Groups

Figure 1-3

References for RAI 1

- [1-1] "Hypothetical Initial Core of GE12"; GE Proprietary; September 10, 2000. (Stored in DRF J11-03558)
- [1-2] TRACG02A User's Manual, NEDC-32956P, Rev. 0, February 2000.

RAI 2

Request:

The staff has examined the special power excersion reactor test benchmark discussed in the qualification topical report. Please provide the input deck so that additional calculations can be run.

Response:

The TRACG input deck and other files needed to run the special power excersion reactor test (SPERT) benchmark calculation are provided in the attached ZIP file RAI2 . ZIP. The included files are summarized in Table 2-1.

Table 2-1 Summary of Files Contained in RAI2.ZIP

Description	File Name	Format
TRACG command file to run steady state and transient	RUN.COM	ASCII
utility command file to delete all output files	CLEAN.COM	ASCII
SPERT test data for comparison	SPERT-TEST.DAT	ASCII
TRACG steady state input file	SPERT SS.INP	ASCII
TRACG transient input file	SPERT TR.INP	ASCII
neutronics steady state input file	SPERT SS.TDT	ASCII
neutronics transient input file	SPERT TR.TDT	ASCII
input file to GRIT graphics output code	SPERT.GRI	ASCII
PANACEA wrapup file	SPERT.WRP	VMS binary

The link below the table title for Table 2-1 can be used to access and view the ZIP file from a PC. Use FTP in binary form to transfer the ZIP file to the VMS computer before expanding it in order to avoid potential machine-dependent conflicts with file and record formats. All the files on the ZIP file are *input* files so it will be most convenient if they are extracted into the VMS directory from which the TRACG code will be executed. How the various input files are used and the output files that will be produced when the RUN.COM file is executed are described in Appendix A of the TRACG02A User's Manual^[2-1]. Changes will be required in the RUN.COM file to specify the appropriate default directory name and to reference the locations where the TRACG and GRIT executables have been installed. The RUN.COM file will execute a steady state case of 20 seconds followed by the transient case. The transient is calculated for only 0.5 seconds but the test data representing the power pulse covers only the first 0.289 seconds. For convenience the GRIT input specified in file SPERT.GRI has been setup to produce ASCII output in column form that can be readily plotted. This ASCII output will be written to SPERT_SS.GRA for the steady state and SPERT_TR.GRA for the transient.

Reference for RAI 2

[2-1] TRACG02A User's Manual, NEDC-32956P, Rev. 0, February 2000.

RAI 3

Request:

Please evaluate the sensitivity of burnup predictions on minimum critical power ratio (MCPR) for the transients of interest.

Response:

The method by which sensitivities to initial conditions are evaluated is described in NEDE-32906P Section 6.2. The issue of burnup prediction is associated with the quantity "core loading pattern and exposure distribution". Reload TRACG analysis will include analysis of reference core loading pattern. Sensitivities to core loading pattern and exposure distribution for each event scenario is provided in NEDE-32906P Section 8.2. Specific conclusions related to core loading pattern and exposure distribution are provided in Section 8.2.4.

RAI 4

Request:

Please evaluate the effects of power distribution uncertainty on MCPR for the transients of interest.

Response:

The method by which sensitivities to initial conditions are evaluated is described in NEDE-32906P Section 6.2. The issue of power distribution is associated with the quantities "axial power distribution" and "radial power distribution". Sensitivities to power distribution for each event scenario are provided in NEDE-32906P Section 8.2. Specific conclusions related to power distribution uncertainty are provided in Section 8.2.4.

The issue of power distribution is also important in the relationship of power distribution to ICPR. This relationship is described in NEDE-32906P Section 7.5.2.4.

RAI 5

Request:

Please discuss the method used to calculate the parameters A_f and A_d for use in the gamma smearing.

Response:

In general the values can be determined by Monte Carlo analyses. For AOO analyses the TRACG inputs SMEAR1 and SMEAR2 are retained at their default values of 1.0 since the net effect of gamma smearing from rod-to-rod is accounted for in the relative pin power distributions that are output from TGBLA. In other words, the R-factors that are based on relative pin powers already reflect the impact of rod-to-rod gamma smearing. Values of SMEAR1 and SMEAR2 less than 1.0 would be appropriate only when the fission densities are used directly to determine the rod peakings as may be done in some LOCA calculations. It is also important to note that the transient responses characterized in terms of $\Delta\text{CPR}/\text{ICPR}$ are insensitive to R-factor as has been demonstrated in Table 7-3 in Section 7.5.2.4 of NEDE-32906P.

RAI 6

Request:

Please evaluate the effect of the update interval for the spatial solution of the kinetics solver on the MCPR for the range of transients being considered for TRACG. Does solving this equation every amplitude/reactivity time step effect the results?

Response:

Table 6-1 Additional Sensitivity Studies to Neutronics Parameters.

10.1.1				
10.1.2				

RAI 7

Request:

Please evaluate the impact of using the implicit vs. explicit solver on the MCPR for the range of transients being considered for TRACG. What user guidance exists to help choosing which solver to use and when? What are the effects of using the explicit method in a component connected to a component using the implicit method?

Response:

The implicit thermal hydraulic solver is used for all AOO transients. The implicit solver was consistently used for the qualification and the proposed application. The explicit solver is only used in the channel component for time domain stability calculations. The central difference was implemented only for sensitivity studies and is not used for any applications.

The following excerpt from the *TRACG02A Users Manual* (NEDC-32956P) indicates how the thermal hydraulic solver is selected and the user guidance that is provided.

W3-I METHOD Methods flag for integration of thermal hydraulic equations. The implicit option is recommended, except for time domain stability calculations (channel only), where the explicit option is recommended.
0 = Explicit first order integration (Euler).
1 = Implicit first order integration (modified Euler).
2 = Second order central integration scheme.
(Default = 1).

Sensitivity of thermal hydraulic instability calculations to numerical method, time step size and nodalization is provided in Section 3.7 of the *TRACG Qualification* (NEDE-32177P, Rev. 2) LTR.

RAI 8

Request:

What is the effect of the "Central Difference Option Flag?" Describe the coding changes made to implement this option.

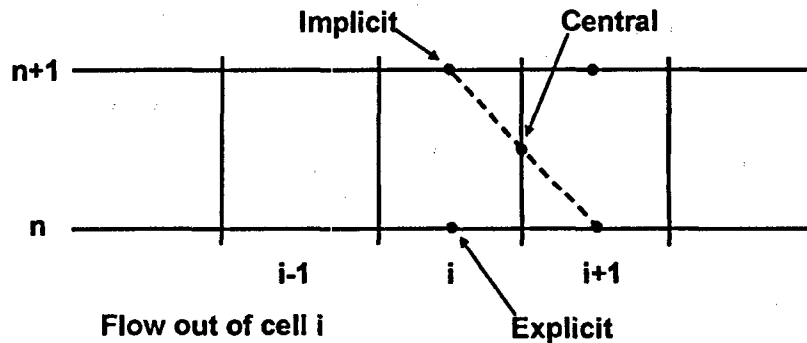
Response:

See the response to RAI 7 for details on which solver options are used. The effect that the hydraulic differencing schemes have on the coding is easiest to explain in terms of how it impacts the fluid property that is convected out of a cell. These impacts are illustrated below.

Explicit: $\rho_i^{n+1} - \rho_i^n = C[\rho_{i-1}^n - \rho_i^n]$; $C = \frac{v\Delta t}{\Delta x} > 0$ **First order**

Implicit: $\rho_i^{n+1} - \rho_i^n = C[\rho_{i-1}^{n+1} - \rho_i^{n+1}]$ **First order**

Central: $\rho_i^{n+1} - \rho_i^n = C[0.5(\rho_{i-1}^{n+1} - \rho_i^n) - 0.5(\rho_i^{n+1} - \rho_{i+1}^n)]$ **Second order**



RAI 9

Request:

How was the effect of channel grouping on MCPR evaluated?

Response:



RAI 10

Request:

What, if any, inconsistencies are present when a plant monitors the reactor with PANAC11 based methods with pin-power reconstruction when the operating and safety limits are determined using TRACG which is based on PANAC10? What are Global Nuclear Fuel's (GNF's) plans for implementing PANAC11 methods into TRACG? The staff considers the introduction of PANAC11 methods into TRACG a model change because the implementation of the kinetics equations into PANAC11 are for a steady-state solver, not a transient code such as TRACG.

Response:

We do not now nor do we intend to commingle these methods. Cores designed with PANAC10/TGBLA04 use GESAM01 which is based on PANAC10 to calculate the safety limit minimum critical power ratio (SLMCPR). Transient responses would be calculated with TRACG using the PANAC10-based methods for these cores. Similarly, cores designed with PANAC11/TGBLA06 use GESAM02 which is based on PANAC11 to calculate the SLMCPR and the transient responses would be evaluated using a TRACG version that has PANAC11-based kinetics.

The steps we intend to follow in performing code updates, process changes and input changes are described in Section 2.6 of the AOO LTR (NEDE-32906P, January 2000).

RAI 11

Request:

What effect does fuel pin grouping within CHAN have on the calculated MCPR and other relevant limits such as strain and linear heat generation rate (LHGR) limits? Justify the use of pre-defined fixed values for the pin power distribution.

Response:

The fuel pin grouping has negligible impact on the bundle hydraulic response since the total energy input at each axial level is not changed by the pin-to-pin power distribution at that level. TRACG does not model sub-channels.

For each rod type, the rod with the highest power determines the LHGR for that type. As is the case for MCPR, the limiting rod of each type can initially be placed on its respective limit using a pre-defined fixed distribution because the initial value is more important than transient variations that may occur within a particular plane. Rods with and without GAD are considered separately since they have different LHGR limits. These LHGR limits are determined such that no thermal-mechanical limits (i.e., plastic strain) will be exceeded during an over-power event. When TRACG is used to determine these LHGR limits, it is necessary to iterate to determine the highest initial LHGR value for each rod type such that the thermal-mechanical considerations are all satisfied even when conservatisms are added to account for uncertainties.

Pin power uncertainties are considered in the SLMCPR uncertainties.

RAI 12

Request:

Please discuss the benchmark values, biases and uncertainties referred to in section CIAX Void Coefficient, H, Pages 5-2 and 5-3 of TRACG Application for Anticipated Operational Occurrences Transient Analyses, NEDE-32906P. These come from MCNP01A to TGBLA04 comparisons.

Response:

Additional details are contained in the responses to RAI 13.

RAI 13: Void Coefficient

This RAI consists of parts (a) through (i). Requests are indicated in *italics*. The response for each part follows immediately after the request. The NRC requests in parts (b), (c), (e), (f), (g), and (i) have been marked as proprietary because they reveal GE proprietary information.

Request 13.a:

a) Given that TGBLA is a deterministic code, the fitted response surface of k_{inf} as a function of water density and exposure must be smooth and basically without residuals. On the other hand, the fitted response surface of k_{inf} for the corresponding MCNP calculation will have an error-in-fit and at each water density - exposure point a Monte Carlo standard error. In terms of these quantities, what is meant by uncertainty and bias? Please give the mathematical expressions for computing them.

Response 13.a:

The void coefficient (C_v) is introduced and defined as

$$C_v \equiv \frac{1}{k} \frac{\partial k}{\partial \alpha} \cong \frac{1}{k_\infty} \frac{\partial k_\infty}{\partial \alpha} \quad (1)$$

Request 13.b:

Response 13.b:

Request 13.c:

Response 13.c:

As stated in the response to part (a), the error is not the Monte Carlo error nor is it attributed to a fitting error. Monte Carlo histories play a limited role only in that there must be a sufficient number of histories so that errors in the k_∞ values from MCNP can be assumed to be negligible.

Request 13.d:

d) Why is a TGBLA calculation necessary to compute the void coefficient? It appears that it can be computed from only the Monte Carlo results. Moreover, since it is assumed the Monte Carlo results to be the "truth", bias would not be an issue.

Response 13.d:

Request 13.e:

Response 13.e:

Request 13.f:

Response 13.f:

Request 13.g:

Response 13.g:

Request 13.h:

h) Please explain why the results of the Anderson-Darling normality test are inconsistent, in a non-systematic fashion, from the percentage points quoted in Kendall and Stuart. In particular, in Figure 5-17 you have an A-Squared of 0.78 gives a p-value of 0.227; the comparable p-value given by Kendall and Stuart is around 0.05. For the cases in Figures 5-17, 5-19 and 5-21 give the Shapiro-Wilk statistic and the related p-value. Give the software package used to compute this statistic.

Response 13.h:

Note that the referenced figures pertain to comparisons of the jet pump calculations with data and have nothing to do with void coefficient. The request and response is addressed here to keep the requests in the same order as received from the NRC.

The source of the cited inconsistency in the Anderson-Darling normality test is not known. The A-Squared value indicated in Fig. 5-17 is 0.476 not 0.78 as cited in the

request. In Figure 5-7 where A-Squared is 0.732, the associated P-value is 0.055 which agrees favorably with the 0.05 P-value quoted in the request for Kendall and Stuart.

The software package used to calculate the Anderson-Darling statistics is *MINITAB for Windows* by Minitab, Inc. located in State College, Pennsylvania. The latest version of the program (Version 12) currently does not perform the requested Shapiro-Wilk test for normality but it does provide two tests for normality in addition to the Andersen-Darling test. One of these is stated by a user note in the program to be similar to Shapiro-Wilk normality test. These tests have been computed for the data in Figures 5-17, 5-19 and 5-21. The results are summarized in Table 13-1.

Table 13-1 Normality Test Results for Requested Quantities

Figure reference	Figure 5-17	Figure 5-19	Figure 5-21
Andersen-Darling Normality Test			
A-Squared	0.476	0.533	0.252
p-value	0.227	0.154	0.693
Ryan-Joiner W-Test for Normality (similar to Shapiro-Wilk)			
R	0.9777	0.9746	0.9856
p-value (approx.)	> 0.1000	> 0.1000	>0.1000
Kolmogorov-Smirnov Normality Test			
D+	0.104	0.171	0.079
D-	0.079	0.085	0.127
D	0.104	0.171	0.127
p-value (approx.)	> 0.15	0.081	>0.15

Note that the results shown in Figure 5-20 of the AOO LTR^[13-4] are not consistent with the statistics presented in Figure 5-21. Figure 5-20 as shown in the AOO LTR was generated using a preliminary jetpump input that is different than the final recommended value. Figure 5-20 based on the correct final code input is provided below. The erroneous figure will be replaced with the correct one shown below when NEDE-32906P is reissued to incorporate the results of the NRC review. Figure 5-21 in the AOO LTR is already correct since it was based on the final results.

Figure 5-20.

Request 13.i:

Response 13.i:

References for RAI-13

- [13-1] *Qualification of the One-dimensional Core Transient Model for Boiling Water Reactors*, NEDO-24154-A and NEDE-24154-P-A, Volumes I, II and III, August 1986.
- [13-2] Sitaraman, S., *MCNP: Light Water Reactor Critical Benchmarks*, NEDO-32028, Class 1, March 1992.
- [13-3] J. G. M. Andersen, et al., *TRACG Model Description*, NEDE-32176P, Rev. 2, December 1999.
- [13-4] J. G. M. Andersen, et al., *TRACG Application for Anticipated Operational Occurrences (AOO) Transient Analyses*, NEDE-32906P, January 2000.

RAI 14

Request:

Pellet Heat Transfer Parameters

What do you mean by "qualifying the overall model against fuel temperature data" at the bottom of page 5-12 of NEDE-32906P? What fuel temperature data? In-core measurements?

Response:

The data are in-core measurements of fuel centerline to coolant temperature differences. The data comes from test reactors such as the Halden reactor and are documented in the approved GESTR Licensing Topical Report:

B. S. Shiralkar, et al., The GESTR-LOCA and SAFER Models for the Evaluation of the Loss-of-Coolant Accident, Volume III: SAFER/GESTR Application Methodology, NEDE-23785-1-PA, Rev. 1, October 1984.

RAI 15.0

Request:

Analysis of Variance

- a) *Give the statistical model, as a mathematical expression, on which the analysis of variance is performed. Give the physical interpretation for each term. That is, what are the so called treatments or factor levels? Are there any interaction effects that should be taken into account? How do you treat the "measurement" error?*
- b) *Please state the statistical hypothesis that is at issue. Give the physical rationale for the choice.*
- c) *In terms of the above statistical model what is the meaning of the sum of squares terms in the context of the TRACG qualification.*
- d) *What are the results of "For the ANOVA technique, the sample variance (s^2) for all the Monte Carlo trails is analyzed" on page 7-6 of NEDE-32906P?*

Response:

All four parts of the request result from the misuse of the expression *Analysis of Variance* in Section 7.3.4 of NEDE-32906P. The method really is just the standard method for deriving tolerance bounds from samples of normal populations. The attached Sections 7.3.3 through 7.5.1 have been re-written to clarify the statistical approach.

ATTACHMENT – RAI 15

7.3.3 Order Statistics Method – Single Bounding Value (GRS)

The Monte Carlo method that has been used in Germany by Gesellschaft für Anlagen-und Reaktorsicherheit (GRS) [24] requires only a modest number of calculations, and automatically includes the effects of interactions between perturbations to different parameters. In this GRS method, Monte Carlo trials are used to vary all uncertain model and plant parameters randomly and simultaneously, each according to its uncertainty and assumed probability density function (PDF), and then a method based on the order statistics of the output values is used to derive upper tolerance bounds (one-sided, upper tolerance limits OSUTLs).

Monte Carlo sampling of each parameter according to its assigned PDF yields the value of that parameter to be used for a particular trial. Given such a trial set of input parameters, the calculation process determines the corresponding output parameter of interest. Therefore, while void coefficient might be set at a -1.5σ value, inter-facial shear might be set to a value of $+2.0\sigma$, each according to its own probability model. In this manner, the effects of interactions between all model parameters are captured in a single calculation. Once all of the trials have been completed, the desired output parameter (e.g., $\Delta\text{CPR}/\text{ICPR}$) is extracted from each of the trials and the set of parameter values is then used to construct an OSUTL for that particular output parameter. Figure 7-1 illustrates this process.

Individual TRACG overlay files containing all the perturbed parameter values are created for each separate trial. For each trial, this overlay file is appended to the end of the base transient input file and the TRACG calculation is performed to determine the output parameter value as a function of time for this particular transient and set of inputs. The process is repeated n times to define the sample values of the output parameter of interest for the particular transient under consideration. Similar samples for other parameters, for the same transient, can be generated at the same time without additional TRACG calculations.

An OSUTL is a function $U = U(x_1, \dots, x_n)$ of the data x_1, \dots, x_n (which will be the values of an output parameter of interest in a set of Monte Carlo trials), defined by two numbers $0 < \alpha, \beta < 1$, so that the proportion of future values of the quantity of interest that will be less than U is $100\alpha\%$, with confidence at least $100\beta\%$ --- this is called an OSUTL with $100\alpha\%$ -content and (at least) $100\beta\%$ confidence level.

The order statistics method, originally developed by Samuel Wilks, produces OSUTLs that are valid irrespective of the probability distribution of the data, requiring only that they be a sample from a continuous PDF. Given values of α and β , the OSUTL can be defined as the largest of the data values, provided the sample size $n \geq \log(1 - \beta) / \log \alpha$ [25]. For 95%-content and 95% confidence level, the minimum sufficient sample size is $n=59$.

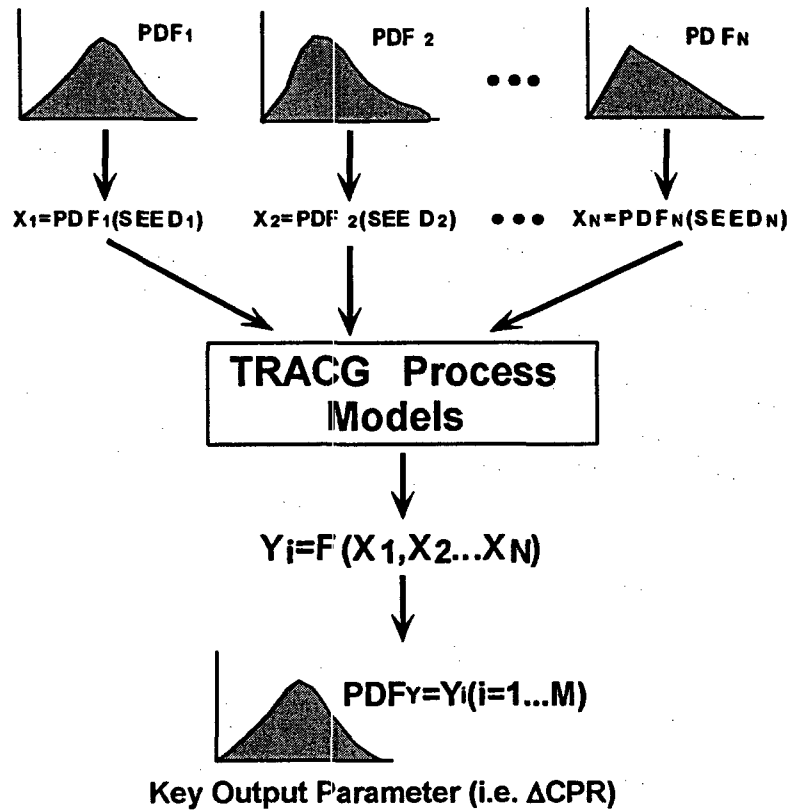


Figure 7-1. Schematic Process for Combining Uncertainties

The order statistics method is generally applicable, irrespective of the probability distribution of the data, and requires only that these be like outcomes of independent random variables with a common probability distribution.

If the method is implemented as described above, whereby the sample size (59) was chosen so that the sample maximum is the upper tolerance bound sought (95% content with 95% confidence), then this bound, as a random quantity, has variability that is typical of the maximum of a sample of that size, which can be substantial, and occasionally may yield an apparently conservative bound.

To mitigate this variability, one can choose a suitably larger sample size so that the bound sought is now given by the second or third largest sample value. For example, the 95% content with 95% confidence tolerance bound is the third largest observation in a sample of size 124: just for the sake of illustration, in normal (that is, Gaussian) populations its variability is about one half of the variability of the maximum in a sample of size 59; and in the more heavily-tailed Student's *t* distribution with 4 degrees of freedom, the variability of the third largest in a sample of size 123 is about one third of the variability of the maximum in a sample of size 59.

The following table summarizes the sample sizes that are required, when the bound is the largest, the second largest, or the third largest order statistic, all for 95% content and 95% confidence:

Order Statistic	Sample Size
Largest	59
2 nd Largest	93
3 rd Largest	124

7.3.4 Normal Distribution One-Sided Upper Tolerance Limit

If the data the tolerance bound will be derived from can reasonably be regarded as a sample from a normal (that is, Gaussian) probability distribution, then this normal distribution one-sided upper tolerance limit (ND-OSUTL) is of the form

$$ND - OSUTL_{\alpha,\beta} \equiv \bar{y} + z_{\alpha,\beta} \cdot s \quad (7-2)$$

where \bar{y} denotes the average of the outcomes of the TRACG trials, and s denotes their standard deviation, and the factor $z_{\alpha,\beta}$ is chosen to guarantee 100 α %-content and 100 β % confidence level. Since this factor $z_{\alpha,\beta}$ depends on the assumption of normality for the data, one must first ascertain whether the data does indeed conform with the Gaussian model, typically using one or several goodness-of-fit tests: for example, Ryan-Joiner's, Shapiro-Wilk's, or Anderson-Darling's. The values of $z_{\alpha,\beta}$ are tabulated in many statistical textbooks [25] as *factors for one-sided normal tolerance limits*. For example, for a sample of size $n = 59$, and a 95% content and a 95% confidence level, $z_{95,95} = 2.024$: as the sample size n increases, this factor approaches 1.645, the 95th percentile of the standard normal distribution. Unlike the order statistics method, this ND-OSUTL method does not require specific minimum sample sizes; but it does require normality. If the data are unlikely to have originated from a normal population, then one should use the order statistics method.

An example in Section 8.4.2.1 shows that the calculated values of Channel 29 Δ CPR/ICPR for the TTNB event may be regarded as a sample from a normal population, to which this ND-OSUTL method can be applied. Although the illustrations are presented only for Δ CPR/ICPR, the same approach can in principle be used to determine the total uncertainty in other calculated results such as centerline temperature, clad strain, vessel pressure, and downcomer water level, again provided the requirement of normality is met.

7.4 Recommended Approach for Combining Uncertainties

This approach to determine the total uncertainty has several advantages over other approaches as summarized in Table 7-2. The following expands on the discussion of these advantages:

-

-

-

-

Table 7-2

COMPARISONS OF METHODS FOR COMBINING UNCERTAINTIES

Method for Combining Uncertainties	Advantages	Disadvantages
Propagation of Errors	<p>Relatively small number computer runs, when the number of input variables is small. The number of cases is linearly related to the number of input parameter uncertainties considered.</p>	<p>Approximate because it involves linearization.</p> <p>Necessary either to demonstrate independence of effects of individual uncertainties on responses, or else must include covariances explicitly.</p>
Response Surface	<p>Very precise statistical characterization of results with a large number of Monte Carlo Trials using response surface.</p> <p>Different distributions can be specified for each input uncertainty.</p> <p>Independence of the effect of individual input parameters on response is not necessary.</p>	<p>Number of computer runs depends on the response surface model and increases exponentially with the number of input parameter uncertainties considered.</p> <p>Interactions between input parameters have to be established and considered in the development of the response surface.</p>
Order Statistics (GRS)	<p>The number of random trials is independent of the number of input parameters considered.</p> <p>The method requires no assumptions about the PDF of the output parameter.</p> <p>It is not necessary to perform separate calculations to determine the sensitivity of the response to individual input parameters.</p> <p>It is not necessary to make assumptions about the effect on the output of interactions of input parameters.</p>	<p>Since the tolerance limits are based on order statistics, they will vary from one set of TRACG trials to another, and these differences may be substantial, especially for small sets of TRACG trials, and particularly if the tolerance bound is the sample extremum.</p>

Normal Distribution One-sided Upper Tolerance Limit (ND-OSUTL)	The number of random trials is independent of the number of input parameters considered. Only a relatively small number of random trials is needed for a precise statistical characterization of the results. It is not necessary to perform separate calculations to determine the sensitivity of the response to individual input parameters. It is not necessary to make assumptions about the effect on the output of interactions of input parameters.	The normality of the PDF for the output variable must be demonstrated.
---	--	--

- The OSUTL for each output parameter of interest can be defined over the entire duration of the transient. That is, it is not limited to using only the peak values for the output variables over the duration of the event analyzed or the values at a particular point in time.

The advantage of the order statistics method is that it does not depend on the PDF of the output variable, and the disadvantage is that the OSUTLs, because they are based on order statistics, will vary from one set of TRACG trials to another, and these differences may be substantial, especially for small sets of TRACG trials, and particularly if the tolerance bound is the sample maximum. The ND-OSUTL method, on the other hand, provides an OSUTL that typically is less sensitive to the particular values in the sample of TRACG trial values, but depends on the output variable being normally distributed.

7-5 Implementation of Statistical Methodology

The purpose of this section is (1) to describe the process by which the statistical results will be used to determine the Operating Limit Minimum Critical Power Ratio (OLMCPR), and (2) to establish that fuel thermal/mechanical performance, peak vessel pressure, and minimum water level all have acceptable margins to design limits. The application to the last three is straightforward, and is discussed in the next section. The determination of the OLMCPR is more involved, and is detailed in the subsequent sections.



RAI 16.0

Request:

Statistical Limits

- a) *Please state the theorem and give the reference to support the statement on page 7-6 of NEDE-32906P: "Statistical theory provides that for an output that is a continuous function of many inputs, the sample mean of this PDF will be approximated by a normal distribution even if the distribution function for the variable itself is not normally distributed."*
- b) *The discussion of one-sided tolerance limits on pages 7-6 and 7-7 of NEDE-32906P appears to confuse the properties of statistical confidence intervals and tolerance intervals. A confidence interval provides an interval estimate for the unknown mean. Tolerance limits differ from confidence intervals in that tolerance limits provide an interval within which at least a specified proportion P of the population lies, with a specified probability $1-\alpha$. What is $z_{95,95}$? Equation (7-2) is incorrect, and all derivations of limits based on it are therefore also incorrect! Therefore, Eqs. 7-3 through 7-7 are not correct.*
- c) *The statement at the bottom of page 7-9: "The p-value must be greater than 0.05 to be considered normal." is too dogmatic.*
- d) *What is the confidence associated with $SLMCRP_{99,9}$ discussed in section 7.5.2.1 of NEDE-32906P? How is it established?*
- e) *In Section 7.5.2.2 of NEDE-32906P how is $\Delta CPR_{95,95}$ precisely defined/computed? Is this value only associated with the limiting transient?*

Response:

- a) The original statement is incorrect, and indeed the exact or approximate normality of the mean of the TRACG results is irrelevant in this context. To apply the method described in 7.3.2, *Normal Distribution One-Sided Upper Tolerance Limit*, one first needs to ascertain that the results of the TRACG trials are not unlike a sample from a normal population, by means of one or several tests of goodness-of-fit: please refer to the attachment to RAI 15, which includes those portions of the report that were re-written and pertain to this issue.
- b) For the revised discussion of tolerance bounds, please refer to the attachment to RAI 15, in particular to 7.3.1, *Order Statistics Method – Single Bounding Value (GRS)*.

c) For the revised version of the relevant passage, please refer to the attachment to RAI 15, in particular to 7.3.2, *Normal Distribution One-Sided Upper Tolerance Limit*.

d) The SLMCPR_{99.9} is determined at a 50% confidence level as described in Appendix IV of GETAB^[16-1].

e) The currently-approved process for calculating $\Delta\text{CPR}_{95/95}$ is defined in Reference [16-2]. The current ODYN process is illustrated in Figure 16-1. The proposed process for TRACG is illustrated in Figure 16-2.

References for RAI 16

[16-1] *General Electric BWR Thermal Analysis Basis (GETAB): Data, Correlation and Design Application*, NEDO-10958-A, January 1977.

[16-2] F. Odar, et al., *Safety Evaluation for the General Electric Topical Report Qualification of the One-Dimensional Core Transient Model for Boiling Water Reactors*, NEDO-24154 and NEDE-24154-P, Volumes I, II and III, Prepared by Reactor Systems Branch, DSI, June 1980.

Figure 16-1

Figure 16-2

RAI 17

Request:

OLMCPR computation issues

- a. In Section 7.5.2.3 of NEDE-32906P, what is meant in Step 1 by:
- (1) "A TRACG statistical study will be performed for each AOO, ..." other than generating the two distributions in Figure 7-6? How many TRACG transient calculations are done "for each type of AOO, for each class of BWR plant type, and for each fuel type"?
 - (2) In the last sentence "the evaluation is performed in the range of operating CPRs rather than at the minimum point in the transient."
 - (3) What is meant by the term "generic" when referring to $\Delta\text{CPR}/\text{ICPR}$?
- b. In the expression $\Delta\text{CPR}/\text{ICPR}$, in the context of Figure 7-6 of NEDE-32906P, are both ΔCPR and ICPR random variables? If so, are they independent?
- c. The use of the term "bias" in this context is confusing. In general, it refers to the difference between the truth and either a calculation or the mean of a series of measurements; you appear to mean the transient component of CPR. Is that correct?
- d. In Step 2 are the "nominal initial conditions" those which lead to the limiting rod?
- e. Are the Monte Carlo calculations in Step 3 for the same plant/cycle/event as in Step 2?

Response:

- a. With respect to Step 1 of Section 7.5.2.3 of NEDE-32906P:
- (2) The process block in Figure 7-5 "Establish Base Core Conditions SLMCPR = Core MCPR" represents the MCPR point in a transient even though the method is a steady state method. The process block in Figure 7-8 "Establish Base Core Conditions OLMCPR = Core MCPR" represents the pre-transient MCPR and therefore an operable condition. The trials shown in Figure 7-8 are performed at conditions representative of operating conditions (approximately 100% core power) rather than at conditions representing the minimum point in the transient (typically greater than 110% core power).

- c. The term "bias" in Section 7.5.2.3 refers to the difference between the nominal value of $\Delta\text{CPR}/\text{ICPR}$ and the mean value of $\Delta\text{CPR}/\text{ICPR}$.

RAI 18

Request:

Validation

- a) *What is "validated" by a code, calculation that shows the output is insensitive to variations in the input? It may be true for the model, but what does it have to do with reality?*
- b) *In the last paragraph on page 7-20 of NEDE-32906P the reference to Figure 7-8 appears to be incorrect.*
- c) *Please comment on the following observation: A TRACG solution is analogous to a correlated time series; the solution at the next time step is dependent on the current solution. In such cases, the error in the solution is cumulative and similar, for example, to the behavior shown in Figures 7-12 and 7-14 of NEDE-32906P. Why does the error in Figures 7-11 and 7-13 decrease past the peak of the function value?*

Response:

- a) The "validation" presented in Section 7.5.2.4 is targeted at how the model is to be applied. Validation of the model itself relative to reality relies on the extensive qualification bases documented in NEDE-32177P. These qualification bases validate the model by showing that all the relevant real phenomena and processes are adequately modeled. The validation presented in Section 7.5.2.4 of NEDE-32906P should be viewed with respect to the components that influence the model's calculation of steady state ICPR and the components that influence the calculation of the transient MCPR. Critical power ratio (CPR) is a calculated quantity for which real data does not exist thus one must validate the processes that are important to determining CPR and the key quantities that are needed to perform these calculations. The steady state process used to get the initial conditions important for determining ICPR has been validated against plant uncertainties. The NRC staff has reviewed and approved this process as documented in: "Acceptance for Referencing of Licensing Topical Reports, *Methodology and Uncertainties for Safety Limit MCPR Evaluations*, NEDC-32601P; *Power Distribution Uncertainties for Safety Limit MCPR Evaluation*, NEDC-32694P; Letter from F. Akstulewicz (NCR) to G. A. Watford (GE) dated March 11, 1999".

Accurate simulation of the transient processes and phenomena has been demonstrated through the extensive qualification in NEDE-32177P. Four of the key full scale plant data comparisons are shown in Section 7.6.

- b) The figure number in the last paragraph on page 7-20 of NEDE-32906P should be Figure 7-9. Furthermore, the figure number in the second to last paragraph on page 7-20 should be Figure 7-6.

RAI 19

Request:

a) *A question has come up regarding the field equations in TRACG, to be more specific, the manner in which density is handled. Please explain how density is defined for steam and noncondensable gas as used in NEDE-32176, Eqn 3.1-22 and following. Addition of simple densities is not correct and should follow the Law of Additive Volumes, or Amagat's equation. This looks like it is using mass forms, but please clarify.*

b) *Also, shouldn't equations B-18 and B-20a be in terms of partial pressure rather than total pressure?*

Response 19a:

There are two methods for dealing with gas mixtures. One method is to apply Amagat's law. This is equivalent to assuming that the components of the gas are segregated each into their own volume. Each volume is determined such that the pressure in each volume is equal. The volumes of the gases are additive and any volume not occupied by liquid is accounted for by the sum of the gas volumes. For this method the pressure in each volume equals the pressure in the other volumes and all are equal to the total pressure for the node. Other relationships that apply for this method are provided in the column labeled "Method 1" of Table 19-1.

Another more common modeling approach is to assume that all gases are mixed as a Gibbs-Dalton mixture in a single gas volume. TRACG02A uses this second approach which is the same model that was first implemented in TRAC-BD1 in 1983^[19-1] when the capability to model noncondensable gases was added. Other TRAC codes^[19-2, 19-3] use the same approach as does RELAP/5^[19-4]. For this second method all gas components (steam and noncondensable gases) are assumed to be intimately mixed so that they occupy the same volume. The individual components are diluted, thus the component densities are reduced relative to the pure fluid component densities. The component reduced or partial densities add to equal the total gas density. The pressures for the individual gas components are partial pressures since they are evaluated using the partial densities. The partial pressures sum to define the total gas pressure according to Dalton's law for partial pressures. For the implementation in TRAC, all the gases are assumed to be at the same temperature which need not be equal to the saturation temperature for the steam. Other relationships that apply for this method are provided in the column labeled "Method 2" of Table 19-1. Method 2 is what is used in TRACG02A.

For both methods the gas volume(s) and the liquid volume sum to the total nodal volume. For both methods the liquid pressure is equal the total gas pressure and this pressure is the total nodal pressure. The key distinction between the methods is the assumption that is made regarding the mixing of the gaseous fluid components. In TRACG02A (as in the other TRAC codes) the assumption is that all the gases are mixed and share a common gas volume. All the fluid relationships consistent with this assumption then follow. They are correctly applied.

Table 19-1 Comparison of Two Methods for Modeling Multi-Component Fluids

	Method 1	Method 2 (used in TRACG)
essential relationship	Amagat's law	Dalton's law of partial pressures
masses	$M = M_l + M_g$ $M_g = M_s + M_a$	$M = M_l + M_g$ $M_g = M_s + M_a$
volumes	$V = V_l + V_g$ $V_g = V_s + V_a$	$V = V_l + V_g$ $V_g = V_s + V_a$
volume fractions	$1 - \alpha = \frac{V_l}{V}$ $\alpha = \frac{V_g}{V} = \frac{V_s + V_a}{V}$ $\beta = \frac{V_a}{V_g}$ $V_a = \beta V_g, V_s = (1 - \beta)V_g$	$1 - \alpha = \frac{V_l}{V}$ $\alpha = \frac{V_g}{V} = \frac{V_s}{V} = \frac{V_a}{V}$ β is not defined (or needed) $V_a = V_g, V_s = V_g$
densities total liquid combined gases	$\rho = \frac{M}{V}$ $\rho_l = \frac{M_l}{V_l}$ $\rho_g = \frac{M_g}{V_g} = \frac{M_s + M_a}{V_s + V_a}$	$\rho = \frac{M}{V}$ $\rho_l = \frac{M_l}{V_l}$ $\rho_g = \frac{M_g}{V_g} = \frac{M_s + M_a}{V_g}$
gas component densities	gas total densities $\rho_s = \frac{M_s}{V_s}$ $\rho_a = \frac{M_a}{V_a}$ $\rho_g = \frac{M_g}{V_g} = \frac{V_s \rho_s + V_a \rho_a}{V_g}$ $= (1 - \beta)\rho_s + \beta\rho_a$	gas reduced densities $\rho_s = \frac{M_s}{V_s} = \frac{M_s}{V_g}$ $\rho_a = \frac{M_a}{V_a} = \frac{M_a}{V_g}$ $\rho_g = \frac{M_g}{V_g} = \frac{V_s \rho_s + V_a \rho_a}{V_g}$ $= \rho_s + \rho_a$
fluid mixture density	$\rho = (1 - \alpha)\rho_l + \alpha\rho_g$ $= (1 - \alpha)\rho_l + \alpha[(1 - \beta)\rho_s + \beta\rho_a]$	$\rho = (1 - \alpha)\rho_l + \alpha\rho_g$ $= (1 - \alpha)\rho_l + \alpha\rho_s + \alpha\rho_a$
pressures	gas total pressures $P = P_g = P_l$ $P_s = P_g = P$ $P_a = P_g = P$	gas partial pressures $P = P_g = P_l$ $P_g = P_s + P_a$

Response 19b:

The TRACG02A code correctly makes the distinction between total pressure and the partial pressure due to steam. The steam properties are evaluated at the partial steam pressure ($P_s = P - P_a$) and the air properties are evaluated at the partial air pressure (P_a). This usage is implied by the context in Appendix B but had not been specifically called out. In Appendix B where steam properties are given, P represents the pressure of the steam, i.e., the partial steam pressure. Similarly, where air properties are given, P represents the pressure of the air, i.e., the partial air pressure.

To eliminate the possibility of confusion, Appendix B has been revised to specifically indicate where partial pressures are used. A copy of the clarified appendix in its entirety follows. Revision bars in the left margin are used to indicate where the revisions have been made. The revision bars on Equations (B-1a, b, c) indicate changes from Rev. 1 of NEDE-32176P and are not associated with the clarifications given in this response. All other indicated revisions are associated with this response.

The TRACG02A code correctly makes the distinction between total pressure and the partial pressure due to steam. To make this evident in the documentation, we will revise Appendix B of NEDE-32176P (as indicated in the attachment to this response) for the next publication.

References for RAI 19

- [19-1] W. L. Weaver, III; *TRAC-BWR Completion Report: Noncondensable Gas Model*, WR-CD-83-062 (Rev), January 1983.
- [19-2] *TRAC-BF1/MOD1: An Advanced Best-Estimate Computer Program for BWR Accident Analysis; Model Description*, NUREG/CR-4356, EGG-2626, Volume 1, August 1992.
- [19-3] *TRAC-PF1/MOD1: An Advanced Best-Estimate Computer Program for Pressurized Water Reactor Thermal Hydraulic Analysis*, NUREG/CR-3858, LA-10157-MS, July 1986.
- [19-4] *RELAP5/MOD2 Models and Correlations*, NUREG/CR-5194, EGG-2531, July 1988.

APPENDIX B

THERMODYNAMIC AND TRANSPORT FLUID PROPERTIES

B.1 Introduction

Thermodynamic and transport property subroutines used in TRACG are based on polynomial fits to steam table data for water and ideal gas behavior for the noncondensable gas. Transport property fits were obtained from Reference B-1 and thermodynamic property fits were obtained from Reference B-2. Both the thermodynamic and transport property routines are used by all TRACG component modules. Tables B-1 through B-6 list the values of the constants. The nomenclature used in this Appendix is consistent with the terminology defined in Section 3.

Table B-1
Polynomial Constants for Thermodynamic Properties of Water and Air

C ₁	= 117.8	C ₂₄	= 1.3
C ₂	= 0.223	C ₂₆	= 0.3
C ₃	= 255.2	C ₂₈	= 1.0 x 10 ⁵
C ₄	= 958.75	C ₄₀	= 273.0
C ₅	= -0.856 6	C ₄₁	= 239.36
C ₆	= 2.619 410 618 x 10 ⁶	C ₄₂	= 2.786 7
C ₇	= -4.995 x 10 ¹⁰	C ₄₃	= -5.776 26
C ₈	= 3.403 x 10 ⁵	C ₄₄	= 3.938
C ₉	= 1.066 554 48	C ₄₅	= 1.0 x 10 ⁻⁶
C ₁₀	= 1.02 x 10 ⁻⁸	C ₄₇	= 1.0 x 10 ³
C ₁₁	= -2.548 x 10 ⁻¹⁵	C ₄₈	= -0.15 x 10 ³
C ₁₂	= 2.589 600 x 10 ⁶	C ₄₉	= -20.0
C ₁₃	= 6.350 x 10 ⁻³	C ₅₁	= 0.657 x 10 ⁻⁶
C ₁₄	= -1.058 2 x 10 ⁻⁹	C ₅₂	= 2.996 018 036 x 10 ³
C ₁₅	= 1.076 4	C ₅₃	= 9.700 016 602 x 10 ³
C ₁₆	= 3.625 x 10 ⁻¹⁰	C ₅₄	= -8.448 077 393 x 10 ³
C ₁₇	= -9.063 x 10 ⁻¹⁷	C ₅₅	= 8.349 824
C ₂₀	= 461.7	C ₅₆	= 3.495 194 44 x 10 ²
C ₂₁	= 2.0 x 10 ⁶	C _{k0}	= -8.335 44 x 10 ⁻⁴
C ₂₃	= 647.3	C _{k2}	= -2.247 45 x 10 ⁻¹⁷
ELC0	= 1.758 80 x 10 ⁴	ELE0	= 2.283 789 029 x 10 ⁹
ELC1	= 3.740 2 x 10 ³	ELE1	= -2.622 156 77 x 10 ⁷
ELC2	= 4.024 35	ELE2	= 1.129 486 67 x 10 ⁵
ELC3	= -0.015 729 4	ELE3	= -2.162 339 85 x 10 ²
ELC4	= 3.130 1 x 10 ⁻⁵	ELE4	= 0.155 283 438
ELD0	= 6.185 27 x 10 ⁶	C _{vg}	= 714.9
ELD1	= -8.145 47 x 10 ⁴	R	= 287.12
ELD2	= 4.465 98 x 10 ²		
ELD3	= -1.041 16		
ELD4	= 9.260 22 x 10 ⁻⁴		

Table B-1
Polynomial Constants for Thermodynamic Properties of Water and Air
(Continued)

CVL1	= 1.002 136 23	CVH1	= 2.252 62
CVL2	= -5.632 785 x 10 ⁻⁵	CVH2	= 0.014 859 4
CVL3	= -8.971 304 77 x 10 ⁻⁹	CVH3	= -7.154 88 x 10 ⁻⁵
CVL4	= -2.282 874 59 x 10 ⁻⁵	CVH4	= -0.010 458 8
CVL5	= 4.765 967 87 x 10 ⁻⁷	CVH5	= -1.029 62 x 10 ⁻⁴
CVL6	= 5.021 318 x 10 ⁻¹⁰	CVH6	= 5.091 35 x 10 ⁻⁷
CVL7	= 4.101 156 58 x 10 ⁻⁶	CVH7	= 2.592 66 x 10 ⁻⁵
CVL8	= -3.803 989 08 x 10 ⁻⁹	CVH8	= 1.724 1 x 10 ⁻⁷
CVL9	= -1.421 997 52 x 10 ⁻¹²	CVH9	= -8.984 19 x 10 ⁻¹⁰

Table B-2
Derived Constants for Thermodynamic Properties of Water and Air

A1	= C ₁ • C ₂ /C ₂₈	A11	= 2 • C ₂₆ /(C ₂₄ • C ₂₀)
A2	= C ₂ - 1.0	A13	= A11 • (1.0 + C ₂₆)
A3	= -C ₄ • C ₅ /C ₂₃	A12	= 1.0/A13
A4	= C ₅ - 1.0	A14	= 1.0/C ₂₈
A5	= C ₄₅ • C ₄₉	A15	= 1.0/C ₂₃
A6	= 2 C ₄₅ • C ₄₈	A16	= 2 • C ₁₁
A7	= 4 • C ₄₄ • C ₄₅	A17	= 2 • C ₁₄
A8	= 3 • C ₄₃ • C ₄₅	A18	= 2 • C ₁₇
A9	= 2 • C ₄₂ • C ₄₅	A19	= 2 • C ₄₈ • C ₄₅
A10	= C ₄₁ • C ₄₅	A20	= C ₄₅ • C ₄₉
DELC0	= ELC1	DELD0	= ELD1
DELC1	= 2 • ELC2	DELD1	= 2 • ELD2
DELC2	= 3 • ELC3	DELD2	= 3 • ELD3
DELC3	= 4 • ELC4	DELD3	= 4 • ELD4
DELE0	= ELE1		
DELE1	= 2 • ELE2		
DELE2	= 3 • ELE3		
DELE3	= 4 • ELE4		

Table B-3
Basic Constants for Transport Properties of Water and Air

B_{0l}	=	$2.394\ 907 \times 10^{-4}$	B_{1l}	=	$-5.196\ 250 \times 10^{-13}$
C_{0l}	=	$1.193\ 203 \times 10^{-11}$	C_{1l}	=	$2.412\ 704 \times 10^{-18}$
D_{0l}	=	$-3.944\ 067 \times 10^{-17}$	D_{1l}	=	$-1.680\ 771 \times 10^{-24}$
		C_{1g}	=	$1.688\ 359\ 68 \times 10^3$	
		C_{2g}	=	$0.602\ 985\ 6$	
		C_{3g}	=	$4.820\ 979\ 623 \times 10^2$	
		C_{4g}	=	$2.953\ 179\ 05 \times 10^7$	
		C_{5g}	=	1.8	
		C_{6g}	=	4.60×10^2	

Table B-4
Liquid Viscosity Constants

A_{0l}	=	$1.299\ 470\ 229 \times 10^{-3}$	B_{0l}	=	$-6.595\ 9 \times 10^{-12}$
A_{1l}	=	$-9.264\ 032\ 108 \times 10^{-4}$	B_{1l}	=	6.763×10^{-12}
A_{2l}	=	$3.810\ 470\ 61 \times 10^{-4}$	B_{2l}	=	$2.888\ 25 \times 10^{-12}$
A_{3l}	=	$-8.219\ 444\ 458 \times 10^{-5}$	B_{3l}	=	$4.452\ 5 \times 10^{-13}$
A_{4l}	=	$7.022\ 437\ 984 \times 10^{-6}$			
D_{0l}	=	$3.026\ 032\ 306 \times 10^{-4}$	E_{0l}	=	$1.452\ 605\ 261\ 2 \times 10^{-3}$
D_{1l}	=	$-1.836\ 606\ 896 \times 10^{-4}$	E_{1l}	=	$-6.988\ 008\ 498\ 5 \times 10^{-9}$
D_{2l}	=	$7.567\ 075\ 775 \times 10^{-5}$	E_{2l}	=	$1.521\ 023\ 033\ 4 \times 10^{-14}$
D_{3l}	=	$-1.647\ 878\ 879 \times 10^{-5}$	E_{3l}	=	$1.230\ 319\ 494\ 6 \times 10^{-20}$
D_{4l}	=	$1.416\ 457\ 633 \times 10^{-6}$			
F_{0l}	=	$-3.806\ 350\ 753\ 3 \times 10^{-11}$	h_0	=	$8.581\ 289\ 699 \times 10^{-6}$
F_{1l}	=	$3.928\ 520\ 767\ 7 \times 10^{-16}$	c_{0n}	=	$4.265\ 884 \times 10^4$
F_{2l}	=	$-1.258\ 579\ 929\ 2 \times 10^{-21}$	P_i	=	$6.894\ 575\ 293 \times 10^5$
F_{3l}	=	$1.286\ 018\ 078\ 8 \times 10^{-27}$			
h_{00}	=	$3.892\ 077\ 365 \times 10^{-6}$	e_{h0}	=	$6.484\ 503\ 981 \times 10^{-6}$
e_{c0n}	=	$5.535\ 88 \times 10^4$	c_n	=	$4.014\ 676 \times 10^5$
h_1	=	2.76×10^5	h_2	=	3.94×10^5

**Table B-5
Vapor Viscosity Constants**

A_{0g}	= 3.53×10^{-8}	B_{1g}	= 0.407×10^{-7}
A_{1g}	= 6.765×10^{-11}	C_{1g}	= 8.04×10^{-6}
A_{2g}	= 1.021×10^{-14}	D_{1g}	= 1.858×10^{-7}
		E_{1g}	= 5.9×10^{-10}
F_{1g}	= -0.2885×10^{-5}	G_{1g}	= 176.0
F_{2g}	= 0.2427×10^{-7}	G_{2g}	= -1.6
F_{3g}	= $-0.6789333 \times 10^{-10}$	G_{3g}	= 0.0048
F_{4g}	= $0.6317037037 \times 10^{-13}$	G_{4g}	= $-0.474074074 \times 10^{-5}$
H_{l1}	= 1.708×10^{-5}	H_{u1}	= 1.735×10^{-5}
H_{l2}	= 5.927×10^{-8}	H_{u2}	= 4.193×10^{-8}
H_{l3}	= 8.14×10^{-11}	H_{u3}	= 1.09×10^{-11}
T_1	= 573.15		
T_2	= 648.15		

**Table B-6
Thermal Conductivity Constants**

h_0	= 5.815×10^5
A_{l0}	= 0.573 738 622
A_{l1}	= 0.253 610 355 1
A_{l2}	= -0.145 468 269
A_{l3}	= 0.013 874 724 85
C	= 2.1482×10^5
A_{g0}	= 1.76×10^{-2}
A_{g1}	= 5.87×10^{-5}
A_{g2}	= 1.04×10^{-7}
A_{g3}	= -4.51×10^{-11}
B_{g0}	= 1.0351×10^{-4}
B_{g1}	= 0.4198×10^{-6}
B_{g2}	= -2.771×10^{-11}

B.2 Thermodynamic Properties

Subroutine THERMO supplies thermodynamic properties for TRACG. The input variables are pressure, liquid, and vapor temperatures. The output variables include (a) saturation temperature, (b) the derivative of T_{sat} with respect to pressure, (c) internal energy, (d) density, (e) the derivatives of internal energy and density with respect to pressure for each phase, and (f) the derivatives of internal energy and density with respect to temperature for each phase. Subroutine THERMO also includes an ideal gas option to calculate the density, internal energy, and their associated derivatives with respect to pressure and temperature for the noncondensable.

The ranges of validity for the thermodynamic properties supplied by THERMO are $280.0 \text{ K} \leq T_{\ell} \leq 647.0 \text{ K}$, $280.0 \text{ K} \leq T_v \leq 3000.0 \text{ K}$, and $1.0 \times 10^3 \text{ Pa} \leq P \leq 190.0 \times 10^5 \text{ Pa}$. If THERMO is provided with data outside this range, it adjusts the data to the corresponding limit and issues a warning message.

Polynomial equations for the various properties used in THERMO are given below. Values of the constants are given in Tables B-1 and B-2.

B.2.1 Saturation Properties

B.2.1.1 Temperature

For $T_{\text{sat}} \leq C_{23}$ (higher saturation temperatures cause THERMO to abort):

$$T_{\text{sat}} = C_1 Y^{C_2} + C_3 - dT_1 - dT_2 \quad (\text{B-1a})$$

where

$$Y = A_{14} P$$

In this expression P can be either the partial steam pressure or the total pressure since saturation temperatures corresponding to both pressures are calculated in TRACG. The general assumption, however, is that the saturation temperature at the interface is given by the partial steam pressure, i.e., $Y = A_{14} P_s$.

dT_1 and dT_2 are correction terms to improve the prediction at low pressures and are given by:

$$dT_1 = -1.298 + Y \left(4.01 \times 10^{-2} - Y \left(3.548 \times 10^{-4} - Y 9.62 \times 10^{-7} \right) \right) \quad (\text{B-1b})$$

$$dT_2 = 11.5 \left(948.55 + \left(2.344785 - \log_{10}(Y) \right)^{6.75} \right)^{0.148148} - 31.75 \quad (\text{B-1c})$$

The derivative of the saturation temperature is obtained by analytical differentiation of the above expressions.

B.2.1.2 Internal Energy

For $P_s \leq C_{21}$

$$e_{\text{sat}} = C_6 + C_7 \left(\frac{1.0}{C_8 + P_s} \right) \quad (\text{B-2a})$$

For $P_s > C_{21}$

$$e_{\text{sat}} = C_{12} + (C_{14} P_s + C_{13}) P_s \quad (\text{B-2b})$$

For $P_s \leq C_{21}$

$$\frac{\partial e_{\text{sat}}}{\partial P_s} = -C_7 \left(\frac{1.0}{C_8 + P_s} \right)^2 \quad (\text{B-2c})$$

and for $P_s > C_{21}$

$$\frac{\partial e_{\text{sat}}}{\partial P_s} = C_{13} + A_{17} P_s \quad (\text{B-2d})$$

B.2.1.3 Heat Capacity

$$C_{\text{ps}} = C_{52} + T_1 (C_{53} T_1 + C_{54}) + \left(\frac{C_{55} + C_{56}}{T_1} \right) \quad (\text{B-3a})$$

and

$$\frac{\partial C_{\text{ps}}}{\partial P} = -A_{15} \frac{\partial T_{\text{sat}}}{\partial P} \left[C_{54} + 2C_{53} T_1 - \frac{\left(\frac{2C_{55} + C_{56}}{T_1} \right)}{T_1^2} \right] \quad (\text{B-3b})$$

where

$$T_1 = 1.0 - A_{15} T_{\text{sat}}$$

B.2.1.4 Enthalpy

$$h_g = e_{\text{sat}} \gamma_s \quad (\text{B-4a})$$

and

$$\left. \frac{\partial h_g}{\partial P_s} = \frac{\partial e_{sat}}{\partial P_s} \gamma_s \right| \quad (B-4b)$$

where

$$\left. \begin{aligned} \gamma_s &= C_9 + (C_{11}P_s + C_{10})P_s \text{ for } P_s \leq C_{21} \\ &= C_{15} + (C_{17}P_s + C_{16})P_s \text{ for } P_s > C_{21} \end{aligned} \right|$$

$$h_f = e_\ell(T_{sat}) + \frac{P}{\rho_\ell(T_{sat})}$$

$$\frac{\partial h_f}{\partial P} = \frac{\partial \rho_\ell}{\partial P} \bigg|_{T_{sat}} + \frac{1}{\rho_\ell(T_{sat})} - \frac{P}{\rho_\ell^2(T_{sat})} \frac{\partial \rho_\ell}{\partial T} \bigg|_{T_{sat}} \left(\frac{\partial T_{sat}}{\partial P} + \frac{\partial \rho_\ell}{\partial P} \right)$$

and e_ℓ , ρ_ℓ , and their derivatives are evaluated using the liquid equations given below.

B.2.2 Liquid Properties

B.2.2.1 Internal Energy

$$TLC = T_\ell - 273.15$$

$$\left. PSL = \frac{\left[\frac{(T_\ell - C_3)^{1/C_2}}{C_1} \right]}{A_{14}} \right|$$

$$ELP = (P - PSL)(C_{k0} + C_{k2} PSL^2)$$

and

$$ERT = \frac{-C_{k0} + C_{k2}(2 \cdot PSL \cdot P - 3 \cdot PSL^2)}{A_1(A_{14} \cdot PSL)^{A_2}}$$

There are three temperature domains used in evaluating the liquid internal energy:

- (1) $T_\ell < 548.15$
- (2) $548.15 \leq T_\ell \leq 611.15$
- (3) $T_\ell > 611.15$

For $T_\ell < 548.15$:

$$e_\ell = ELC0 + ELC1 \cdot TLC + ELC2 \cdot TLC^2 + ELC3 \cdot TLC^3 + ELC4 \cdot TLC^4 + ELP \quad (B-5a)$$

$$\frac{\partial e_\ell}{\partial T} = \text{DELCO} + \text{DELC1} \cdot \text{TLC} + \text{DELC2} \cdot \text{TLC}^2 + \text{DELC3} \cdot \text{TLC}^3 + \text{ERT}. \quad (\text{B-5b})$$

For $548.15 \leq T_\ell \leq 611.15$:

$$e_\ell = \text{ELD0} + \text{ELD1} \cdot \text{TLC} + \text{ELD2} \cdot \text{TLC}^2 + \text{ELD3} \cdot \text{TLC}^3 + \text{ELD4} \cdot \text{TLC}^4 + \text{ELP}. \quad (\text{B-6a})$$

$$\frac{\alpha e_\ell}{\partial T} = \text{DELD0} + \text{DELD1} \cdot \text{TLC} + \text{DELD2} \cdot \text{TLC}^2 + \text{DELD3} \cdot \text{TLC}^3 + \text{ERT}. \quad (\text{B-6b})$$

For $T_\ell > 611.15$:

$$e_\ell = \text{ELE0} + \text{ELE1} \cdot \text{TLC} + \text{ELE2} \cdot \text{TLC}^2 + \text{ELE3} \cdot \text{TLC}^3 + \text{ELE4} \cdot \text{TLC}^4 + \text{ELP}. \quad (\text{B-7a})$$

$$\frac{\alpha e_\ell}{\partial T} = \text{DELE0} + \text{DELE1} \cdot \text{TLC} + \text{DELE2} \cdot \text{TLC}^2 + \text{DELE3} \cdot \text{TLC}^3 + \text{ERT}. \quad (\text{B-7b})$$

For all three temperature domains:

$$\frac{\partial e_\ell}{\partial P} = C_{k0} + C_{k2} \cdot \text{PSL}^2. \quad (\text{B-8})$$

B.2.2.2 Density

Define $\text{PBAR} = 1.0 \times 10^{-5} P$ and $\text{TLC} = T_\ell - 273.15$. There are three temperature domains:

- (1) $T_\ell > 525.15$
- (2) $T_\ell < 521.15$
- (3) $521.15 \leq T_\ell \leq 525.15$

For $T_\ell > 525.15$:

$$\rho_\ell = 1.43 + \frac{1000}{(\text{CVH1} + \text{CVH2} \cdot \text{PBAR} + \text{CVH3} \cdot \text{PBAR}^2 + \beta_1 \cdot \text{TLC} + \gamma_1 \cdot \text{TLC}^2)} \quad (\text{B-9a})$$

$$\frac{\partial \rho_\ell}{\partial P} = -(\rho_\ell - 1.43)^2 \cdot 1.0 \times 10^{-8} [\text{CVH2} + 2 \cdot \text{CVH3} \cdot \text{PBAR} + \text{TLC}(\text{CVH5} + 2 \cdot \text{CVH6} \cdot \text{PBAR}) + \text{TLC}^2(\text{CVH8} + 2 \cdot \text{CVH9} \cdot \text{PBAR})] \quad (\text{B-9b})$$

$$\frac{\partial \rho_\ell}{\partial T_\ell} = -(\rho_\ell - 1.43)^2 \cdot 1.0 \times 10^{-3} (\beta_1 + 2 \cdot \gamma_1 \cdot \text{TLC}) \quad (\text{B-9c})$$

where

$$\beta_1 = CVH4 + CVH5 \cdot PBAR + CVH6 \cdot PBAR^2$$

and

$$\gamma_1 = CVH7 + CVH8 \cdot PBAR + CVH9 \cdot PBAR^2.$$

For $T_\ell < 521.15$:

$$\rho_\ell = \frac{1000}{(CVL1 + CVL2 \cdot PBAR + CVL3 \cdot PBAR^2) + \beta_1 \cdot TLC + \gamma_1 \cdot TLC^2} - 2.01 \quad (B-10a)$$

$$\frac{\partial \rho_\ell}{\partial P} = -(\rho_\ell + 2.01)^2 \cdot 1.0 \times 10^{-8} [CVL2 + 2 \cdot CVL3 \cdot PBAR + TLC(CVL5 + 2 \cdot CVL6 \cdot PBAR) + TLC^2 (CVL8 + 2 \cdot CVL9 \cdot PBAR)] \quad (B-10b)$$

$$\frac{\partial \rho_\ell}{\partial T_\ell} = -(\rho_\ell + 2.01)^2 \cdot 1.0 \times 10^{-3} (\beta_1 + 2 \cdot \gamma_1 \cdot TLC) \quad (B-10c)$$

where

$$\beta_1 = \text{CVL4} + \text{CVL5} \cdot \text{PBAR} + \text{CVL6} \cdot \text{PBAR}^2$$

$$\gamma_1 = \text{CVL7} + \text{CVL8} \cdot \text{PBAR} + \text{CVL9} \cdot \text{PBAR}^2.$$

For $521.15 \leq T_\ell \leq 525.15$, an average of the functions in Equations B-9 and B-10 is used in this range. Call the two values $\rho_{\ell a}$ and $\rho_{\ell b}$, then:

$$\rho_\ell = \left(\frac{525.15 - T_\ell}{4.0} \right) \rho_{\ell b} + \left(\frac{T_\ell - 521.15}{4.0} \right) \rho_{\ell a} \quad (\text{B-11a})$$

$$\frac{\partial \rho_\ell}{\partial P} = \left(\frac{525.15 - T_\ell}{4.0} \right) \frac{\partial \rho_{\ell b}}{\partial P} + \left(\frac{T_\ell - 521.15}{4.0} \right) \frac{\partial \rho_{\ell a}}{\partial P} \quad (\text{B-11b})$$

$$\frac{\partial \rho_\ell}{\partial T_\ell} = \left(\frac{525.15 - T_\ell}{4.0} \right) \frac{\partial \rho_{\ell b}}{\partial T_\ell} + \left(\frac{T_\ell - 521.15}{4.0} \right) \frac{\partial \rho_{\ell a}}{\partial T_\ell} + \frac{\rho_{\ell a} - \rho_{\ell b}}{4.0} \quad (\text{B-11c})$$

After evaluation above, a pressure correction is applied to ρ_ℓ and its derivatives. In the following, the values calculated in Equations B-9a through B-11c are denoted by a tilde (~).

(a) $P \geq 4.0 \times 10^5 \text{ Pa}$

$$\left(\frac{\partial \rho_\ell}{\partial T_\ell} \right)_P = \left(1 - \frac{1000}{P} \right) \left(\frac{\partial \tilde{\rho}_\ell}{\partial T_\ell} \right)_P$$

$$\left(\frac{\partial \rho_\ell}{\partial P} \right)_{T_\ell} = \left(1 - \frac{1000}{P} \right) \left(\frac{\partial \tilde{\rho}_\ell}{\partial P} \right)_{T_\ell} + \frac{1000 \tilde{\rho}_\ell}{P^2}$$

$$\rho_\ell = \left(1 - \frac{1000}{P} \right) \tilde{\rho}_\ell.$$

(b) $P \leq 4.0 \times 10^5 \text{ Pa}$

$$\left(\frac{\partial \rho_\ell}{\partial T_\ell} \right)_P = (0.995 + 6.25 \times 10^{-9} P) \left(\frac{\partial \tilde{\rho}_\ell}{\partial T_\ell} \right)_P$$

$$\left(\frac{\partial \rho_\ell}{\partial P} \right)_{T_\ell} = (0.995 + 6.25 \times 10^{-9} P) \left(\frac{\partial \tilde{\rho}_\ell}{\partial P} \right)_{T_\ell} + 6.25 \times 10^{-9} \tilde{\rho}_\ell$$

$$\rho_\ell = (0.995 + 6.25 \times 10^{-9} P) \tilde{\rho}_\ell.$$

B.2.2.4 Enthalpy

Enthalpy is not evaluated by the water property routines, but may be evaluated easily through:

$$h_\ell = e_\ell + \frac{P}{\rho_\ell} \quad (\text{B-12})$$

B.2.3 Vapor Properties

B.2.3.1 Superheated Vapor

$$(T_v - T_{\text{sat}}) > 0.$$

B.2.3.1.1 Internal Energy

$$e_s = e_{\text{sat}} + A_{12} \left[(T_v - T_{\text{sat}}) + (T_v^2 - \beta) \right]^{1/2} - \frac{T_{\text{sat}}}{(A_{11} C_{\text{ps}} - 1.0)} \quad (\text{B-13})$$

where

$$\beta = T_{\text{sat}}^2 \left[1.0 - \frac{1.0}{(A_{11} C_{\text{ps}} - 1.0)^2} \right]$$

$$\frac{\partial e_s}{\partial T_v} = \left[\frac{A_{13}}{2} \left(1.0 - \frac{\beta}{k^2} \right) \right]^{-1.0}$$

$$k = A_{13} (e_s - e_{\text{sat}}) + T_{\text{sat}} \left[1.0 + \frac{1.0}{(A_{11} C_{\text{ps}} - 1.0)} \right]$$

$$\frac{\partial e_s}{\partial P_s} = -\frac{1}{2} \left(\frac{\partial e_s}{\partial T_v} \right) \left[\left(1.0 - \frac{\beta}{k^2} \right) \frac{\partial k}{\partial P_s} + \frac{1}{k} \frac{\partial \beta}{\partial P_s} \right]$$

$$\frac{\partial k}{\partial P_s} = -A_{13} \frac{\partial e_{\text{sat}}}{\partial P_s} + \left[1.0 + \frac{1.0}{(A_{11} C_{\text{ps}} - 1.0)} \right] \frac{\partial T_{\text{sat}}}{\partial P_s}$$

$$-T_{\text{sat}} A_{11} \left[\frac{1.0}{(A_{11} C_{\text{ps}} - 1.0)^2} \right] \frac{\partial C_{\text{ps}}}{\partial P_s}$$

and

$$\frac{\partial \beta}{\partial P_s} = \frac{2.0}{T_{sat}} \left[\beta \left(\frac{\partial T_{sat}}{\partial P_s} \right) + \frac{T_{sat}^3 A_{11}}{(A_{11} C_{ps} - 1.0)^3} \right] \left(\frac{\partial C_{ps}}{\partial P_s} \right)$$

B.2.3.1.2 Density

$$\rho_s = \frac{P_s}{[(\gamma_s - 1.0)e_{sat} + C_{26}(e_s - e_{sat})]} \quad (B-14a)$$

$$\frac{\partial \rho_s}{\partial T_v} = - \left(\frac{\partial e_s}{\partial T_v} \right) \left[\frac{C_{26} \rho_s}{(\gamma_s - 1.0)e_{sat} + C_{26}(e_s - e_{sat})} \right] \quad (B-14b)$$

and

$$\frac{\partial \rho_s}{\partial P_s} = \rho_s \left\{ \left[\frac{1.0}{P_s} e_{sat} \left(\frac{\partial \gamma_s}{\partial P_s} \right) + (\gamma_s - 1.0 - C_{26}) \frac{\partial e_{sat}}{\partial P_s} \right] \right. \\ \left. \left[\frac{1.0}{(\gamma_s - 1.0)e_{sat} + C_{26}(e_s - e_{sat})} \right] \right\} + \left(\frac{\partial \rho_s}{\partial e_s} \right) \left(\frac{\partial e_s}{\partial P_s} \right) \quad (B-14c)$$

where

$$\frac{\partial \gamma_s}{\partial P_s} = C_{10} + A_{16} P_s \quad \text{for } P_s \leq C_{21}$$

$$\frac{\partial \gamma_s}{\partial P_s} = C_{16} + A_{18} P_s \quad \text{for } P_s > C_{21}$$

and

$$\frac{\partial \rho_s}{\partial e_s} = \frac{-C_{26} \rho_s}{[(\gamma_s - 1.0)e_{sat} + C_{26}(e_s - e_{sat})]}$$

If ρ_s exceeds $0.9\rho_\ell$ or is < 0 , Equation B-14 is superseded by

$$\rho_s = 0.9\rho_\ell \quad (\text{B-15a})$$

$$\frac{\partial \rho_s}{\partial T_v} = 0.9 \left(\frac{\partial \rho_\ell}{\partial T_\ell} \right) \quad (\text{B-15b})$$

and

$$\frac{\partial \rho_s}{\partial P_s} = 0.9 \left(\frac{\partial \rho_\ell}{\partial P} \right) \quad (\text{B-15c})$$

B.2.3.1.3 Enthalpy

Enthalpy is not evaluated by the water property routines, but may be calculated easily through:

$$h_s = e_s + \frac{P_s}{\rho_s} \quad (\text{B-16})$$

B.2.3.2 Subcooled and Saturated Vapor

$$(T_v - T_{\text{sat}}) \leq 0.$$

B.2.3.2.1 Internal Energy

$$e_s = e_{\text{sat}} + (T_v - T_{\text{sat}}) \frac{C_{\text{ps}}}{C_{24}} \quad (\text{B-17a})$$

$$\frac{\partial e_s}{\partial T_v} = \frac{C_{\text{ps}}}{C_{24}} \quad (\text{B-17b})$$

$$\frac{\partial e_s}{\partial P_s} = - \left(\frac{\partial e_s}{\partial T_v} \right) \left\{ \frac{\partial T_{\text{sat}}}{\partial P_s} - \left(\frac{C_{24}}{C_{\text{ps}}} \right) \left[\frac{\partial e_{\text{sat}}}{\partial P_s} + \frac{(e_s - e_{\text{sat}})}{C_{\text{ps}}} \left(\frac{\partial C_{\text{ps}}}{\partial P_s} \right) \right] \right\} \quad (\text{B-17c})$$

B.2.3.2.2 Density

The formulas are identical to the superheated vapor case above, but the subcooled or saturated vapor energy is used in this case.

B.2.3.2.3 Enthalpy

Enthalpy is not evaluated by the water property routines, but may be calculated easily through:

$$h_s = e_s + \frac{P_s}{\rho_s} \quad (\text{B-18})$$

B.2.3.3 Noncondensable Gas (Air)

The density and internal energy of the noncondensable gas are computed from the perfect gas law. The default noncondensable gas is air. The option to overlay the gas constant (R) and specific heat (C_{vg}) to model other gas(es) is available.

B.2.3.3.1 Internal Energy

$$e_a = C_{vg} T_g \quad (\text{B-19a})$$

$$\frac{\partial e_a}{\partial T_v} = C_{vg} \quad (\text{B-19b})$$

$$\frac{\partial e_a}{\partial P_s} = 0.0 \quad (\text{B-19c})$$

B.2.3.3.2 Density

$$\rho_s = \frac{P_s}{RT_v} \quad (\text{B-20a})$$

$$\frac{\partial \rho_s}{\partial P_s} = \frac{1.0}{RT_v} \quad (\text{B-20b})$$

$$\frac{\partial \rho_s}{\partial T_v} = -R\rho_s \left(\frac{\partial \rho_s}{\partial P_s} \right) \quad (\text{B-20c})$$

where R is the universal gas constant divided by the molecular weight for the noncondensable.

B.2.3.4 Properties of Water Mixtures

The internal energy of a mixture of steam and noncondensable gas is given by the density-weighted average of the internal energies of the two species. The density of a mixture of steam and noncondensable gas is the sum of the densities of the two species.

B.3 Transport Properties

Subroutine FPROP is used to obtain transport water properties for TRACG. The input variables for this routine are (a) the saturation temperature, (b) pressure, (c) enthalpies of each phase, (d) vapor density, and (e) the vapor temperature. The output transport variables include (a) the latent heat of vaporization, (b) surface tension, (c) constant pressure specific heat, (d) viscosity, and (e) thermal conductivity of each phase. The transport property calls are function calls within Subroutine FPROP. The polynomial equation fits for the transport

properties used in FPROP are described below. Values of the constants are given in Tables B-3 through B-6.

B.3.1 Latent Heat of Vaporization

$$h_{fg} = h_g - h_f \quad (\text{B-21})$$

where h_g is calculated using Equation B-4a and

$$h_f = e_\ell + \frac{P}{\rho_\ell}$$

where e_ℓ and ρ_ℓ are calculated at saturation conditions according to Section B.2.2.

B.3.2 Constant Pressure Specific Heats

Constants used in this section are given in Table B-3.

$$c_{p\ell} = \left\{ h_\ell \left[h_\ell (D_{0\ell} + D_{1\ell}P) + (C_{0\ell} + C_{1\ell}P) \right] + B_{0\ell} + B_{1\ell}P \right\}^{-1} \quad (\text{B-22})$$

$$c_{pg} = c_{1g} + C_{2g}T_v + \frac{C_{3g}P_s}{(C_{5g}T_v - C_{6g})^{2.4}} + \frac{C_{4g}P_s^3}{(C_{5g}T_v - C_{6g})^9} \quad (\text{B-23})$$

Specific heat of the noncondensable gas is 1037.0.

B.3.3 Fluid Viscosities

B.3.3.1 Liquid

Constants used in this section are given in Table B-4. The evaluation of liquid viscosity is divided into three different enthalpy ranges:

- (1) $h_\ell \leq h_1$
- (2) $h_1 < h \leq h_2$
- (3) $h_\ell > h_2$

For $h_\ell \leq h_1$:

$$\mu_\ell = \left(A_{0\ell} + A_{1\ell}x + A_{2\ell}x^2 + A_{3\ell}x^3 + A_{4\ell}x^4 \right) - \left(B_{0\ell} + B_{1\ell}\eta + B_{2\ell}\eta^2 + B_{3\ell}\eta^3 \right) (P - P_i) \quad (\text{B-24a})$$

where

$$x = (h_\ell - c_{0n})h_0$$

and

$$\eta = (h_\ell - e_{c0n})e_{h0}$$

In the range $h_1 < h \leq h_2$

$$\begin{aligned} \mu_\ell = & (E_{0\ell} + E_{1\ell}h_\ell + E_{2\ell}h_\ell^2 + E_{3\ell}h_\ell^3) \\ & + (F_{0\ell} + F_{1\ell}h_\ell + F_{2\ell}h_\ell^2 + F_{3\ell}h_\ell^3)(P - P_i). \end{aligned} \quad (\text{B-24b})$$

For $h_\ell > h_2$

$$\mu_\ell = (D_{0\ell} + D_{1\ell}z + D_{2\ell}z^2 + D_{3\ell}z^3 + D_{4\ell}z^4) \quad (\text{B-24c})$$

where

$$z = (h_\ell - c_n)h_{00}$$

B.3.3.2 Vapor

Constants used in this section are given in Table B-5. Three vapor temperature ranges are used to represent the data:

- (1) $T_v \leq T_1$
- (2) $T_1 < T_v < T_2$
- (3) $T_v \geq T_2$

For $T_v \leq T_1$:

$$\mu_s = [B_{1g}(T_v - 273.15) + C_{1g}] - \rho_s [D_{1g} - E_{1g}(T_v - 273.15)]. \quad (\text{B-25a})$$

If $\mu_s < 10^{-7}$, it is set to that value.

For $T_1 < T_v < T_2$:

$$\begin{aligned} \mu_s = & B_{1g}(T_v - 273.15) + C_{1g} - \rho_s \left[F_{1g} + F_{2g}(T_v - 273.15) \right. \\ & \left. + F_{3g}(T_v - 273.15)^2 + F_{4g}(T_v - 273.15)^2 \right] \\ & + \rho_s \left[G_{1g} + G_{2g}(T_v - 273.15) + G_{3g}(T_v - 273.15)^2 \right. \\ & \left. + G_{4g}(T_v - 273.15)^3 \right] \left(A_{0g} + A_{1g}\rho_s + A_{2g}\rho_s^2 \right). \end{aligned} \quad (\text{B-25b})$$

For $T_v \geq T_2$:

$$\mu_s = B_{1g}(T_v - 273.15) + C_{1g} - \rho_s \left(A_{0g} + A_{1g}\rho_s + A_{2g}\rho_s^2 \right). \quad (\text{B-25c})$$

B.3.3.3 Noncondensable Gas

For the ideal gas, two ranges of T_v are used:

(1) $T_v \leq 502.15$

(2) $T_v > 502.15$

For $T_v \leq 502.15$:

$$\mu_a = H_{\ell 1} + H_{\ell 2}(T_v - 273.15) + H_{\ell 3}(T_v - 273.15)^2. \quad (\text{B-26a})$$

For $T_s > 502.15$:

$$\mu_a = H_{u 1} + H_{u 2}(T_v - 273.15) + H_{u 3}(T_v - 273.15)^2. \quad (\text{B-26b})$$

B.3.4 Fluid Thermal Conductivities

B.3.4.1 Liquid

The liquid thermal conductivity is given by:

$$k_\ell = A_{\ell 0} + A_{\ell 1}x_k + A_{\ell 2}x_k^2 + A_{\ell 3}x_k^3 \quad (\text{B-27})$$

where

$$x_k = \frac{h_\ell}{h_0}$$

and the constants are given in Table B-6.

B.3.4.2 Vapor

For the vapor, thermal conductivity is given by:

$$k_s = x_1 + \rho_s \left[x_2 + \frac{Cp_s}{(T_v - 273.15)^{4.2}} \right] \quad (\text{B-28})$$

where

$$x_1 = A_{g0} + A_{g1}(T_v - 273.15) + A_{g2}(T_v - 273.15)^2 + A_{g3}(T_v - 273.15)^3$$

and

$$x_2 = B_{g0} + B_{g1}(T_v - 273.15) + B_{g2}(T_v - 273.15)^2.$$

The constants are given in Table B-6. The thermal conductivity of the noncondensable gas is 0.0228.

B.3.5 Surface Tension

For $T_{\text{sat}} < 374.15^\circ\text{C}$:

$$\sigma = S_{21}TR^2 + S_3TR^3 + S_4TR^4 + S_5TR^5 \quad (\text{B-29})$$

$$S_{21} = S_2 + \left(\frac{S_1}{1 + S_0TR} \right)$$

where

$$TR = 647.3 - T_{\text{sat}}$$

$$S_0 = 0.83$$

$$S_1 = 1.160936807 \times 10^{-4}$$

$$S_2 = 1.12140468 \times 10^{-6}$$

$$S_3 = -5.752805180 \times 10^{-9}$$

$$S_4 = 1.286274650 \times 10^{-11}$$

$$S_5 = -1.149719290 \times 10^{-14}$$

For $T_{\text{sat}} \geq 374.15^\circ\text{C}$:

$$\sigma = 0.$$

(B-30)

This completes the description of the functional fits to the water transport properties.

B.4 Verification

The TRACG thermodynamic and transport fluid properties are consistent with the properties used in TRAC-BD1. These properties have been compared to steam table data over a wide range of conditions in Reference B-3. This assessment found good agreement for both thermodynamic and transport properties throughout the saturation and nonequilibrium regions. Additional assessment to confirm this conclusion was performed by comparing the TRACG values to ASME steam table values. A summary of these comparisons is provided in Tables B-7 through B-9.

Table B-7
Comparison of Saturation Properties
(14.7 < P < 1500 psia)

Property	RMS Error*(%)	
	Liquid	Vapor
Saturation Temperature	0.17	
Enthalpy	0.16	0.07
Specific Volume	0.23	0.49
Specific Heat	2.94	5.13
Thermal Conductivity	2.28	0.17
Viscosity	2.27	0.14
Surface Tension	0.21	

*Error = (ASME-TRACG)/ASME

Table B-8
RMS Error* (%) of Subcooled Liquid Properties (100°F < T < T_{sat})

Property	Pressure (psia)						
	14.7	250	500	750	1000	1250	1500
Enthalpy	1.78	0.84	0.56	0.43	0.48	0.63	0.82
Specific Volume	0.20	0.20	0.18	0.19	0.22	0.23	0.24
Specific Heat	0.38	0.27	0.23	0.30	0.42	0.60	0.89
Thermal Conductivity	0.72	1.07	1.09	1.10	0.98	0.84	0.68
Viscosity	2.16	2.95	2.71	2.47	2.18	1.91	1.70

*Error = (ASME-TRACG)/ASME

Table B-9**RMS Error* (%) of Superheated Steam Properties ($1500^{\circ}\text{F} > T > T_{\text{sat}}$)**

Property	Pressure (psia)						
	14.7	250	500	750	1000	1250	1500
Enthalpy	0.74	0.52	0.33	0.30	0.55	0.96	1.59
Specific Volume	0.40	2.35	1.86	1.30	0.55	0.74	2.16
Specific Heat	1.16	1.25	1.38	1.21	1.10	0.67	0.87
Thermal Conductivity	< 0.01	0.05	0.07	0.07	0.05	0.13	0.38
Viscosity	< 0.01	0.03	0.06	0.10	0.15	0.21	0.31

***Error = (ASME-TRACG)/ASME**

B.5 References

- B-1 W.A. Coffman and L.L. Lynn, *WATER: A Large Range Thermodynamic and Transport Water Property FORTRAN-IV Computer Program*, Bettis Atomic Power Laboratory, WAPD-TM-568, December 1966.
- B-2 W.C. Rivard and M.D. Torrey, *Numerical Calculations of Flashing from Long Pipes Using a Two-Fluid Model*, Los Alamos National Laboratory, LA-6104-MS, 1975.
- B-3 J.W. Spore, et. al., *TRAC-BD1: An Advanced Best Estimate Computer Program for Boiling Water Reactor Loss-of-Coolant Accident Analysis*, NUREG/CR-2178, EGG-2109, October 1981.

RAI 20

Request:

The staff wishes to perform AOO transient calculations to better assess the capability and applicability of TRACG02A. To facilitate the staff review of the code, please provide in electronic form all the input files needed to reproduce the following AOO cases that are listed in the identified sections of the TRACG Qualification LTR (NEDE-32177P, Rev. 2):

- 1. Peach Bottom 2 turbine trip test #2 (Section 7.1);*
- 2. Hatch 2 two-pump trip test (Section 7.2);*
- 3. Nine Mile Point 2 pump upshift test (Section 7.8);*
- 4. Leibstadt loss of feedwater test with HPCS unavailable (Section 7.9).*

Response:

All the input files for the four requested test cases are provided in electronic form on the CD transmitted by Reference 20-1. All the files for a particular test case are collected in a single VMS saveset file. A fifth saveset named UNPACK.SAV can be restored and used to unpack the other four savesets. Each of the four AOO cases will be expanded into a separate directory that contains all the input files needed to reproduce the results documented in NEDE-32177P, Rev. 2. For each AOO test case, three command files are provided: (1) RUN_S.COM will run the steady state job, (2) RUN_T.COM will run the transient job, (3) RUN.COM will run both the steady state and transient jobs. Each AOO case includes a PANAC10 wrapup file (*.WRP) that is used to supply the inputs for the 3D neutron kinetics. Each AOO case also includes a graphics input file (*.GRI) that can be used together with the GRIT utility that was provided previously for use in extracting key calculated values from the TRACG02A output graphics file (*.GRF file).

References for RAI 20

- [20-1] GE/NRC Letter FLN-2001-003, G. A. Watford to U.S. NRC Document Control Desk, "Transmittal of GE Proprietary Information Contained in Electronic form on CD labeled: 'Input Files for Four Selected TRACG02A Qualification Cases (3/15/2001)'", March 15, 2001.

RAI 21

Request:

The staff has performed a series of audit calculations with TRAC-BF1 and NESTLE using the TRACG model provided by GNF. Analysis of a main steam isolation valve (MSIV) closure event with TRAC-BF1/NESTLE predicts a significantly different power when compared to TRACG (refer to Figure 1, attached). The staff has assessed both models and has not found any deficiencies in either the TRACG or the TRAC-BF1/NESTLE input. The boundary conditions, for example, are identical. In order for the staff to proceed with the review, the following information is needed to assist us as we attempt to reconcile the differences in the predicted results.

- a. Provide all of the calculated k-infinity values from the TGBLA code at the cross section generation branch points.*
- b. Describe the model used to account for the bypass and water rod density in the cross section formulation. How are changes in the bypass and water rod density accounted for in the cross section generation code and how are these effects averaged into a form suitable for TRACG analysis?*
- c. Describe the mathematical form of the cross section model and relate the coefficients in the TRACG kinetics output file to coefficients in the model.*
- d. Describe the form and content of the PANACEA wrap-up file.*

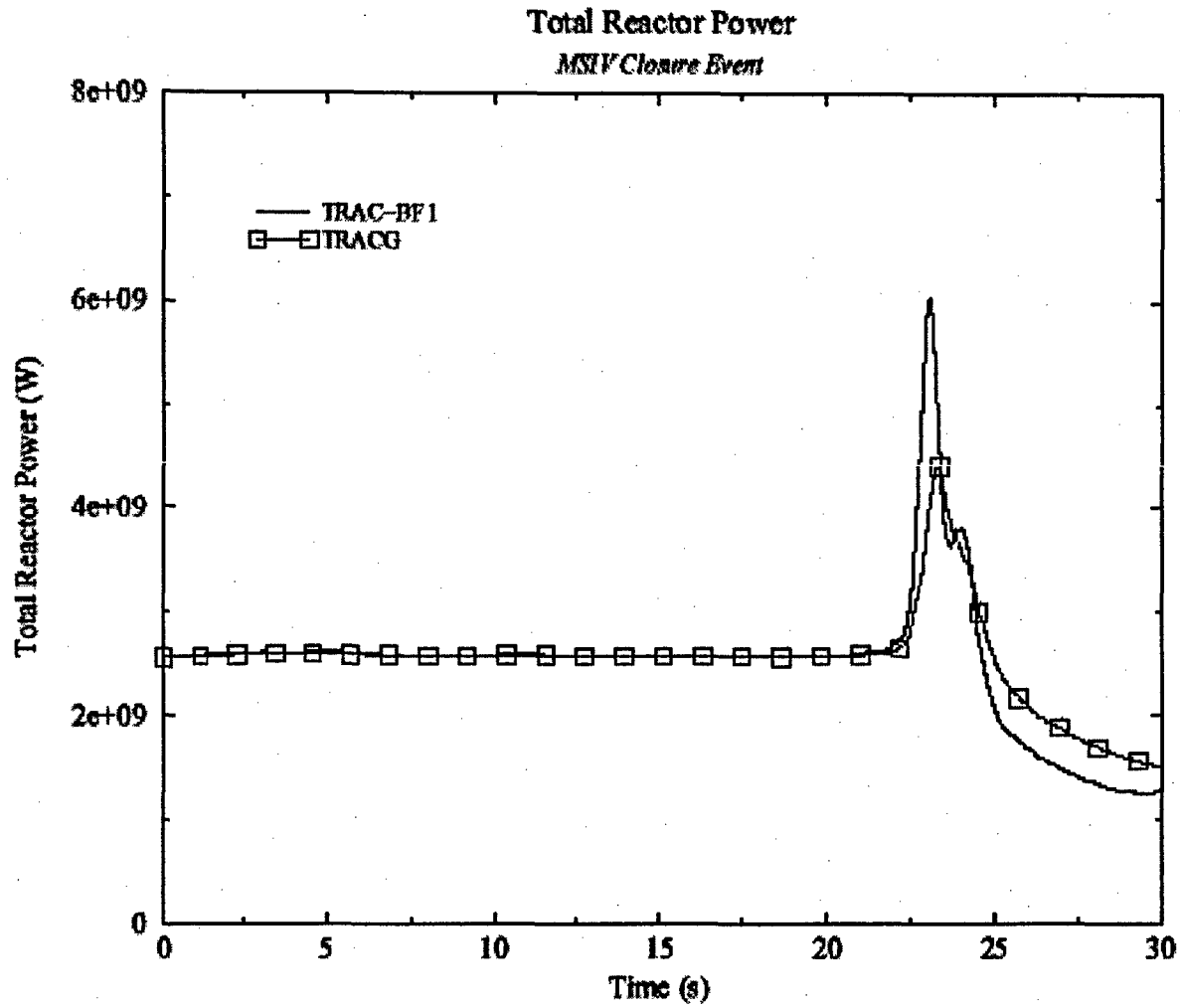


Figure 1 Total Reactor Power with unmodified TRACG

Responses

The responses are contained in four parts corresponding to the four parts of the request. For convenience the request for each part is repeated prior to providing the response. Each part begins on a new page. References for all four parts are consolidated below. Proprietary information is indicated by a solid bar in the right margin.

References for RAI-21

[21-1] "Hypothetical Initial Core of GE12"; GE Proprietary; September 10, 2000. (Stored in DRF J11-03558)

[21-2] J. G. M. Andersen et. al., *TRACG Model Description*, NEDE-32176P, Revision 2, December 1999.

[21-3] *Steady-State Nuclear Methods*, NEDE-30130-P-A, April 1985.

[21-4] *PANACEA BWR Core Simulator*, NEDE-20884, Volume 2, January 1993.

Request 21-b:

- b. Describe the model used to account for the bypass and water rod density in the cross section formulation. How are changes in the bypass and water rod density accounted for in the cross section generation code and how are these effects averaged into a form suitable for TRACG analysis.

Response 21-b:

Section 9.2 of Reference 21-2 states:

Void dependence is represented by the ratio of cell average water density relative to the reference water density used in the lattice cell calculation. This ratio is given by:

$$U = \frac{\rho}{\rho_0}$$

The cell average water density is the volume weighted average water density in the $6 \times 6 \times 6$ in³ cell used in the nuclear model. The cell size is identical to the pitch of the fuel channels, and therefore the cell will include the channel and half of the bypass region between the channel and the neighboring channel. The cell average water density is calculated by:

$$\rho = F_{AC} [(1 - \alpha)\rho_l + \alpha\rho_v]_{AC} + F_{BP} [(1 - \alpha)\rho_l + \alpha\rho_v]_{BP} \\ + F_{WR} [(1 - \alpha)\rho_l + \alpha\rho_v]_{WR}$$

where: F_{AC} is the relative volume in the active channel excluding the water rods.

F_{BP} is the relative volume in the bypass region between channels

F_{WR} is the relative volume in the water rods

α is the void fraction

ρ_l is the liquid density

ρ_v is the vapor density

Note, the volume fractions must satisfy:

$$F_{AC} + F_{BP} + F_{WR} = 1.0$$

For each fuel type the nuclear parameters have been fitted in terms of U.

In the approved 3D core simulator PANACEA [21-3] the water rod volume is lumped together with the bypass volume. When these volumes are lumped together, the above equation reduces to:

$$\rho = F_{AC} [(1 - \alpha)\rho_l + \alpha\rho_v]_{AC} + (1 - F_{AC}) [(1 - \alpha)\rho_l + \alpha\rho_v]_{OC}$$

where the subscript "OC" designate the out-of-channel density, or the average density in the lumped bypass and water rod channel. This expression is identical to the calculation of the cell averaged water density in PANACEA [21-3]. From the above derivation it is seen that the calculation of the relative water density in TRACG is the same as in PANACEA, except for the capability of TRACG to distinguish between the out-of-channel water in the bypass and the water rods.

The nuclear parameters as used both in the approved PANACEA [21-3] and TRACG [21-2] are correlated in terms of the average relative water density U and exposure. The correlations in terms of the average relative density are obtained from lattice calculations at different in-channel void fractions and exposures. A zero out-of-channel void fraction is used in the lattice calculations and the assumption is made that the worth of the water is the same in the 6^3 in³ cell independent of whether the water is in the channel or out of the channel.

Request 21-c:

- c. *Describe the mathematical form of the cross section model and relate the coefficients in the TRACG kinetics output file to coefficients in the model.*

Response 21-c:

TRACG provides outputs that indicate the cross section information contained on the PANACEA wrapup (See response to Request 21-d). PANACEA bundle types are assigned in a map as shown by the example in Exhibit 21-c.1. The example shows the core loading corresponding to the PANACEA wrapup that was provided in response to RAI-1. All the information shown in these exhibits was extracted from the TT_TOT file produced by running the sample problems described in the response to RAI-1.

PANACEA bundles are also referred to as assemblies and their corresponding index is denoted by IAT. A particular IAT consists of one or more fuel types (lattices) that are stacked axially to define the assembly. Each lattice has a unique fuel type index (IFT or IF) so that a particular IAT is defined by how the IF values are stacked. For the wrapup supplied in response to RAI-1, nine assembly types were defined as shown in Exhibit 21-c.2. Note that only the first five of these assemblies were actually used in the core as indicated by the map in Exhibit 21-c.1.

Exhibit 21-c.1 BUNDLE TYPEs from TRACG Kinetics Output File (*.TOT)

Exhibit 21-c.2 FUEL TYPEs from TRACG Kinetics Output File (*.TOT)

Exhibit 21-c.3 CROSS SECTION Edits from TRACG Kinetics Output File (*.TOT)

Request 21-d:

d. Describe the form and content of the PANACEA wrap-up file.

Response 21-d:

The following discussion is specific to PANAC10A and was extracted from the user documentation contained in Reference [21-4].

The terms wrapup, wrapup file, restart and restart file are used frequently throughout the PANACEA documentation. The following discussion is included to acquaint the User with the concepts these terms represent. The PANACEA program makes use of an input/output system which partitions data into a number of "classes" or "data sets". The content of each data set for PANACEA is summarized in the following table. A wrapup is a collection of classes of data which is identified by a label or wrapup ID (WRAPID). This collection of data may reside on a magnetic tape, a temporary disc file, or a permanent disc file. The wrapup format is a fixed record length binary ("unformatted") file. The wrapup may contain all the data sets necessary to run PANACEA or some subset of the required data sets.

A wrapup file is simply one or more wrapups, each having a WRAPID, residing on a storage device. The wrapup file is always ended by a pseudo-wrapup (WRAPID = EOWRAP) which consists of just an identification block.

A restart is equivalent to a wrapup. The name change is meant to indicate the role the data plays in the PANACEA case. A wrapup is output from a PANACEA case while a restart is input. It is normal procedure for the wrapup from one case to be the restart of another. A restart file is, therefore, the same as a wrapup file.

The following table gives a quick index of all classes in PANACEA which are wrapped up. For those classes, the size, internal coding name, and a quick description are provided. Classes that are not listed are not wrapped up.

PANACEA CLASS SUMMARY						
<u>CLASS</u>	<u>TYPE</u>	<u>NAME</u>	USER INPUT SYMBOL <u>OR CLASS SIZE</u>	REC. NO.	NO. OF <u>REC.</u>	<u>DESCRIPTION</u>

RAI 22

Request:

The prediction of safety limits using TRACG depends on the consistency between TRACG predictions and test measurements used for the GENE critical power ratio correlation. Please provide assessment information on the ability of TRACG to predict pressure drops for different flow rates, inlet subcoolings, powers, and different fuel bundle designs in the test facility used for critical power ratio testing.

Response:

The models for frictional pressure drop are described in Section 6.2 of Ref. [22-1]. This section documents the models for wall friction and form losses and includes application range and applicability to BWR as well accuracy of the models. The GE design correlation is based on the Chisholm correlation which has been tested against a wide range of data as documented in Section 6.2.1.6 of Ref. [22-1]. Form losses are calculated using the homogeneous two phase multiplier. This model has been extensively tested against full scale ATLAS pressure drop data for spacers and tie plates as documented in Section 6.2.2.5 of Ref. [22-1]. Finally the applicability of the pressure drop model is discussed in Section 6.2.3 of Ref. [22-1]. It is shown that the models apply for the operating range of the BWR and that BWR bundle pressure drops are very accurately calculated with these models.

Section 3.5 of Ref. [22-2] contains qualification against full scale ATLAS test data for a large range of power and flow (0-8MW and 135-2034kg/m²s). These comparisons showed a small 5% over-prediction of the pressure drop, and a standard deviation of 3.9%.

References for RAI 22

[22-1] TRACG Model Description, NEDE-32176P, Rev. 2, December 1999.

[22-2] TRACG Qualification, NEDE-32177P, Rev. 2, January 2000.

[22-3] J. G. M. Andersen, et al., *TRACG Application for Anticipated Operational Occurrences (AOO) Transient Analyses*, NEDE-32906P, January 2000.

RAI 23

Request:

TRACG uses the rate of change of void fraction, pressure, non-condensable gas pressure, and liquid and vapor temperatures to control the timestep size. In reactivity transients such as a rod drop the key parameters that should control timestep size are the rate of control rod reactivity insertion and the rate of change in fuel temperatures. What steps does GENE take to insure that they get numerically converged results for rod drop transients in light of the fact that the TRACG timestep control algorithm does not monitor the rate of change in the key controlling parameters in the event?

Response:

In TRACG a distinction is made between numerical convergence and temporal discretization error as indicated in Section 8.2.4 of Ref. [23-1]. The numerical convergence criteria are several orders of magnitude tighter than the rate of change restrictions. The time step size is regulated to control the inaccuracies associated with temporal discretization. These inaccuracies are a result of the fundamental assumption that critical parameters remain constant during the time interval of one time step. As indicated in Section 8.2.4 of Ref. [23-1], the time step size in TRACG is a function of the rate of change for the nodal values of the five independent hydraulic variables (1) pressure, (2) void fraction, (3) vapor temperature, (4) liquid temperature and (5) non-condensable gas pressure. In addition to these, TRACG regulates the time step size to control the rates of change for (6) heat slab temperatures, (7) fuel rod temperatures, and (8) nodal powers from the 3D neutron kinetics model. Thus TRACG does indeed monitor key controlling parameters for fast reactor transients by checking and controlling the rates of change for nodal power and fuel rod temperatures.

For each of the eight quantities identified in the previous paragraph there is an associated TRACG code input parameter RATEOK(i). The RATEOK default values are documented in Appendix G of Ref. [23-2]. To provide additional detail on how the RATEOK values are used in the rate of change equations, the five rate of change equations originally presented in Section 8.2.4.2 of Ref. [23-1] have been rewritten by replacing the default value with its symbolic RATEOK(i) name. In addition, the three rate-of-change equations for items (6), (7) and (8) that were not provided previously in Ref. [23-1] have been added. All the equations given in this RAI response will be included in the next revision of the TRACG Model Description LTR.

$$\zeta_p = \max \left(\frac{|P_i^n - P_i^{n-1}|}{\max(5.0 \cdot 10^4, \text{RATEOK}(1) \cdot P_i^n)} \right)$$

$$\zeta_{\alpha} = \max \left(\frac{|\alpha_i^n - \alpha_i^{n-1}|}{\text{RATEOK}(2)} \right)$$

$$\zeta_{T_v} = \max \left(\frac{|T_{vi}^n - T_{vi}^{n-1}|}{\text{RATEOK}(3)} \right)$$

$$\zeta_{T_t} = \max \left(\frac{|T_{ti}^n - T_{ti}^{n-1}|}{\text{RATEOK}(4)} \right)$$

$$\zeta_{P_a} = \max \left(\frac{|P_{ai}^n - P_{ai}^{n-1}|}{\max(5.0 \cdot 10^4, \text{RATEOK}(5) \cdot F_i^n)} \right)$$

$$\zeta_{T_w} = \max \left(\frac{|T_{wj}^n - T_{wj}^{n-1}|}{\text{RATEOK}(6)} \right)$$

$$\zeta_{T_{fuel}} = \max \left(\frac{|T_{fuel,j,k}^n - T_{fuel,j,k}^{n-1}|}{\text{RATEOK}(7)} \right)$$

$$\zeta_P = \max \left(\frac{|P_{k,chan}^n - P_{k,chan}^{n-1}|}{\text{RATEOK}(8)} \right)$$

Note that the first five equations above reduce to those given previously in Section 8.2.4.2 of Ref. [23-1] when the default values of the RATEOK(i) inputs are specified. All the AOO calculations presented in references [23-3] and [23-4] were run using the default values. The symbols for the first five equations above are the same as defined in Section 8.2.4.2 of Ref. [23-1] except the "η" in the original expressions for T_v , T_t , and P_a should have been "ζ". The new symbols associated with the last three equations are:

T_w is the slab temperature which may be a single value for a lumped slab or an array of values for a single-sided or double-sided slab with more than one node;

T_{fuel} is the fuel rod temperature which is defined for multiple radial nodes in the fuel pellet and cladding at multiple axial locations in any number of rod groups for each CHAN component;

P is the nodal power in an axial node (k) of a CHAN (normalized to 1 real bundle).

The limiting rate-of-change ratio is quantified by ζ which is defined as the maximum of the eight individual rate of change ratios defined above. Allowable values for ζ must satisfy

$$\zeta = \max(\zeta_P, \zeta_{\alpha}, \zeta_{T_v}, \zeta_{T_b}, \zeta_{P_a}, \zeta_{T_w}, \zeta_{T_{fuel}}, \zeta_P) \leq \text{XRATOK}$$

The value of XRATOK may be input as described in Section 3.2 of Ref. [23-2], but the default value of 1.25 is almost always used. (All the AOO calculations used XRATOK=1.25.) When ζ is greater than XRATOK the time step fails and is repeated using a time step size that is at least a factor of 2 smaller but not more than a factor of 10 smaller depending on the actual value of ζ . For values of $\zeta \leq \text{XRATOK}$ a gain is defined that is the reciprocal of ζ . This gain is not allowed to exceed 1.5. This gain times the current time step size defines the time step size that will be used for the next step provided the new time step size is not otherwise restricted by a high iteration count or by any of the other criteria given in Section 8.2.4.3 of Ref. [23-1]. In the absence of these other restrictions, the rate-of-change logic is such that the time step sizes will tend to float smoothly around values that result in a value for ζ that is near unity.

Note that TRACG does indeed monitor key controlling parameters for fast reactor transients by checking and controlling the rates of change for nodal power and fuel rod temperatures. The rod drop accident (RDA) is not classified as an AOO event; nevertheless, the time step control algorithm restricts the time step size to limit the maximum local changes in nodal power and fuel temperature that may result in the event of a local prompt criticality from a RDA or some other postulated reactivity insertion accident (RIA). The limits on nodal power and fuel temperature also are relevant for boron dilution situations during an ATWS. Convergence of the 3D flux shape is addressed separately and is controlled by specifying the parameters listed on page 35 of Ref. [23-2]. For a LOCA, the rate of change for nodal power will not be relevant although the rate of change for fuel temperature (including clad) may be important especially during the quenching of hot fuel rods.

The capability of TRACG to control the time step size for AOO events is evident from the sensitivity studies documented in Section 6.9 of Ref. [23-3]. In these studies performed for a fast pressurization transient, changes in maximum allowed time step size produced negligible changes in the calculated values for the key safety parameters. Additional sensitivity studies were performed in response to RAI 6 to quantify the impact of varying other parameters related to the neutron kinetics solver. Of course, these sensitivity studies are designed to address a particular type of application, i.e., AOOs. Other applications of TRACG for non-AOO events such as LOCA, ATWS and RDA/RIA have different critical parameters and thus have different sensitivities to time step size that must be quantified for these specific applications. Some additional non-AOO time step sensitivity studies are included in Ref. [23-3] Sections 3.1.5.4 and 3.7.5 in addition to those previously mentioned for AOOs in Section 6.9.

References for RAI 23

[23-1] TRACG Model Description, NEDE-32176P, Rev. 2, December 1999.

[23-2] TRACG02A User's Manual, NEDC-32956P, Rev. 0, February 2000.

[23-3] TRACG Qualification, NEDE-32177P, Rev. 2, January 2000.

[23-4] J. G. M. Andersen, et al., *TRACG Application for Anticipated Operational Occurrences (AOO) Transient Analyses*, NEDE-32906P, January 2000.

ENCLOSURE 3

MFN 06-042

Affidavit

General Electric Company

AFFIDAVIT

I, **Louis M. Quintana**, state as follows:

- (1) I am Manager, Licensing, General Electric Company ("GE"), and have been delegated the function of reviewing the information described in paragraph (2) which is sought to be withheld, and have been authorized to apply for its withholding.
- (2) The information sought to be withheld is contained in the GE proprietary report, NEDE-32906P-A, *TRACG Application for Anticipated Operational Occurrences (AOO) Transient Analyses, Revision 1*, Class III (GE Proprietary Information), dated April 2003. This document was originally prepared in 2003 but was not formally issued. The proprietary information is indicated by "sidebars" drawn in the right-hand margin of the report. The sidebars refer to Paragraph (3) of this affidavit, which provides the basis for the proprietary determination.
- (3) In making this application for withholding of proprietary information of which it is the owner, GE relies upon the exemption from disclosure set forth in the Freedom of Information Act ("FOIA"), 5 USC Sec. 552(b)(4), and the Trade Secrets Act, 18 USC Sec. 1905, and NRC regulations 10 CFR 9.17(a)(4), and 2.390(a)(4) for "trade secrets" (Exemption 4). The material for which exemption from disclosure is here sought also qualify under the narrower definition of "trade secret", within the meanings assigned to those terms for purposes of FOIA Exemption 4 in, respectively, *Critical Mass Energy Project v. Nuclear Regulatory Commission*, 975F2d871 (DC Cir. 1992), and *Public Citizen Health Research Group v. FDA*, 704F2d1280 (DC Cir. 1983).
- (4) Some examples of categories of information which fit into the definition of proprietary information are:
 - a. Information that discloses a process, method, or apparatus, including supporting data and analyses, where prevention of its use by General Electric's competitors without license from General Electric constitutes a competitive economic advantage over other companies;
 - b. Information which, if used by a competitor, would reduce his expenditure of resources or improve his competitive position in the design, manufacture, shipment, installation, assurance of quality, or licensing of a similar product;
 - c. Information which reveals aspects of past, present, or future General Electric customer-funded development plans and programs, resulting in potential products to General Electric;

- d. Information which discloses patentable subject matter for which it may be desirable to obtain patent protection.

The information sought to be withheld is considered to be proprietary for the reasons set forth in paragraphs (4)a. and (4)b. above.

- (5) To address 10 CFR 2.390 (b) (4), the information sought to be withheld is being submitted to NRC in confidence. The information is of a sort customarily held in confidence by GE, and is in fact so held. The information sought to be withheld has, to the best of my knowledge and belief, consistently been held in confidence by GE, no public disclosure has been made, and it is not available in public sources. All disclosures to third parties including any required transmittals to NRC, have been made, or must be made, pursuant to regulatory provisions or proprietary agreements which provide for maintenance of the information in confidence. Its initial designation as proprietary information, and the subsequent steps taken to prevent its unauthorized disclosure, are as set forth in paragraphs (6) and (7) following.
- (6) Initial approval of proprietary treatment of a document is made by the manager of the originating component, the person most likely to be acquainted with the value and sensitivity of the information in relation to industry knowledge. Access to such documents within GE is limited on a "need to know" basis.
- (7) The procedure for approval of external release of such a document typically requires review by the staff manager, project manager, principal scientist or other equivalent authority, by the manager of the cognizant marketing function (or his delegate), and by the Legal Operation, for technical content, competitive effect, and determination of the accuracy of the proprietary designation. Disclosures outside GE are limited to regulatory bodies, customers, and potential customers, and their agents, suppliers, and licensees, and others with a legitimate need for the information, and then only in accordance with appropriate regulatory provisions or proprietary agreements.
- (8) The information identified in paragraph (2), above, is classified as proprietary because it contains the detailed results including the process and methodology for application of TRACG to the performance of evaluations of AOOs for GE BWRs. This TRACG code has been developed by GE for over fifteen years, at a total cost in excess of three million dollars. The reporting, evaluation and interpretations of the results, as they relate to the BWR, was achieved at a significant cost to GE.

The development of the evaluation process along with the interpretation and application of the analytical results is derived from the extensive experience database that constitutes a major GE asset.

- (9) Public disclosure of the information sought to be withheld is likely to cause substantial harm to GE's competitive position and foreclose or reduce the availability of profit-making opportunities. The information is part of GE's comprehensive BWR safety and technology base, and its commercial value extends

beyond the original development cost. The value of the technology base goes beyond the extensive physical database and analytical methodology and includes development of the expertise to determine and apply the appropriate evaluation process. In addition, the technology base includes the value derived from providing analyses done with NRC-approved methods.

The research, development, engineering, analytical and NRC review costs comprise a substantial investment of time and money by GE.

The precise value of the expertise to devise an evaluation process and apply the correct analytical methodology is difficult to quantify, but it clearly is substantial.

GE's competitive advantage will be lost if its competitors are able to use the results of the GE experience to normalize or verify their own process or if they are able to claim an equivalent understanding by demonstrating that they can arrive at the same or similar conclusions.

The value of this information to GE would be lost if the information were disclosed to the public. Making such information available to competitors without their having been required to undertake a similar expenditure of resources would unfairly provide competitors with a windfall, and deprive GE of the opportunity to exercise its competitive advantage to seek an adequate return on its large investment in developing these very valuable analytical tools.

I declare under penalty of perjury that the foregoing affidavit and the matters stated therein are true and correct to the best of my knowledge, information, and belief.

Executed on this 6th day of February 2006.



Louis M. Quintana
Manager, Licensing

ENCLOSURE 1 - CD-ROM

MFN 06-042

GE Licensing Topical Report NEDE-32906P-A, Revision 1,
“TRACG Application for Anticipated Operational Occurrences (AOO)
Transient Analyses

GE Proprietary Information

PROPRIETARY INFORMATION NOTICE

This enclosure contains proprietary information of the General Electric Company (GE) and is furnished in confidence solely for the purpose(s) stated in the transmittal letter. No other use, direct or indirect, of the document or the information it contains is authorized. Furnishing this enclosure does not convey any license, express or implied, to use any patented invention or, except as specified above, any proprietary information of GE disclosed herein or any right to publish or make copies of the enclosure without prior written permission of GE. The header of each page in this enclosure carries the notation “GE Proprietary Information.”

The proprietary information of the GE Company is indicated by “bars” drawn in the right-hand margin of the report (as shown to the right of this paragraph). The sidebars refer to Paragraph (3) of the affidavit, which provides the basis for the proprietary determination.